Electronic Supplementary Information

Hydrogen Bonds and Dispersion Forces Serving as Molecular Locks for Tailored Group 11 Bis(amidine) Complexes

Janet Arras,[a] Omar Ugarte Trejo,[a] Nattamai Bhuvanesh,[b] Colin D. McMillen,[c] and Michael Stollenz*[a]

[a] Department of Chemistry and Biochemistry, Kennesaw State University, 370 Paulding Avenue NW, MD#1203, Kennesaw, Georgia 30144, USA. [b] Department of Chemistry, Texas A&M University, 580 Ross Street, P.O. Box 30012, College Station, Texas 77842-3012, USA. [c] Department of Chemistry, Clemson University, 379 Hunter Laboratories, Clemson, SC 29634-0973, USA

*E-mail: Michael.Stollenz@kennesaw.edu.

Table of Contents

Experimental and Computational Sections

General Procedures. All synthetic procedures involving air- and moisture-sensitive compounds were carried out by using Schlenk techniques under an atmosphere of dry argon. Glassware was heat-sealed with a heat gun under vacuum. *Solvents*: Prior to use, tetrahydrofuran (THF), diethyl ether, and toluene were freshly distilled from sodium/benzophenone. CH_2Cl_2 was distilled from CaH_2. Alternatively, the aforementioned solvents were purified using a PPT Solvent Purification System. For non-inert manipulations, CH_2Cl_2, diethyl ether, and pyridine were used as received without further purification. *Deuterated solvents*: $CDCl_3$ (Cambridge Isotope Laboratories, Inc., D, 99.8% + 0.03% v/v tetramethylsilane, TMS), C_6D_6 (Cambridge Isotope Laboratories, Inc., D, 99.5%), and pyridine-d_5 (C_5D_5N, Cambridge Isotope Laboratories, Inc., D, 99.9%) were used as received without further purification. *Reactants*: [(Me_2S)AuCl] (Aldrich), CuCl (Alfa Aesar, 99.999%), AgCl (Alfa Aesar, 99.9%), and 2-mesitylmagnesium bromide (Acros Organics, 1 M in THF) used as received without further purification. The syntheses of **L**H_2[S2] and **4** (Method A)[S3] were previously described. Elemental analyses were performed by Atlantic Microlab, Inc. Melting points were determined with an SRS (Stanford Research Systems) Digi Melt instrument using open capillaries; values are uncorrected (the heating rate was 2 K/min). NMR measurements were recorded on a Bruker Avance III 400 spectrometer at 300 K unless otherwise noted. ^{13}C NMR resonances were obtained with proton broadband decoupling and referenced to the solvent signals of $CDCl_3$ at 77.0, C_6D_6 at 128.0, and C_5D_5N at 123.9 (^1H NMR: 7.24 ($CHCl_3$), 7.15 (benzene), and 7.22 (pyridine), respectively). ^{13}C NMR assignments are based on HSQC and HMBC 2D experiments. $\Delta G_c^{\ddagger}$ values were determined by monitoring the CH_2 signals of **1** and **2** in dependence from the temperature and calculated using the Gutowsky-Holm equation $k_{Tc} = \pi\delta\nu/\sqrt{2}$ (k_{Tc}: rate constant at T_c; ν: difference of separated signals in Hz) and the Eyring equation.[S4,S5] Mass-spectrometric analyses were performed on a Bruker Ultraflex II Tof instrument (MALDI), on a Waters Q-Tof API US quadrupole time of flight MS system (low resolution ESI), and on a Thermo Obitrap Velos Pro MS system (high resolution ESI). IR spectra were measured on a PerkinElmer Spectrum One FT-IR Spectrometer equipped with a Universal ATR Sampling Accessory.

Synthesis of 1. A solution of **L**H_2 (0.714 g, 1.75 mmol) in THF (20 mL) was added to a suspension of CuCl (0.350 g, 3.54 mmol) in THF (30 mL) with stirring. Over the course of 5 d, a colorless precipitate was formed. This solid was isolated by filtration, washed with cold THF (0 °C, 3 × 4 mL), and dried in oil pump vacuum for 24 h. A colorless microcrystalline powder was obtained. Yield 1.013 g (1.670 mmol, 95%). Mp: 170–175 °C (decomposition into a black oil). Anal. Calcd. for $C_{24}H_{36}N_6Cu_2Cl_2$: C, 47.52; H, 5.98; N, 13.85; Cl, 11.69. Found: C, 47.73; H, 5.94; N, 13.79; Cl, 11.63. ^1H NMR (400.1 MHz, $CDCl_3$): δ 1.25 (s, 18 H, CH_3, ^{t}Bu), 2.58 (s, 6 H, CH_3, 6-Py), 3.65 (broad s, 4 H, CH_2), 6.56 (d, $^3J_{HH}$ = 8.1 Hz, 2 H, Py H^3), 6.64 (s, 2 H, NH), 6.68 (d, $^3J_{HH}$ = 7.4 Hz, 2 H, CH, Py H^5), 7.46 (t, $^3J_{HH}$ = 7.8 Hz, 2 H, CH, Py

H^4). ^{1}H NMR (400.1 MHz, C_6D_6): δ 1.31 (s, 18 H, CH_3, ^{t}Bu), 1.97 (s, 6 H, CH_3, 6-Py), 4.02 (s, 4 H, CH_2), 5.91 (d, $^3J_{HH}$ = 7.3 Hz, 2 H, CH, Py H^5), 6.21 (d, $^3J_{HH}$ = 8.1 Hz, 2 H, CH, Py H^3), 6.71 (t, $^3J_{HH}$ = 7.8 Hz, 2 H, CH, Py H^4), 7.45 (s, 2 H, NH). ^{13}C{^{1}H} NMR (100.6 MHz, $CDCl_3$): δ 25.8 (CH_3, 6-Py), 30.4 (CH_3, ^{t}Bu), 38.9 (CH_2), 41.0 (C, ^{t}Bu), 114.5 (CH, Py C^3), 115.2 (CH, Py C^5), 139.3 (CH, Py C^4), 155.7 (C, Py C^6), 163.1 (C, CN_2), 163.9 (C, Py C^2). ^{13}C{^{1}H} NMR (100.6 MHz, C_6D_6): δ 25.1 (CH_3, 6-Py), 30.5 (CH_3, ^{t}Bu), 39.2 (CH_2), 41.2 (C, ^{t}Bu), 114.4 (CH, Py C^3), 114.6 (CH, Py C^5), 138.9 (CH, Py C^4), 155.8 (C, Py C^6), 163.1 (C, CN_2), 164.3 (C, Py C^6). MS (ESI(+)): *m*/*z* (relative intensity): 471 (23) [**L**H_2Cu] $^+$, 409 (100) [**L**H_2 + H]$^+$, 205 (44) [**L**H_2 + 2 H]$^{2+}$. HRMS (ESI(+)): *m*/*z* calcd for $C_{24}H_{36}N_6Cu$ [**L**H_2Cu]$^+$ 471.2297, found 471.2292. MS (MALDI(+)): *m*/*z* (relative intensity): 571 (100) [M – Cl + 1]$^+$. IR (neat, cm^{-1}): 3378 (s, ν(N–H)), 2992, 2968, 2923, 2893, 2872 (w, (ν-C–H)), 1627 (vs, ν(C=N)), 1599 (s), 1559 (m), 1530 (vs), 1483 (m), 1455 (vs), 1401 (s), 1385, 1370, 1363, 1342 (m), 1285 (s), 1255 (m), 1218 (s), 1194 (vs), 1160 (s), 1119, 1094, 1077 (m), 1023 (s), 984 (w), 970, 960 (m), 944, 929 (w), 882 (m), 850 (w), 832, 806 (s), 788 (vs), 749 (s), 707 (w).

Synthesis of 2. A solution of **L**H_2 (0.435 g, 1.06 mmol) in THF (20 mL) was added to a solution of [(Me_2S)AuCl] (0.629 g, 2.14 mmol) in THF (50 mL) with stirring under exclusion of light. Over the course of 3 h, a colorless precipitate was formed. This solid was isolated by filtration, washed with CH_2Cl_2 (3 × 10 mL), and dried in oil pump vacuum for 24 h. A colorless microcrystalline powder was obtained. Yield: 0.784 g (0.898 mmol, 85%). Mp: 180–181 °C (decomposition into a dark purple oil). Anal. Calcd. for $C_{24}H_{36}N_6Au_2Cl_2$: C, 33.00; H, 4.15; N, 9.62; Cl, 8.12. Found: C, 33.02; H, 4.20; N, 9.45; Cl, 8.28. ^{1}H NMR (400.1 MHz, $CDCl_3$): δ 1.26 (s, 18 H, CH_3, ^{t}Bu), 2.67 (s, 6 H, CH_3, 6-Py), 3.78 (broad s, 4 H, CH_2), 6.43 (s, 2 H, NH), 6.68 (d, $^3J_{HH}$ = 8.2 Hz, 2 H, CH, Py H^3), 6.75 (d, $^3J_{HH}$ = 7.3 Hz, 2 H, CH, Py H^5), 7.49 (t, $^3J_{HH}$ = 7.8 Hz, 2 H, CH, Py H^4). ^{1}H NMR (400.1 MHz, C_6D_6): δ 1.32 (s, 18 H, CH_3, ^{t}Bu), 2.09 (s, 6 H, CH_3, 6-Py), ≈ 3.65, 4.66 (broad, 4 H, CH_2), 5.90 (d, $^3J_{HH}$ = 7.4 Hz, 2 H, CH, Py H^5), 6.26 (d, $^3J_{HH}$ = 8.2 Hz, 2 H, CH, Py H^3), 6.65 (t, $^3J_{HH}$ = 7.8 Hz, 2 H, CH, Py H^4), ≈ 7.15 (br, 2 H, NH, overlaid by the C_6D_6 signal). ^{13}C{^{1}H} NMR (100.6 MHz, $CDCl_3$): δ 26.5 (CH_3, 6-Py), 30.2 (CH_3, ^{t}Bu), 39.4 (CH_2), 41.3 (C, ^{t}Bu), 115.3 (CH, Py C^3), 115.4 (CH, Py C^5), 139.3 (CH, Py C^4), 155.8 (C, Py C^6), 162.6 (C, CN_2), 163.4 (C, Py C^2). ^{13}C{^{1}H} NMR (100.6 MHz, C_6D_6): δ 25.8 (CH_3, 6-Py), 30.3 (CH_3, ^{t}Bu), 39.8 (CH_2), 41.6 (C, ^{t}Bu), 114.9 (CH, Py C^5), 115.1 (CH, Py C^3), 138.7 (CH, Py C^4), 155.8 (C, Py C^6), 162.8 (C, CN_2), 163.7 (C, Py C^2). MS (ESI(+)): *m*/*z* (relative intensity): 605 (93) [**L**H_2Au]$^+$, 409 (100) [**L**H_2 + H]$^+$. MS (MALDI(+)): *m*/*z* (relative intensity): 837 (31) [M – Cl]$^+$, 641 (19) [**L**H_2AuCl + H]$^+$, 605 (100) [**L**H_2Au]$^+$, 409 (40) [**L**H_2 + H]$^+$. HRMS (MALDI(+)): *m*/*z* calcd for $C_{24}H_{36}N_6Au_2Cl$ [M – Cl]$^+$ 837.2021, found 837.2029. IR (neat, cm^{-1}): 3391 (s, ν(N–H)), 2998, 2965, 2910, 2868 (w, (ν-C–H)), 1637 (vs, ν(C=N)), 1602 (s), 1560 (m), 1524 (vs), 1483 (m), 1458 (vs), 1399 (s), 1378, 1364, 1343 (m), 1283 (s), 1256, 1237

(w), 1216 (s), 1190 (s), 1163 (s), 1122 (w), 1096 (m), 1063 (m), 1032, 1021 (m), 972, 962, 943, 925, 882, 874, 849 (w), 833 (m), 813 (w), 804 (m), 785 (vs), 744 (m), 707 (w).

Synthesis of 3/3'. A solution of **L**H_2 (0.473 g, 1.16 mmol) in pyridine (20 mL) was added to a suspension of AgCl (0.332 g, 2.32 mmol) in pyridine (20 mL) with stirring. After 24 h, the solvent was removed from the off-white reaction mixture using a trap-to-trap distillation and the isolated colorless crystalline solid was dried in oil pump vacuum for 24 h. Yield 0.335 g (0.25 mmol, 43% of solvent-free complex **3'**).[S6] Mp: 139–142 °C (decomposition into a grey solid). Anal. Calcd. for $C_{48}H_{72}N_{12}Ag_3Cl_3 \cdot 0.7AgCl$:[S6] C, 42.79; H, 5.39; N, 12.47; Cl, 9.74. Found: C, 43.26; H, 5.33; N, 12.28; Cl, 9.87. ^{1}H NMR (400.1 MHz, C_5H_5N): δ 1.42 (s, 18 H, CH_3, ^{t}Bu), 2.46 (s, 6 H, CH_3, 6-Py), 3.42 (s, 4 H, CH_2), 5.09 (broad s, 2 H, NH), 6.66–6.70 (m, 4 H, Py $H^{3,5}$), 7.43 (t, $^3J_{HH}$ = 7.7 Hz, 2 H, CH, Py H^4). $^{13}C\{^1H\}$ NMR (100.6 MHz, C_5H_5N): δ 25.2 (CH_3, 6-Py), 30.0 (CH_3, ^{t}Bu), 40.0 (C, ^{t}Bu), 44.0 (CH_2), 114.1 (broad s, CH, Py C^3), 115.5 (CH, Py C^5), 138.1 (CH, Py C^4), 156.7 (C, Py C^6), 163.9 (C, CN_2). The signal of Py C^2 is likely hidden or too broad to be detected. MS (ESI(+)): *m/z* (relative intensity): 515 (5) [**L**H_2Ag]$^+$, 409 (39) [**L**H_2 + H]$^+$, 205 (100) [**L**H_2 + 2 H]$^{2+}$. MS (MALDI(+)): m/z (relative intensity): 657 (5) [**L**$H_2Ag_2Cl]^+$, 515 (88) [**L**H_2Ag]$^+$, 409 (100) [**L**H_2 + H]$^+$. IR (neat, cm^{-1}): 3310, 3283 (w, ν(N–H)), 3060, 2959, 2940, 2908, 2869 (w, (ν-C–H)), 1638, 1622 (s, ν(C=N)), 1609 (m), 1590 (s), 1550, 1532 (vs), 1491 (w), 1482 (m), 1453, 1441 (vs), 1399 (m), 1367 (s), 1337, 1327, 1293 (m), 1273, 1258 (w), 1244, 1218, 1196, 1157 (m), 1103, 1086, 1067, 1034, 1002, 952, 903, 895, 879 (w), 851 (m), 832 (w), 813 (m), 788 (m), 779, 750 (m), 737 (w), 716, 697 (m), 663 (w).

Synthesis of 4. *Method A:* This method was previously described.[S3] *Method B:* A solution of 2-mesitylmagnesium bromide (1.16 mL, 1.16 mmol) was added dropwise to a solution of complex **2** (0.251 g, 0.287 mmol) in THF (100 mL) at –78 °C with stirring. After 30 min, the reaction mixture was allowed to warm to room temperature. Water (5 mL) was added and the mixture was extracted with CH_2Cl_2 (100 mL). The organic phase was separated and dried over anhydrous Na_2SO_4, followed by filtration and evaporation of all volatiles. The residue was washed with diethyl ether (10 mL) at room temperature and dried in oil pump vacuum for 24 h to yield a colorless, microcrystalline solid. Yield 0.239 g (0.230 mmol, 80%).

X-ray Crystallography. Single crystals of **1** were grown as colorless plates from a saturated THF solution at –35 °C. Suitable colorless plates of **2** were obtained as colorless plates from a THF solution that was layered with diethyl ether and stored at –35 °C. Single crystals of **3** were obtained as colorless blocks by allowing diethyl ether vapor to slowly diffuse into a pyridine solution at 4 °C. X-ray data for **2** were collected on a D8 goniostat equipped with a Bruker Photon 100 CMOS detector at Beamline 11.3.1 at the Advanced Light Source (Lawrence Berkeley National Laboratory) using synchrotron radiation tuned to λ = 0.7749 Å. For data collection, frames were measured for a duration of 1 s at 0.5° intervals of

ω at 100 K. X-ray data for **1** and **3** were collected on a Bruker D8 Venture diffractometer (CuKa radiation, λ = 1.54178 Å (**1**) or MoKa radiation, λ = 0.71073 Å (**3**) by using ω and φ scans at 100 K (**1**) or 140 K (**3**, Tables S1 and S2). The integrated intensities for each reflection were obtained by reduction of the data frames with the program APEX3.[S7] Cell parameters were obtained and refined with 64056 (5293 unique, **1**), 23380 (3420 unique, **2**), and 32126 (5853 unique, **3**) reflections, respectively. The integrated intensity information for each reflection was obtained by reduction of the data frames by using the SAINT algorithm of APEX3. The integrated data were corrected for absorption by using SADABS.[S8] The structures of **1** and **2** were solved by direct methods and refined (weighted least squares refinement on F^2) by using SHELXL-97.[S9] The structure of **3** was solved by intrinsic phasing (SHELXT) and refined on F^2 using SHELXL-2016. The hydrogen atoms were placed in idealized positions, and refined by using a riding model. For all structures **1**, **2**, and **3**, absence of additional symmetry and voids was confirmed using PLATON (ADDSYM).[S10] CCDC 2093837 (**1**), 2093838 (**2**), and 2101719 (**3**) contain the supplementary crystallographic data for this paper. These data can be obtained free of charge from The Cambridge Crystallographic Data Centre via www.ccdc.cam.ac.uk/data_request/cif.

Computational details. The crystal structures of [**L**H_2(CuCl)$_2$] (**1a**) and [**L**H_2(AuCl)$_2$] (**2a**) and the rationally derived structures **1b-d** and **2b-d** were fully geometry-optimized using TURBOMOLE v7.4.1.[S11] Density functional theory was used with the B3LYP functional.[S12] together with the RIDFT module,[S13] dispersion correction[S14] and the def2-TZVP basis set.[S15] No symmetry constraints were imposed on any structures during optimization. The energetic minimum of the calculated structures was confirmed by vibration analyses performed analytically (aoforce).[S16]

Thermochemical corrections were calculated with the Gaussian16 program package (revision A.03).[S17] applying the BP86 functional[S18] and dispersion correction[S14] (for **1a-d** without dispersion correction) with def2-SVP[S19] basis sets on all elements.

Quantum Theory of Atoms in Molecules (QTAIM)[S20] analyses for **1a** and **2a** were carried out with AIMAll[S21] on wave function files obtained from Gaussian16 (revision A.03).[S17] For these wave function files we used the B3LYP functional[S12] together with dispersion correction[S22] and the 6-311G(d)[S23] basis set on all atoms except for gold and copper. For gold we used the effective core potential, ECP60MDF, for copper the effective core potential, ECP10MDF, with the corresponding triple-ζ quality basis set cc-pVTZ-PP.[S24] Electrostatic potential maps (ESP) were created on that level of theory with GaussView 6.0.16.[S25]

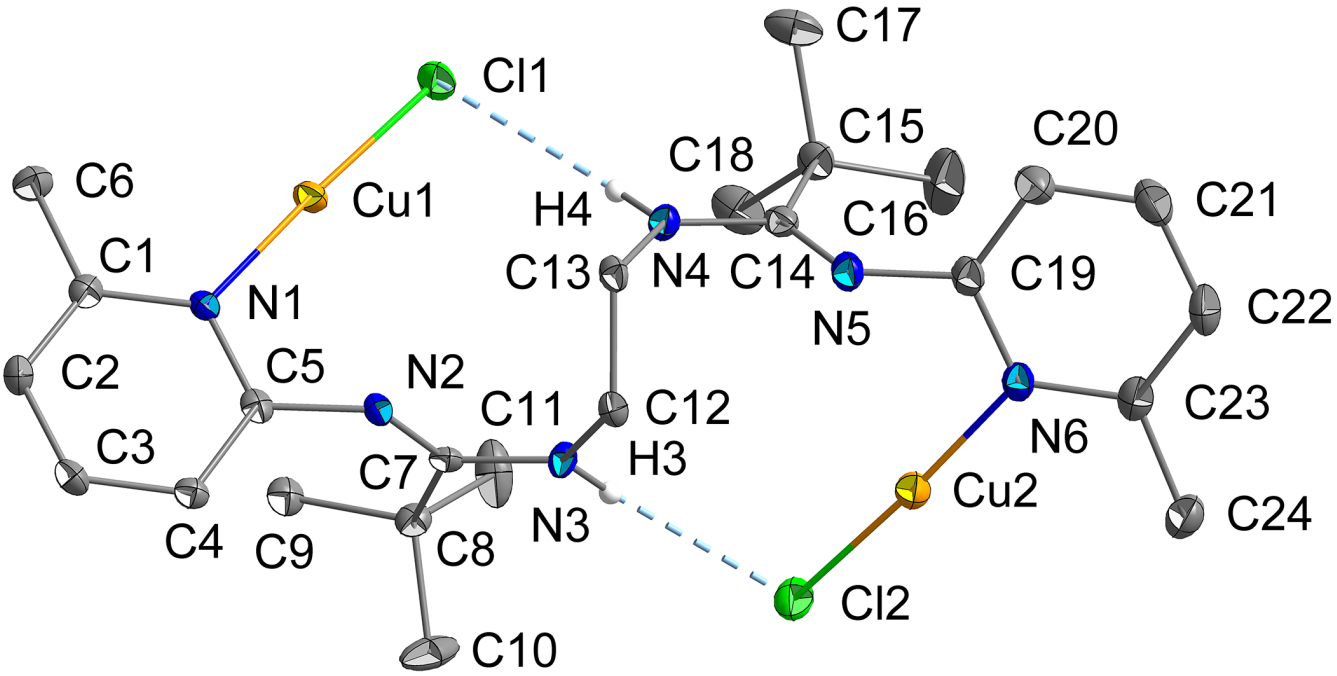

Figure S1: Molecular structure of **1** showing ellipsoids with anisotropic displacement factors of 50% probability. Hydrogen atoms except for NH functionalities and hydrogen bonds have been omitted for clarity. H3 and H4 are represented in standard ball and stick mode. Selected interatomic distances (Å), bond angles (deg), and torsion angles (deg): Cu1–Cl1 2.0961(6), Cu2–Cl2 2.1001(6), Cu1–N1 1.8934(16), Cu2–N6 1.8932(17), C12–C13 1.533(3), N3–C12 1.451(2), N3–C7 1.347(2), N2–C7 1.294(2), N2–C5 1.376(2), N1–C5 1.359(3), N1–C1 1.363(2), N4–C13 1.450(2), N4–C14 1.348(3), N5–C14 1.289(3), N5–C19 1.371(3), N6–C19 1.363(3), N6–C23 1.359(3), N1–Cu1–Cl1 175.87(5), N6–Cu2–Cl2 174.37(6), Cu1–N1–C1 126.22(13), Cu1–N1–C5 114.02(13), Cu2–N6–C23 126.23(15), Cu2–N6–C19 113.80(13), N3–C12–C13 113.58(16), C7–N3–C12 123.56(16), N2–C7–N3 116.91(17), C5–N2–C7 129.28(17), N1–C5–N2 116.70(17), C1–N1–C5 119.76(17), N4–C13–C12 113.55(16), C14–N4–C13 122.87(17), N5–C14–N4 116.47(18), C19–N5–C14 130.66(19), N6–C19–N5 115.63(19), C23–N6–C19 119.86(18), Cu1–N1–C1–C6 –4.5(2), Cu1–N1–C5–N2 –6.8(2), Cu2–N6–C23–C24 3.3(3), Cu2–N6–C19–N5 –10.1(2), N3–C12–C13–N4 51.1(2), C7–N3–C12–C13 73.2(2), N1–C5–N2–C7 100.1(2), C14–N4–C13–C12 74.4(2), N6–C19–N5–C14 106.6(3).

Hydrogen bonds (Å) and associated angles (deg): N3···Cl2 3.3583(17), N4···Cl1 3.3449(17), H3··· Cl2 2.53, H4···Cl1 2.52, N3–H3···Cl2 156.6, N4–H4···Cl1 156.1.

Symmetry operation used to generate equivalent atoms of the depicted enantiomer: $-x + 1, -y + 1, -z + 1$.

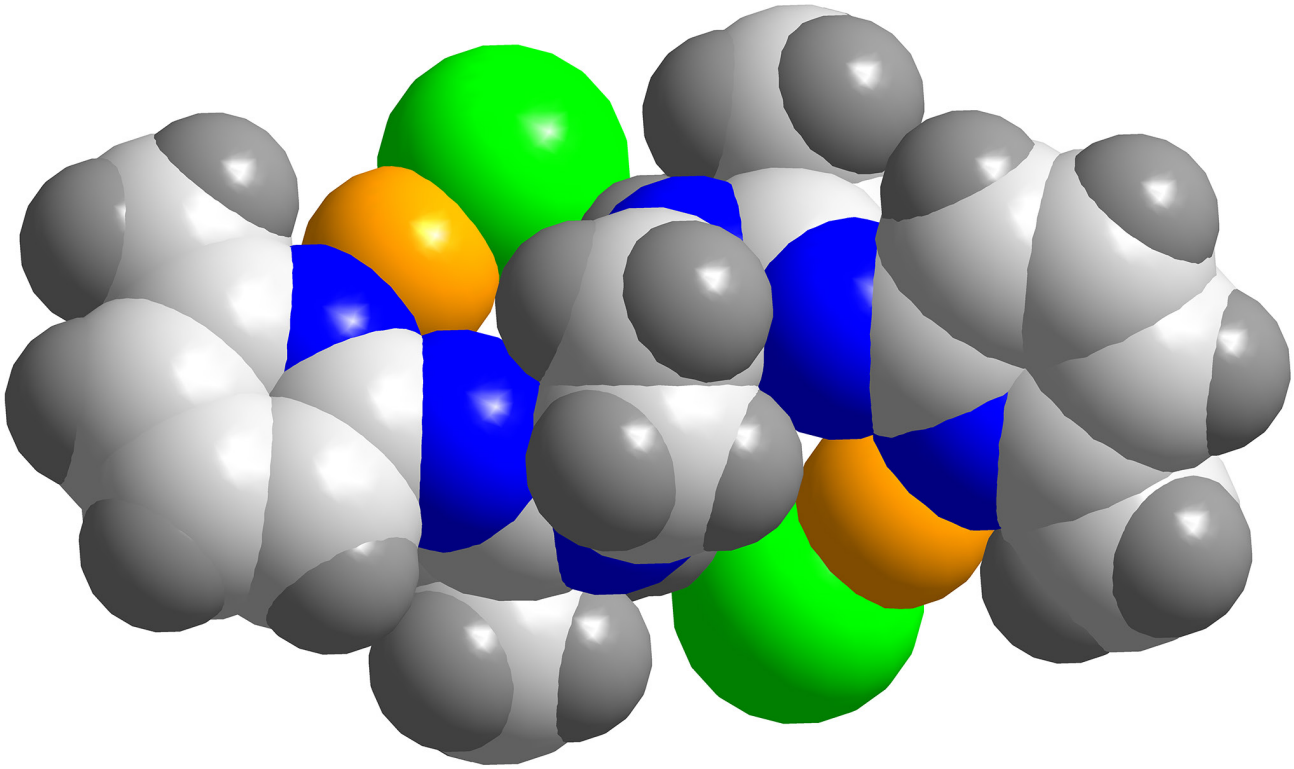

Figure S2: Space filling representation of the molecular structure of **1**.

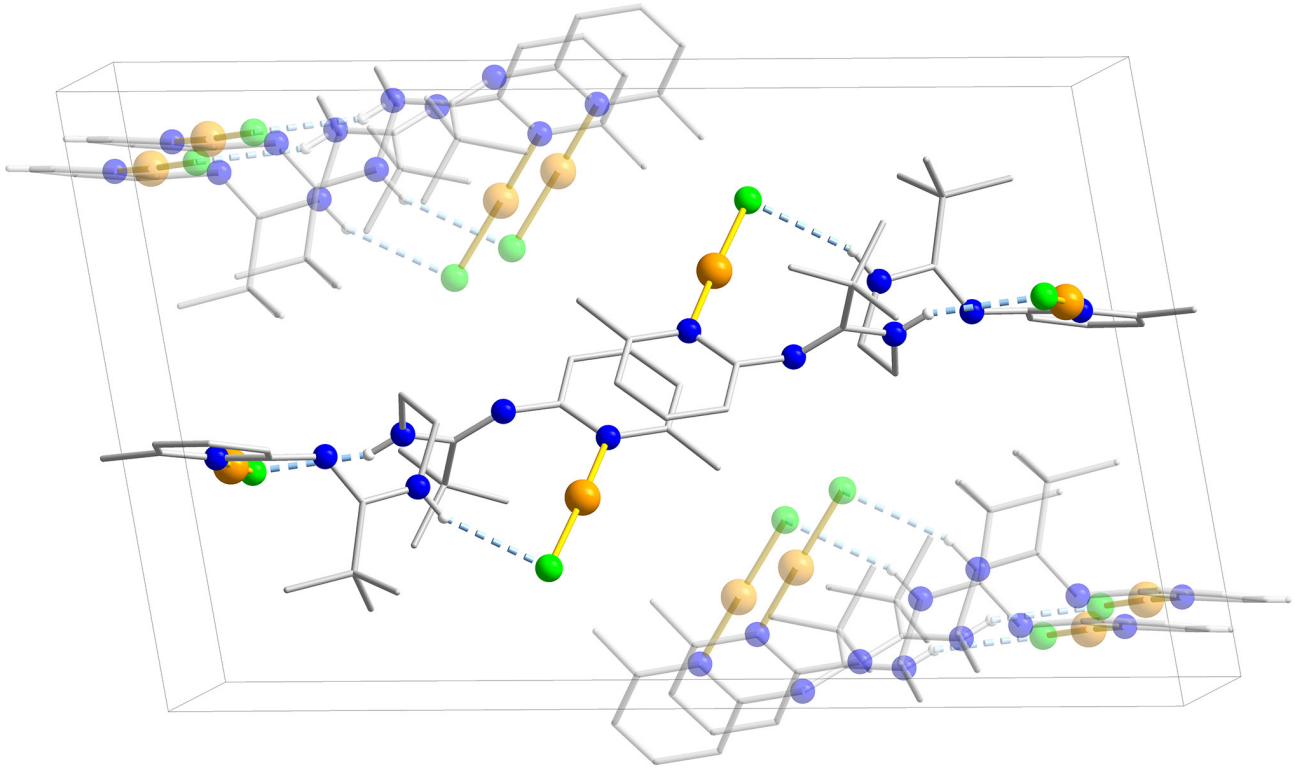

Figure S3: Crystal packing diagram and unit cell of **1**. Hydrogen atoms except for NH functionalities and hydrogen bonds have been omitted for clarity.

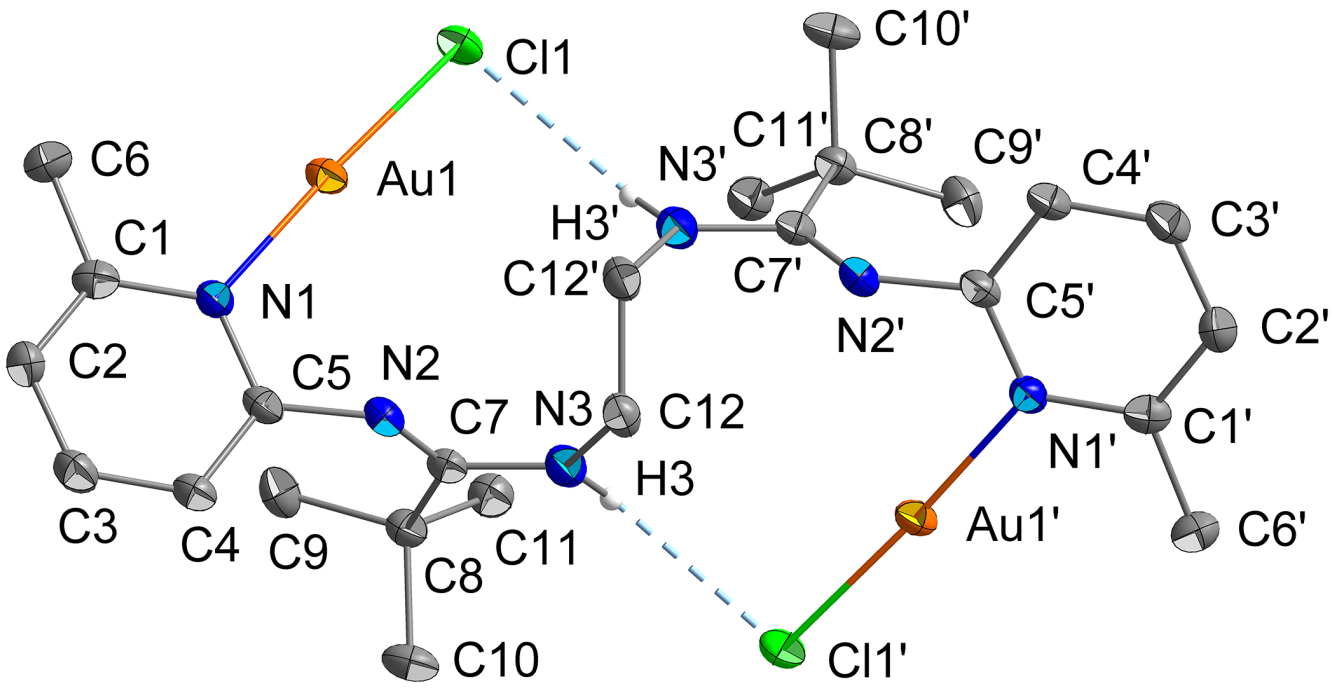

Figure S4: Molecular structure of **2** showing ellipsoids with anisotropic displacement factors of 50% probability. Hydrogen atoms except for NH functionalities and hydrogen bonds have been omitted for clarity. H3 and H3' are represented in standard ball and stick mode. Selected interatomic distances (Å), bond angles (deg), and torsion angles (deg): Au1–Cl1 2.2573(11), Au1–N1 2.028(4), C12–C12' 1.534(9), N3–C12 1.452(6), N3–C7 1.349(6), N2–C7 1.286(6), N2–C5 1.370(6), N1–C5 1.359(6), N1–C1 1.372(6), N1–Au1–C11 176.66(12), Au1–N1–C1 123.5(3), Au1–N1–C5 117.0(3), N3–C12–C12' 113.2(3), C7–N3–C12 123.3(4), N2–C7–N3 116.1(4), C5–N2–C7 130.2(4), N1–C5–N2 117.4(4), C1–N1–C5 119.5(4), Au1–N1–C1–C6 2.0(6), Au1–N1–C5–N2 4.6(5), N3–C12–C12'–N3' –55.9(5),[S26] C7–N3–C12–C12' –73.7(6), N1–C5–N2–C7 –99.5(6).

Hydrogen bonds (Å) and associated angles (deg):[S26] N3···Cl1' 3.389(4), H3··· Cl1' 2.614(1), N3–H3···Cl1' 147.4(3).

Symmetry operation used to generate equivalent atoms in the crystal packing (') $-x+1, y, -z+3/2$.

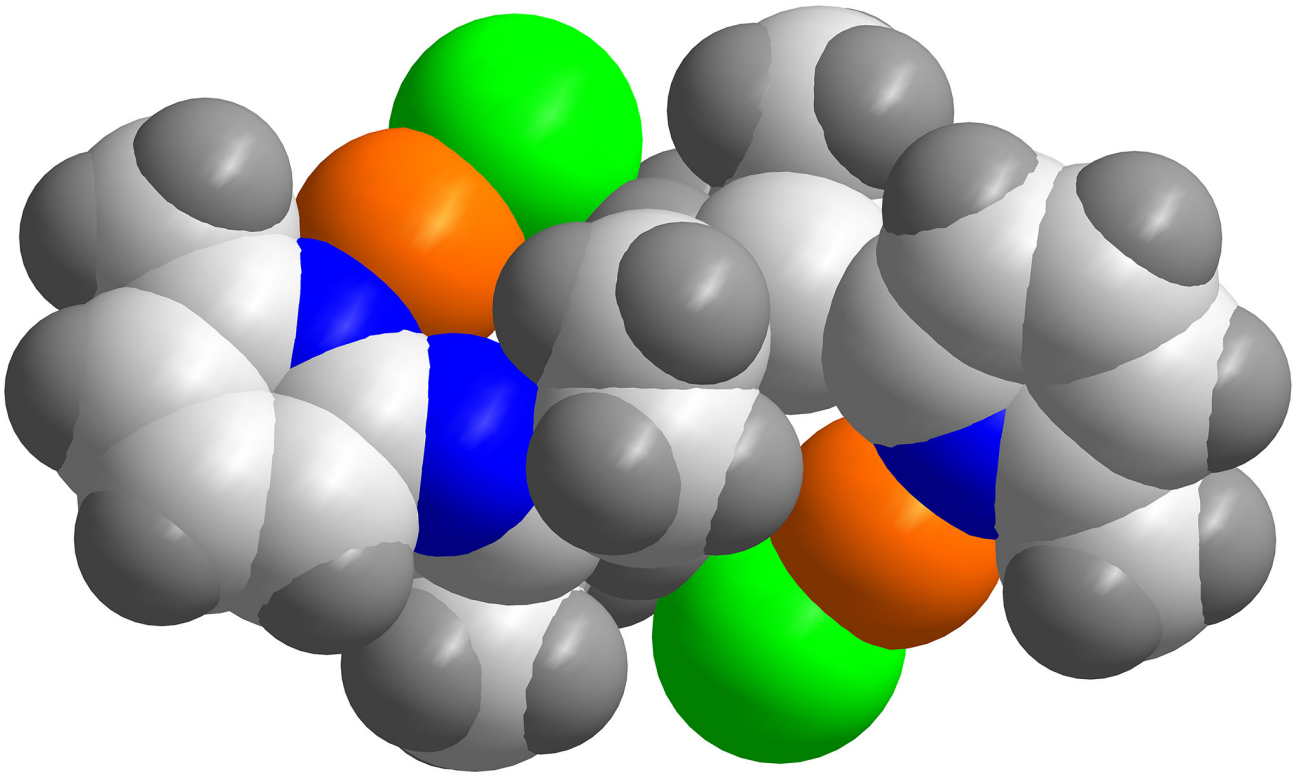

Figure S5: Space filling representation of the molecular structure of **2**.

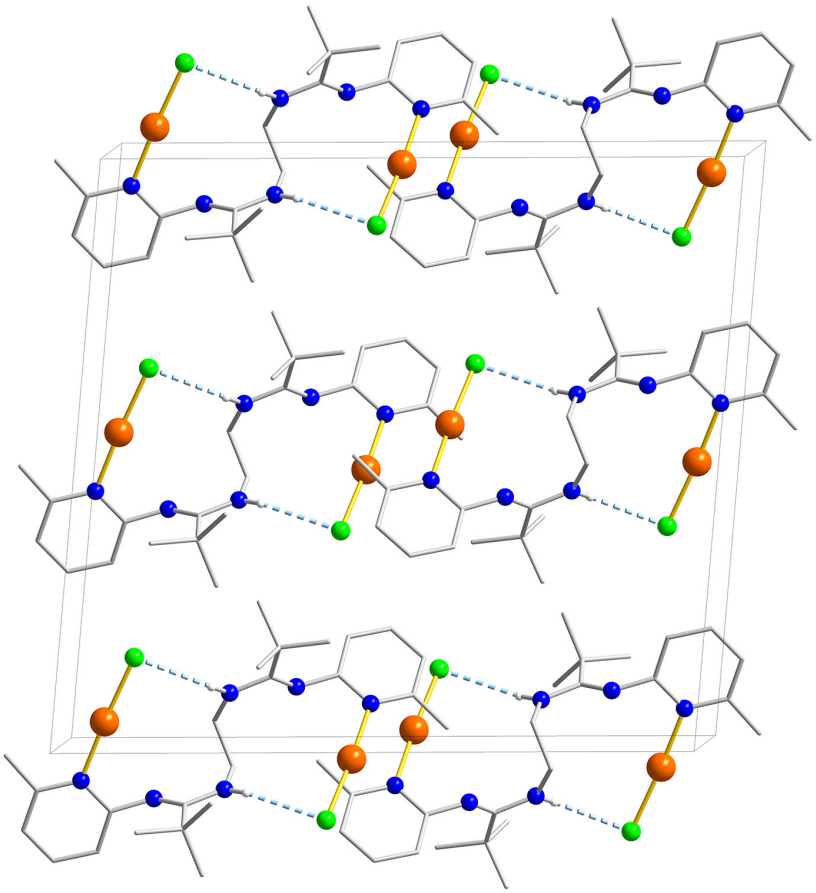

Figure S6: Crystal packing diagram and unit cell of **2**. Hydrogen atoms except for NH functionalities and hydrogen bonds have been omitted for clarity.

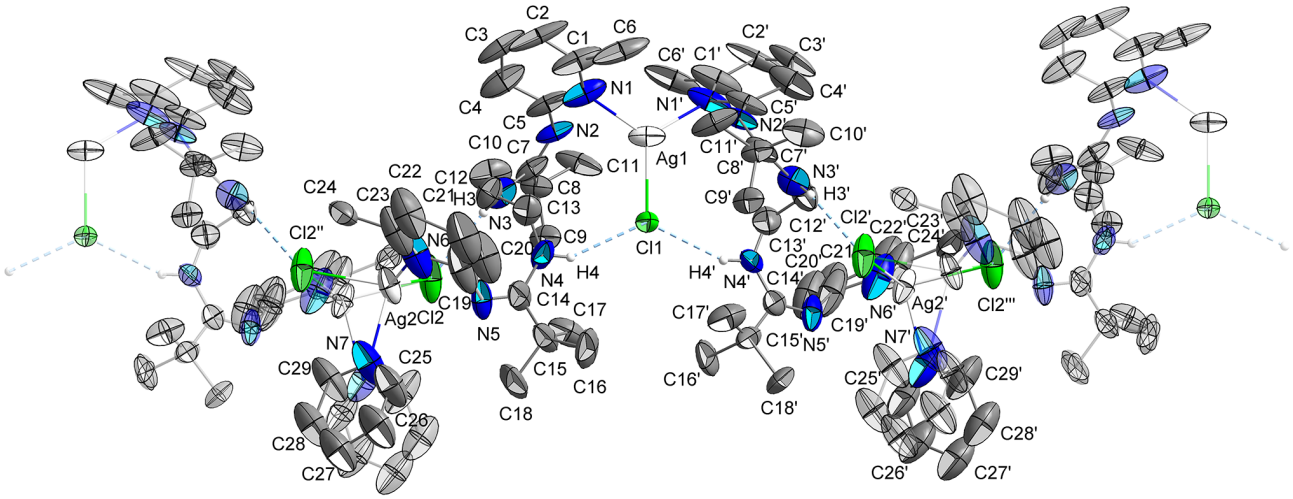

Figure S7: Molecular structure of **3** showing ellipsoids with anisotropic displacement factors of 50% probability. Solvent molecules and hydrogen atoms except for NH functionalities and hydrogen bonds have been omitted for clarity. These hydrogen atoms are represented in standard ball and stick mode.

Selected interatomic distances (Å), bond angles (deg), and torsion angles (deg): Ag1–Cl1 2.494(6), Ag1–N1 2.259(17), Ag2–Cl2 2.570(5), Ag2–Cl2" 2.662(5), Ag2–N6 2.27(2), Ag2–N7 2.39(3), C12–C13 1.47(3), N3–C12 1.44(2), N3–C7 1.38(3), N2–C7 1.28(3), N2–C5 1.36(2), N1–C5 1.35(3), N1–C1 1.36(2), N4–C13 1.37(3), N4–C14 1.38(2), N5–C14 1.25(3), N5–C19 1.38(4), N6–C19 1.43(4), N6–C23 1.32(4), N1–Ag1–C11 120.6(5), N1–Ag1–N1' 118.7(10), Ag1–N1–C1 131.7(18), Ag1–N1–C5 111.6(11), N6–Ag2–Cl2 125.0(5), N6–Ag2–Cl2" 118.4(7), N6–Ag2–N7 103.9(9), N7–Ag2–Cl2 114.3(7), N7–Ag2–Cl2" 89.1(7), Cl2–Ag2–Cl2" 100.69(17), Ag2–N6–C23 135.1(17), Ag2–N6–C19 108.7(18), N3–C12–C13 113.1(16), C7–N3–C12 132.8(19), N2–C7–N3 127.2(15), C5–N2–C7 128.5(19), N1–C5–N2 117.3(18), C1–N1–C5 117(2), N4–C13–C12 118(2), C14–N4–C13 127.9(17), N5–C14–N4 126(2), C19–N5–C14 127(2), N6–C19–N5 118.4(19), C23–N6–C19 116(2), Cl1–Ag1–N1–C1 110(2),[S26] Cl1–Ag1–N1–C5 –66(2),[S26] Ag1–N1–C1–C6 3(3),[S26] Ag1–N1–C5–N2 –10(2),[S26] Cl2–Ag2–N6–C23 136(3),[S26] Cl2–Ag2–N6–C19 –53(2),[S26] Cl2"–Ag2–N6–C23 7(3),[S26] Cl2"–Ag2–N6–C19 177(2),[S26] N7–Ag2–N6–C23 –90(3),[S26] N7–Ag2–N6–C19 81(2),[S26] Ag2–N6–C23–C24 –14(4),[S26] Ag2–N6–C19–N5 –4(3),[S26] N3–C12–C13–N4 –60(3),[S26] C7–N3–C12–C13 66(3),[S26] N1–C5–N2–C7 131(2),[S26] C14–N4–C13–C12 –69(3),[S26] N6–C19–N5–C14 128(3).[S26]

Hydrogen bonds (Å) and associated angles (deg):[S26] N3···Cl2 3.24(2), N4···Cl1 3.247(16), H3··· Cl2 2.44, H4··· Cl1 2.46, N3–H3···Cl2 151.3, N4–H4···Cl1 148.6.

Symmetry operation used to generate equivalent atoms in the crystal packing (') $-x, y, -z$; (") $-x, y, -z + 1$; ("') $x, y, z - 1$.

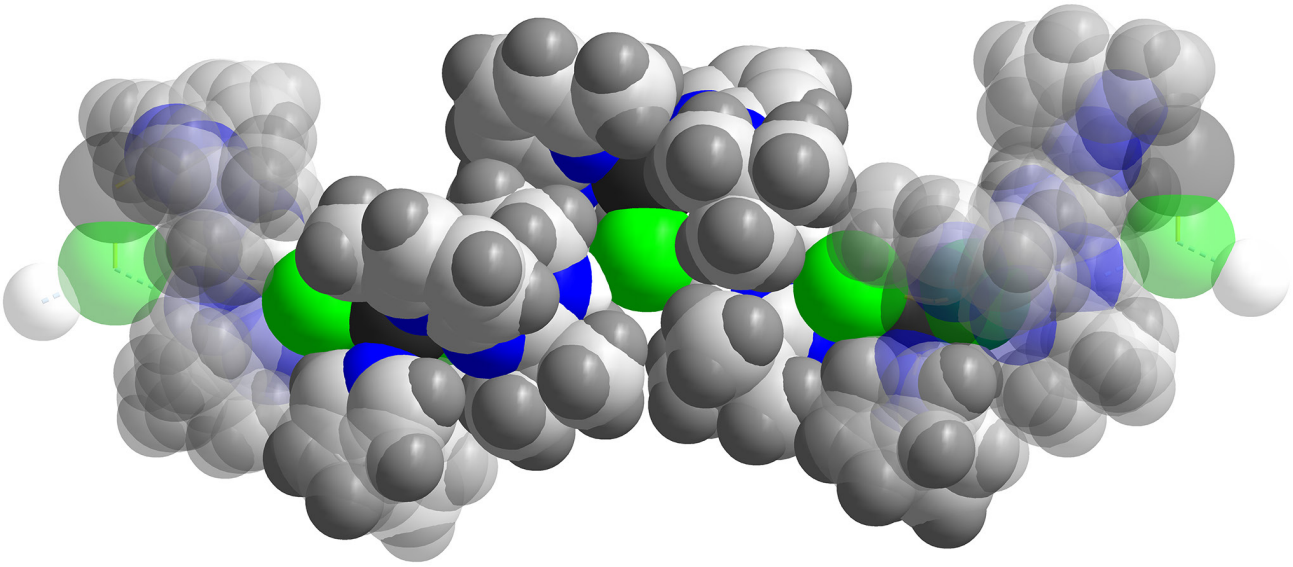

Figure S8: Space filling representation of the molecular structure of **3**. Solvent molecules have been omitted for clarity.

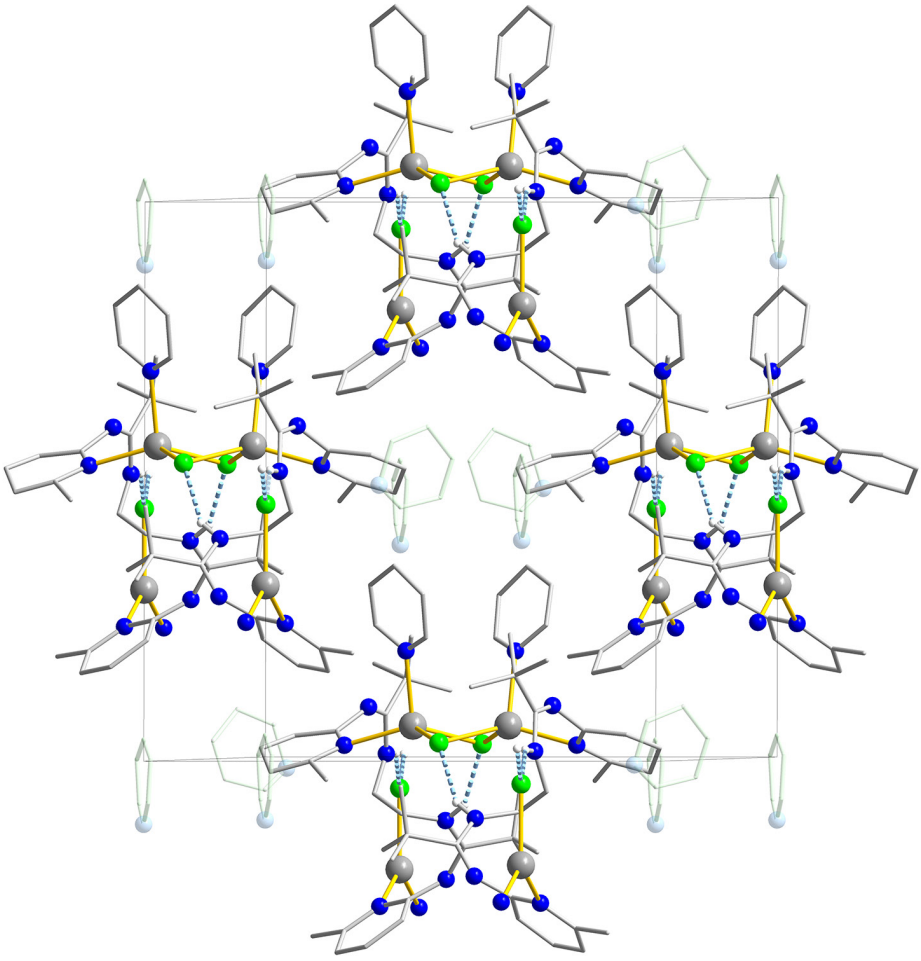

Figure S9: Crystal packing diagram and unit cell of **3**. Hydrogen atoms except for NH functionalities and hydrogen bonds have been omitted for clarity.

Table S1: Crystal data and refinement details for **1**–**3**.

	1	**2**	**3**
Empirical formula	$C_{24}H_{36}N_6Cu_2Cl_2$	$C_{24}H_{36}N_6Au_2Cl_2$	$C_{73}H_{97}N_{17}Ag_3Cl_3$
M_r	606.57	873.42	1642.63
Crystal size [mm]	0.234 × 0.076 × 0.027	0.04 × 0.03 × 0.01	0.056 × 0.071 × 0.072
Crystal system	monoclinic	monoclinic	monoclinic
Space group	*P* 1 2_1/*c* 1	*C* 1 2/*c* 1	*C* 1 2 1
a [Å], α [°]	21.9310(5), 90	18.294(2), 90	16.2306(17), 90
b [Å], β [°]	9.5330(2), 99.5570(10)	7.6496(8), 95.371(5)	17.1928(17), 117.364(3)
c [Å], γ [°]	13.5026(3), 90	19.769(2), 90	16.4118(16), 90
V [Å^3]	2783.78(11)	2754.4(5)	4067.3(7)
Z	4	4	2
$\rho_{calcd.}$ [g cm^{-3}]	1.447	2.106	1.341
F(000)	1256	1656	1692
μ [mm^{-1}]	3.828	13.074	0.863
T_{max}/T_{min}	0.7533 / 0.6182	0.4248 / 0.2997	0.9530 / 0.9400
hkl range	±26, –9 +11, ±16	±24, ±10, ±26	±18, ±19, ±18
θ range [°]	4.088 – 70.161	3.149 – 31.303	2.51 – 23.32
Measured refl.	64056	23380	32126
Unique refl. [R_{int}]	5293 [0.0509]	3420 [0.0661]	5853 [0.0757]
Data / restr. / param.	5293 / 0 / 315	3420 / 0 / 158	5853 / 73 / 437
Goodness-of-fit	1.076	1.054	1.049
*R*1 (I>2σ(I))	0.0289	0.0294	0.0768
*wR*2 (all data)	0.0702	0.0830	0.2144
Resid. electron dens. [e Å^{-3}]	0.395 / –0.306	3.328 / –1.150	1.519 / –0.854

Table S2: Key crystallographic bond distances and angles of **L**H_2 and **1**–**4**.

	LH_2[S2]	**1**	**2**	**3**	**4**[S3]
	bond/angle [Å]/[°]				
M–X*	-	2.0961(6) 2.1001(6)	2.2573(11)	2.494(6) 2.570(5) 2.662(5)	2.010(3) 2.014(3)
M–N	-	1.8934(16) 1.8932(17)	2.028(4)	2.259(17) 2.27(2) 2.39(3)	2.102(2) 2.111(2)
CH_2–CH_2	1.5469(15)	1.533(3)	1.534(9)	1.47(3)	1.518(4)
CH_2–NH	1.4477(14) 1.4521(14)	1.451(2) 1.450(2)	1.452(6)	1.44(2) 1.37(3)	1.446(4) 1.444(4)
$C_{amidine}$–N	1.3466(14) 1.3558(15)	1.347(2) 1.348(3)	1.349(6)	1.38(3) 1.38(2)	1.350(3) 1.354(3)
$C_{amidine}$=N	1.2910(15) 1.2866(15)	1.294(2) 1.289(3)	1.286(6)	1.28(3) 1.25(3)	1.289(4) 1.290(3)
N–M–X*	-	175.87(5) 174.37(6)	176.66(12)	120.6(5) 125.0(5) 118.4(7) 114.3(7) 89.1(7)	177.4(1) 173.35(10)
N_{Ar}–C–$N_{amidine}$	120.30(10) 119.00(10)	116.70(17) 115.63(19)	117.4(4)	127(2) 128.5(19)	117.1(2) 118.6(2)
N=C–NH	129.40(10) 128.85(10)	116.70(17) 116.47(18)	116.1(4)	127.2(15) 126(2)	117.0(2) 116.4(2)
$C_{Py\text{-}2}$–N=$C_{amidine}$	130.38(10) 128.50(10)	129.28(17) 130.66(19)	130.2(4)	128.5(19) 127(2)	128.6(2) 127.5(2)
N–CH_2–CH_2–N	28.8(1)[S26]	51.1(2)[S26]	–55.9(5)[S26]	–60(3)[S26]	56.4(3)

*) X = Cl (**1**–**3**), X = C (**4**)

Table S3. Δ_{CN} parameter[S27],[S28] of **L**H_2, **1**, **2**, and **4**.

LH_2[S2]	**1**	**2**	**4**[S3]
d(C–N) – d(C=N) [Å]			
0.0556 / 0.0692	0.053 / 0.059	0.063	0.061 / 0.064

Table S4. N–H IR stretching modes of {$CH_2NH(^tBu)C{=}N{-}Mes\}_2$, **L**$H_2$, and **1**–**4** (neat).

	{$CH_2NH(^tBu)C{=}N{-}Mes\}_2$[S29]	**L**H_2[S2]	**1**	**2**	**3**	**4**[S3]
	$\tilde{\nu}$ [cm^{-1}]					
ν(N–H)	3447	3308	3378	3391	3310, 3283	3413

Table S5. Experimental (**1** and **2**) and calculated (**1a** and **2a**) N–H stretching modes of **1** and **2**.

	exp.		calc.	
			(Gaussian BP-86/def2-SVP)	(Gaussian DFT-D3/BP-86/def2-SVP)
	1	**2**	**1a**	**2a**
	$\tilde{\nu}$ [cm^{-1}]			
ν(N–H)	3378	3391	3277.73, 3280.58	3320.72, 3323.02
ν(C=N)	1627	1637	1681.59, 1686.77	1691.12, 1696.02

Table S6. Calculated (Gaussian BP-86/def2-SVP) N–H and C=N IR stretching modes of **1a**, the intermediate of the conformational ring inversion (**1b**), and alternative isomers without hydrogen bonds (**1c** and **1d**).

	1a	**1b**	**1c**	**1d**
	$\tilde{\nu}$ [cm^{-1}]			
ν(N–H)	3277.73, 3280.58	3272.73, 3278.16	3553.67, 3553.94	3551.25, 3551.38
ν(C=N)	1681.59, 1686.77	1645.13, 1653.28	1652.34, 1660.69	1656.26, 1665.45

Table S7. Calculated (Gaussian DFT-D3/BP-86/def2-SVP) N–H and C=N IR stretching modes of **2a**, the intermediate of the conformational ring inversion (**2b**), and alternative isomers without hydrogen bonds (**2c** and **2d**).

	2a	**2b**	**2c**	**2d**
	$\tilde{\nu}$ [cm^{-1}]			
ν(N–H)	3320.72, 3323.02	3280.32, 3285.70	3553.51, 3553.56	3552.03, 3552.18
ν(C=N)	1691.12, 1696.02	1675.37, 1682.29	1650.75, 1660.54	1657.34, 1666.64

Table S8: Selected ^{1}H NMR shifts of {CH$_2$NH(^{t}Bu)C=N–Mes}$_2$ and **L**H$_2$.

	{CH$_2$NH(^{t}Bu)C=N–Mes}$_2$[S29]	**L**H$_2$[S2]
	δ (CDCl$_3$) [ppm] δ (C$_6$D$_6$) [ppm]	
NH	4.05	5.57
	3.91	≈ 6.60
^{t}Bu–CN$_2$	1.20	1.18
	1.12	1.25
CH$_3$ (6-Py)	-	2.40
	-	2.36
CH$_2$	2.45	3.09
	2.42	3.07–3.10
Py H^3 (d)	-	6.44 ($^3J_{HH}$ = 7.3 Hz)
	-	6.69 ($^3J_{HH}$ = 8.0 Hz)
PyH^4 (t)	-	7.33 ($^3J_{HH}$ = 7.7 Hz)
	-	7.10 ($^3J_{HH}$ = 7.7 Hz)
PyH^5 (d)	-	6.60 ($^3J_{HH}$ = 7.3 Hz)
	-	6.39 ($^3J_{HH}$ = 7.3 Hz)

Table S9: Selected ^{1}H NMR shifts of **1**, **2**, **3'**, and **4**.

	1	**2**	**3'**	**4**[S3]
		δ ($CDCl_3$) [ppm] δ (C_6D_6) [ppm]		
NH	6.64	6.43	5.09*	4.95
	7.45	≈ 7.15**		5.26
^{t}Bu–CN_2	1.25	1.26	1.42*	0.82
	1.31	1.32		0.90
CH_3 (6-Py)	2.58	2.67	2.46*	2.72
	1.97	2.09		2.44
CH_2	3.65	3.78	3.42*	≈ 3.75 (broad)
	4.02	≈ 3.65, 4.66		≈ 3.60, 4.73 (broad)
Py H^3 (d)	6.56 ($^3J_{HH}$ = 8.1 Hz)	6.68 ($^3J_{HH}$ = 8.2 Hz)	6.66–6.70*,***	6.58 ($^3J_{HH}$ = 8.1 Hz)
	6.21 ($^3J_{HH}$ = 8.1 Hz)	6.26 ($^3J_{HH}$ = 8.2 Hz)		6.19 ($^3J_{HH}$ = 8.1 Hz)
PyH^4 (t)	7.46 ($^3J_{HH}$ = 7.8 Hz)	7.49 ($^3J_{HH}$ = 7.8 Hz)	7.43* ($^3J_{HH}$ = 7.7 Hz)	7.44 ($^3J_{HH}$ = 7.8 Hz)
	6.71 ($^3J_{HH}$ = 7.8 Hz)	6.65 ($^3J_{HH}$ = 7.8 Hz)		6.75 ($^3J_{HH}$ = 7.8 Hz)
PyH^5 (d)	6.68 ($^3J_{HH}$ = 7.4 Hz)	6.75 ($^3J_{HH}$ = 7.3 Hz)	6.66–6.70*,***	6.71 ($^3J_{HH}$ = 7.3 Hz)
	5.91 ($^3J_{HH}$ = 7.3 Hz)	5.90 ($^3J_{HH}$ = 7.4 Hz)		6.07 ($^3J_{HH}$ = 7.3 Hz)

*) C_5D_5N, **) overlaid by residual benzene signal, ***) multiplet

Table S10: Selected $^{13}C\{^{1}H\}$ NMR shifts of $\{CH_2NH(^tBu)C{=}N{-}Mes\}_2$ and $\mathbf{L}H_2$.

	$\{CH_2NH(^tBu)C{=}N{-}Mes\}_2$[S29]	$\mathbf{L}H_2$[S2]
		δ ($CDCl_3$) [ppm] δ (C_6D_6) [ppm]
$C(\underline{\boldsymbol{C}}H_3)_3$	29.1	29.3
	29.1	29.5
$\underline{\boldsymbol{C}}(CH_3)_3$	38.5	39.1
	38.7	39.2
CH_3 (6-Py)	-	24.4
	-	24.4
CH_2	43.0	43.5
	43.4	43.5
C (Py C^2)	-	162.7
		163.5
CH (Py C^3)	-	113.4
	-	114.7
CH (Py C^4)	-	136.9
	-	137.0
CH (Py C^5)	-	115.3
		115.0
C (Py C^6)	-	156.5
	-	156.1
CN_2	158.4	162.7
	158.0	163.2

Table S11: Selected $^{13}C\{^{1}H\}$ NMR shifts of **1**, **2**, **3'**, and **4**.

	1	**2**	**3'**	**4**[S3]
			δ ($CDCl_3$) [ppm] δ (C_6D_6) [ppm]	
$C(\underline{\boldsymbol{C}}H_3)_3$	30.4	30.2	30.0*	29.2
	30.5	30.3		29.5
$\underline{\boldsymbol{C}}(CH_3)_3$	41.0	41.3	40.0*	39.8
	41.2	41.6		40.1
CH_3 (6-Py)	25.8	26.5	25.2*	25.0
	25.1	25.8		24.8
CH_2	38.9	39.4	44.2*	39.9
	39.2	39.8		40.1
C (Py C^2)	163.9	163.4	-**	162.9
	164.3	163.7		163.4
CH (Py C^3)	114.5	115.3	114.1*	115.1
	114.4	115.1		115.0
CH (Py C^4)	139.3	139.3	138.1*	138.6
	138.9	138.7		138.5
CH (Py C^5)	115.2	115.4	115.5*	116.0
	114.6	114.9		115.6
C (Py C^6)	155.7	155.8	156.7*	156.7
	155.8	155.8		156.7
CN_2	163.1	162.6	163.9*	161.4
	163.1	162.8		161.2

*) C_5D_5N, **) too broad to be detected or likely hidden by another signal

Table S12: T_c and activation barrier $\Delta G^{\ddagger}_c$ of the conformational ring inversion for **1**, **2**, and **4**.

	1	**2**	**4**[S3]
		[°C]	
		[kcal·mol^{-1}]	
$CDCl_3$	–29.2	9.9	16.5
	11.1	12.9	13.0
C_6D_6	–10.0*	27.2	36.0
	11.9*	13.5	13.8

*) C_7D_8

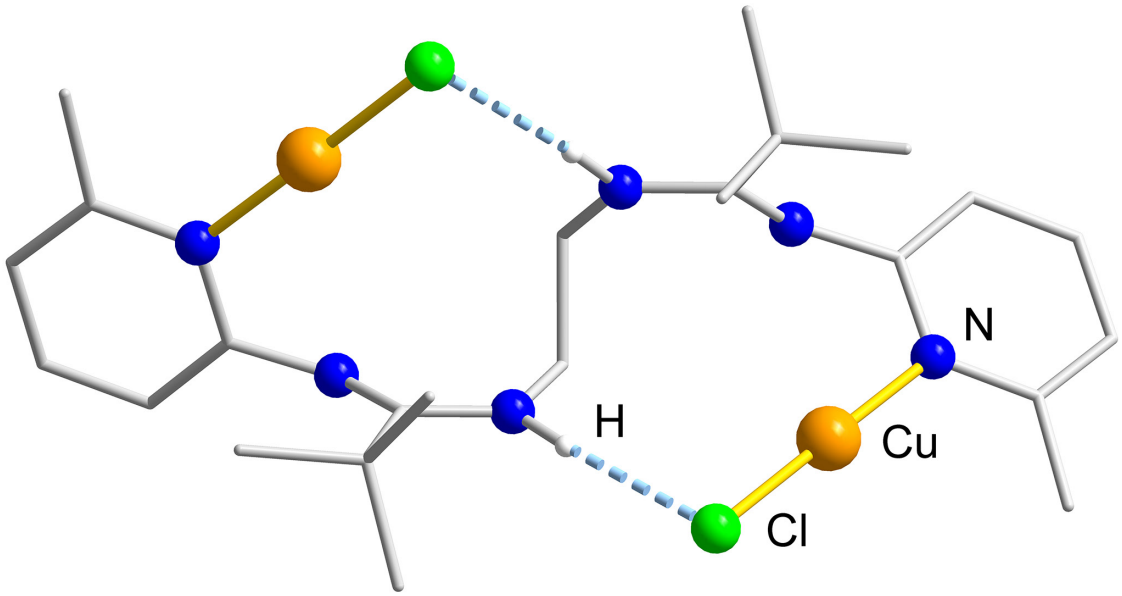

Figure S10: Computational structure of **1a** (RIDFT-D3/B3LYP/def2-TZVP).

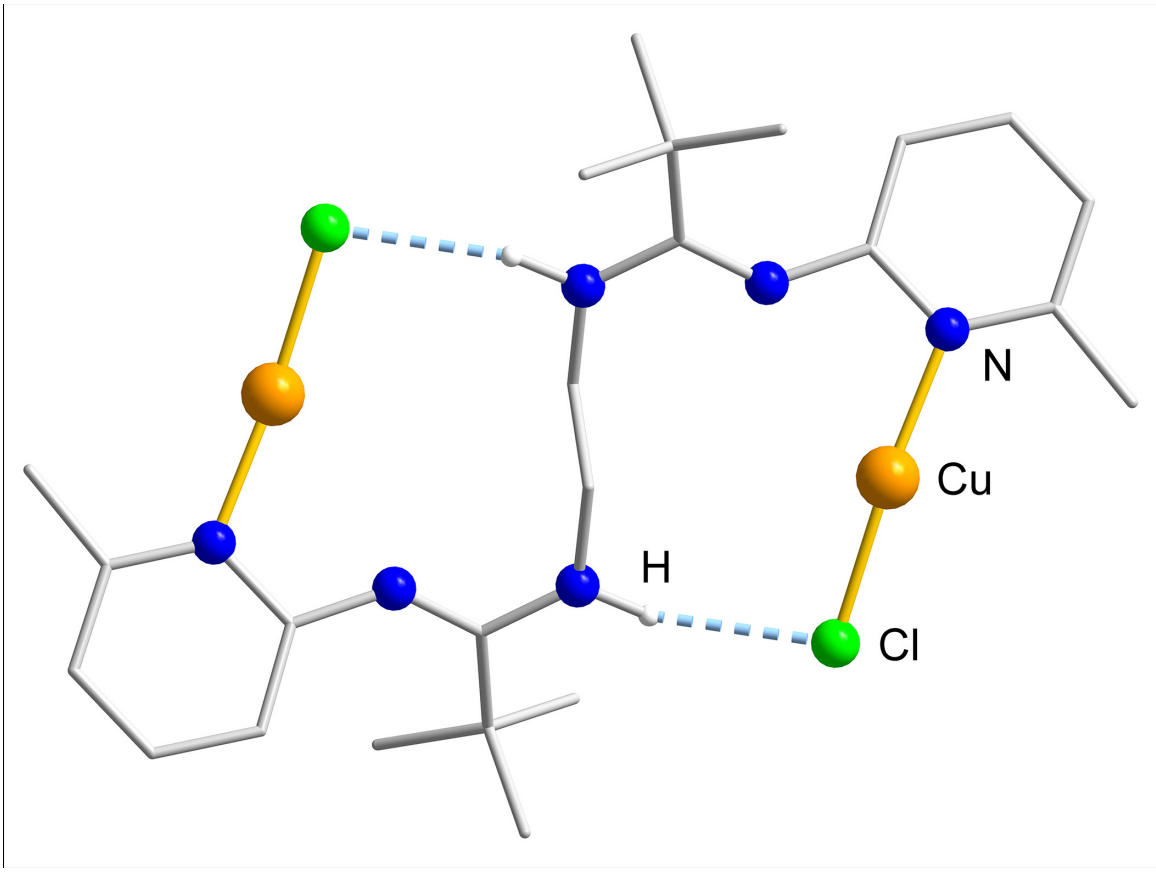

Figure S11: Computational structure of **1b** (RIDFT-D3/B3LYP/def2-TZVP).

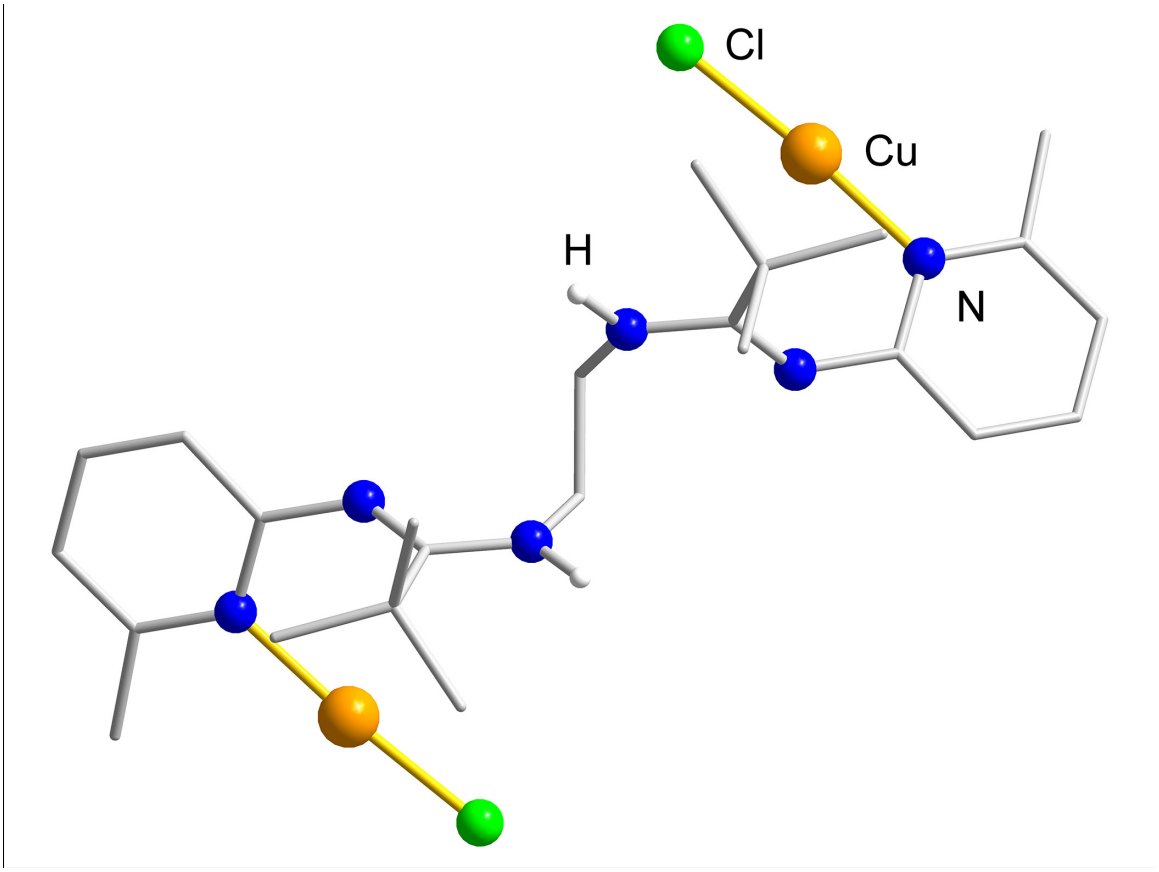

Figure S12: Computational structure of **1c** (RIDFT-D3/B3LYP/def2-TZVP).

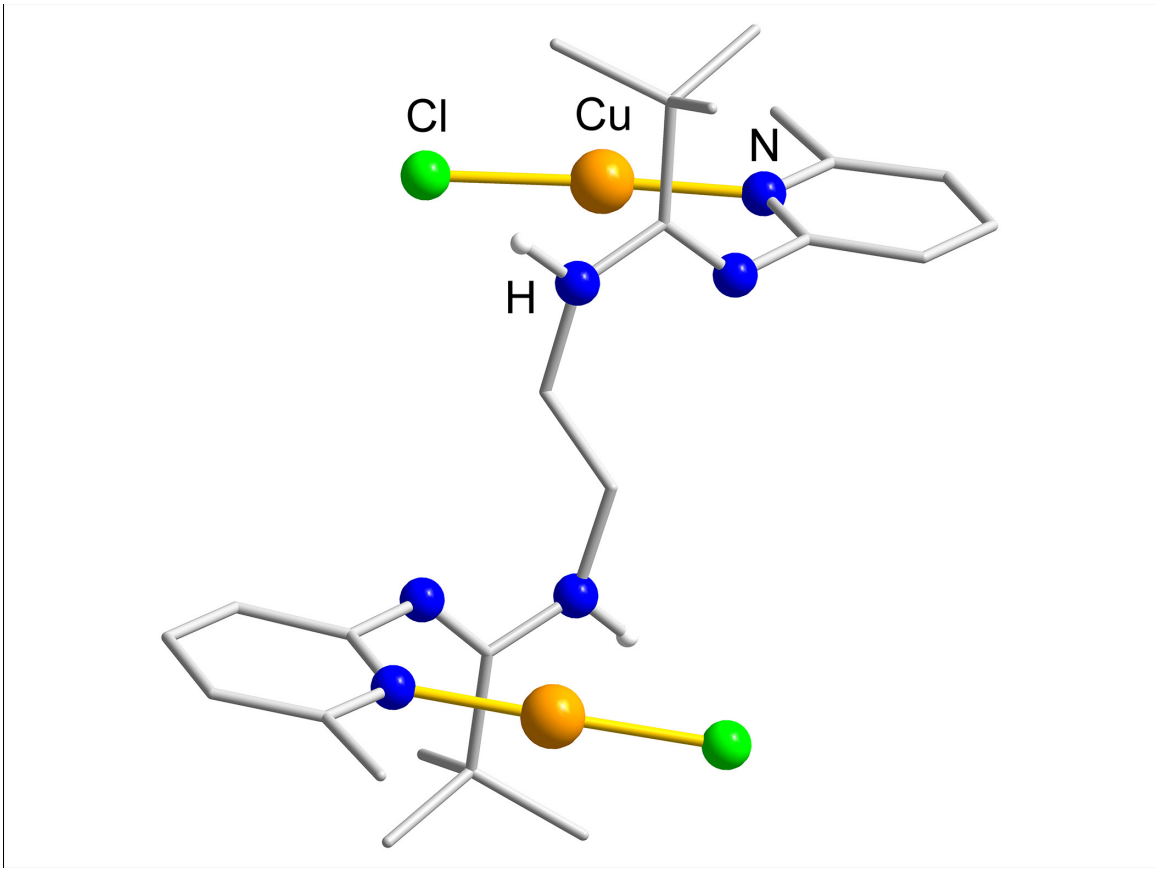

Figure S13: Computational structure of **1d** (RIDFT-D3/B3LYP/def2-TZVP).

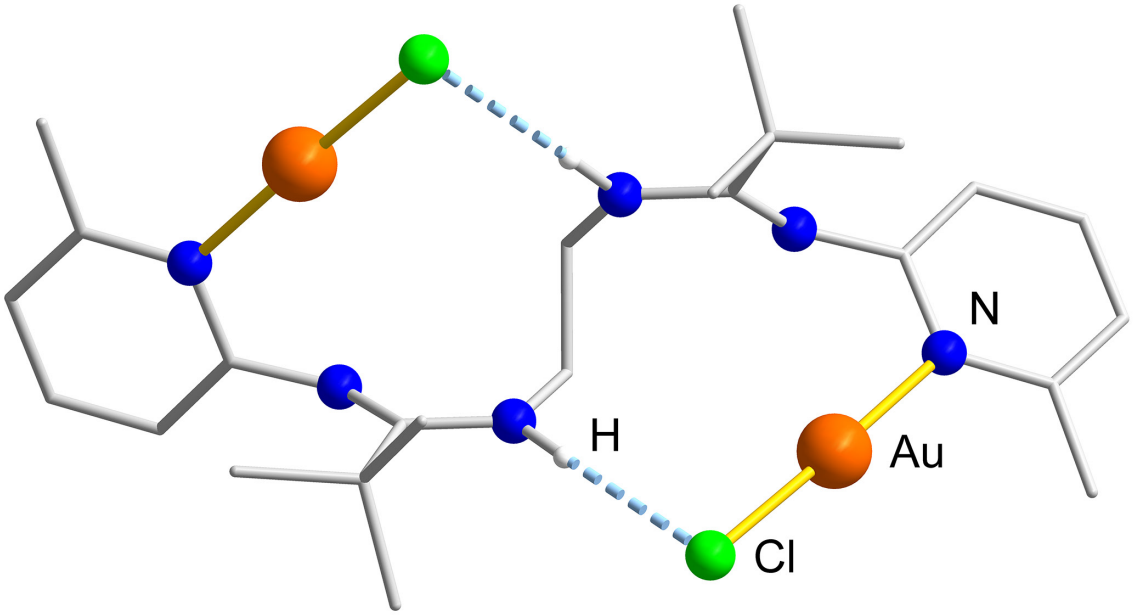

Figure S14: Computational structure of **2a** (RIDFT-D3/B3LYP/def2-TZVP).

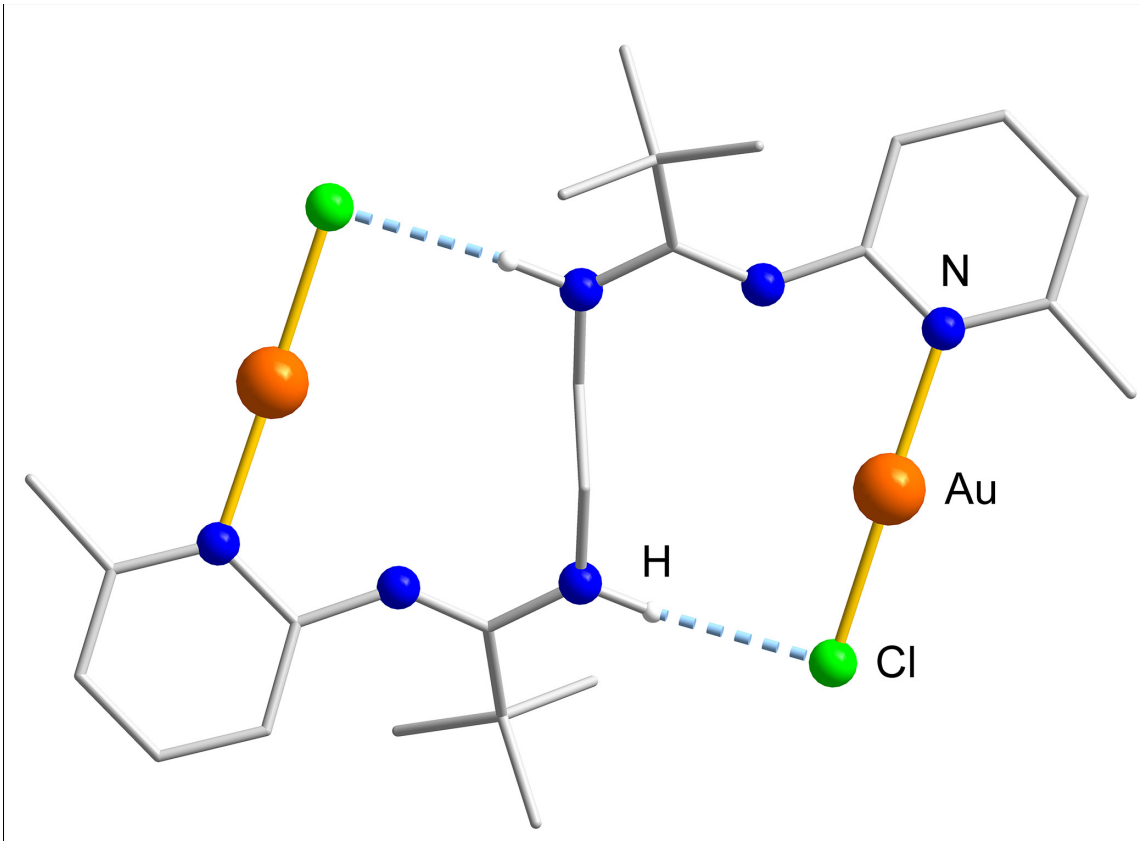

Figure S15: Computational structure of **2b** (RIDFT-D3/B3LYP/def2-TZVP).

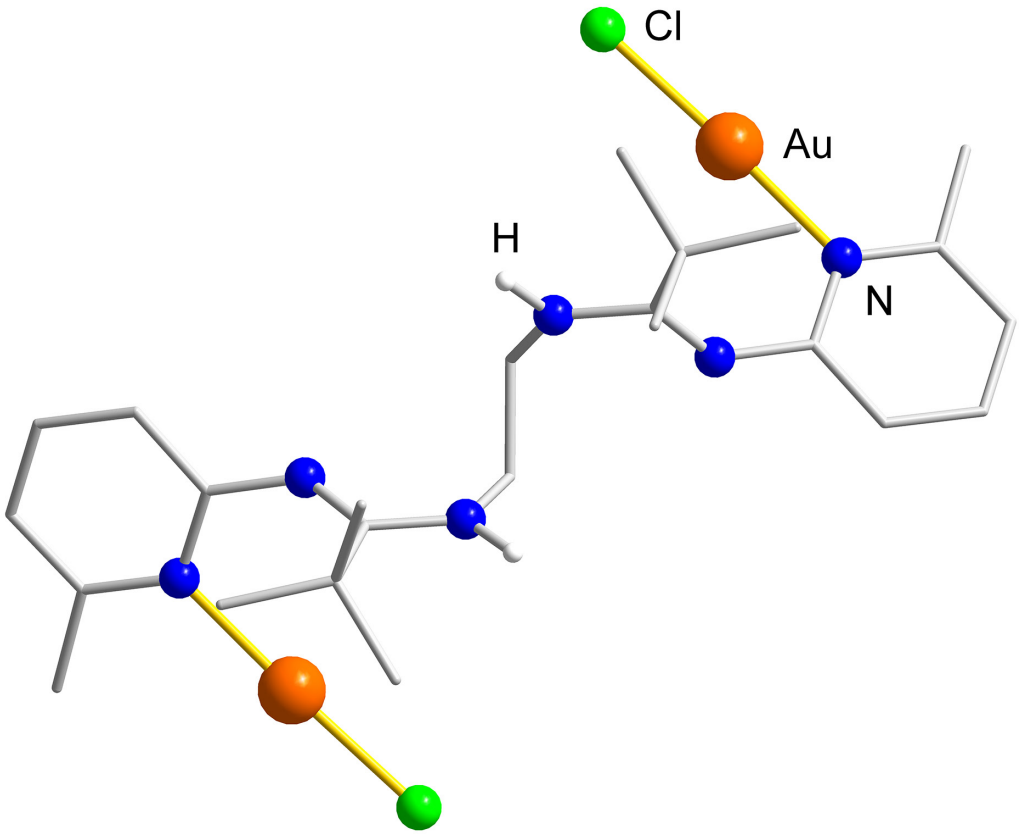

Figure S16: Computational structure of **2c** (RIDFT-D3/B3LYP/def2-TZVP).

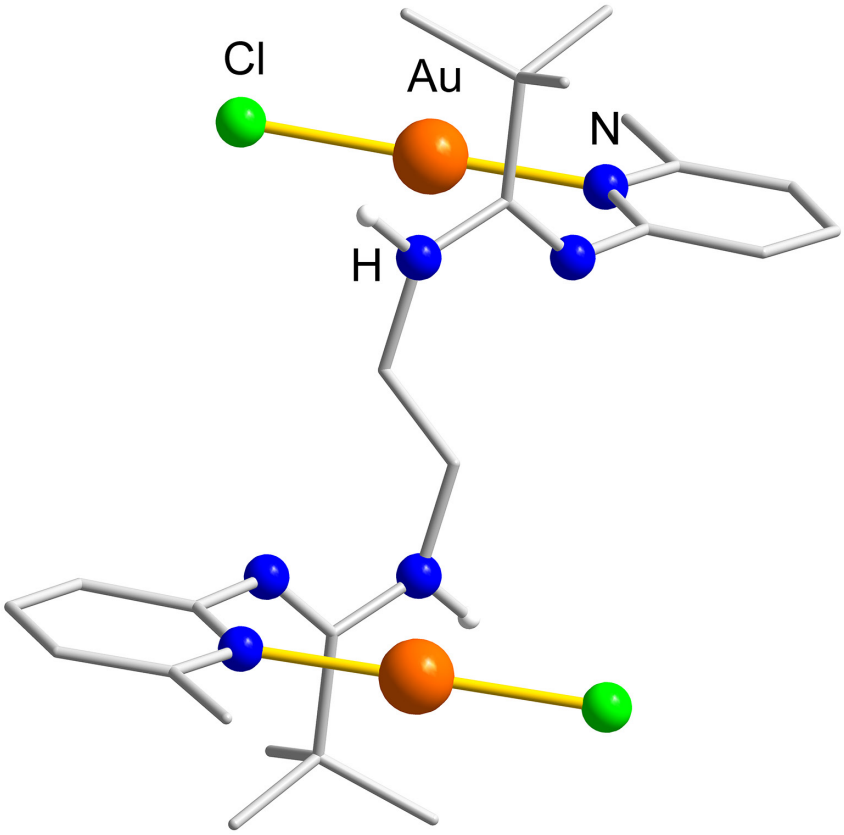

Figure S17: Computational structure of **2d** (RIDFT-D3/B3LYP/def2-TZVP).

Table S13: Calculated energies E and G (kcal/mol) of **1a**–**1d**.

	Energy E* [kcal/mol]: RIDFT-D3/B3LYP/def2-TZVP	Free Energy G** [kcal/mol]: BP-86/def2-SVP on structures **1a**–**1d**
1a	−3,429,975.84***	−3,429,272.01***
1b	−3,429,962.18	−3,429,264.01
1c	−3,429,952.49	−3,429,254.76
1d	−3,429,952.35	−3,429,254.85

*) Geometry optimization with TURBOMOLE.
**) Thermochemical correction obtained from reoptimization and frequency calculations with GAUSSIAN.
***) Structure is based on XRD data

Table S14: Calculated energies E and G (kcal/mol) of **2a**–**2d**.

	Energy E* [kcal/mol]: RIDFT-D3/B3LYP/def2-TZVP	Free Energy G** [kcal/mol]: DFT-D3/BP-86/def2-SVP on structures **2a**–**2d**
2a	−1,541,466,376***	−1,540,941.87***
2b	−1,541,452.553	−1,540,927.966
2c	−1,541,445.014	−1,540,919.448
2d	−1,541,444.633	−1,540,918.476

*) Geometry optimization with TURBOMOLE.
**) Thermochemical correction obtained from reoptimization and frequency calculations with GAUSSIAN.
***) Structure is based on XRD data

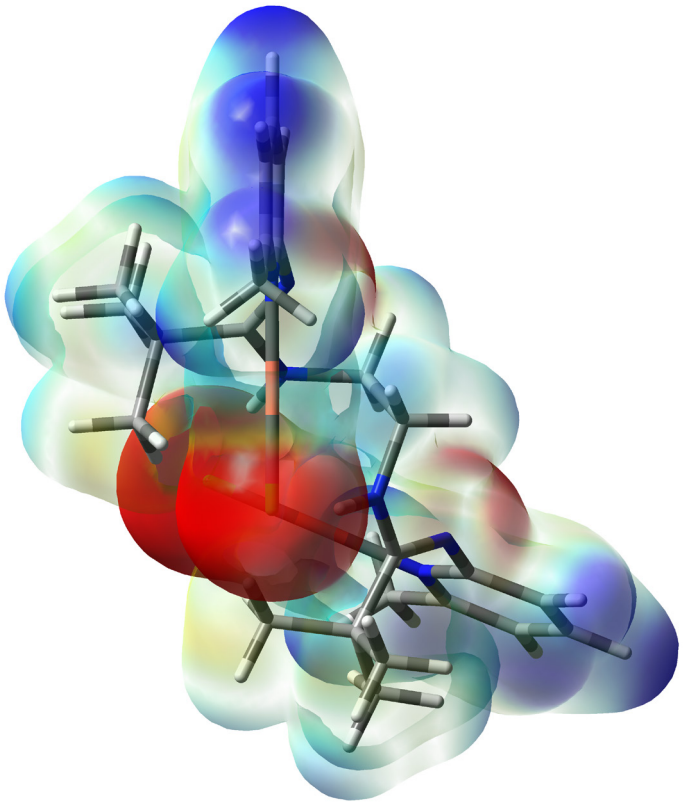

Figure S18: Electron density of **1a** mapped with electrostatic potential on the 0.006 au electron density isosurface. Color code (au): blue > 0.05706 > –0.02706 > red. Side view, transparent and fade.

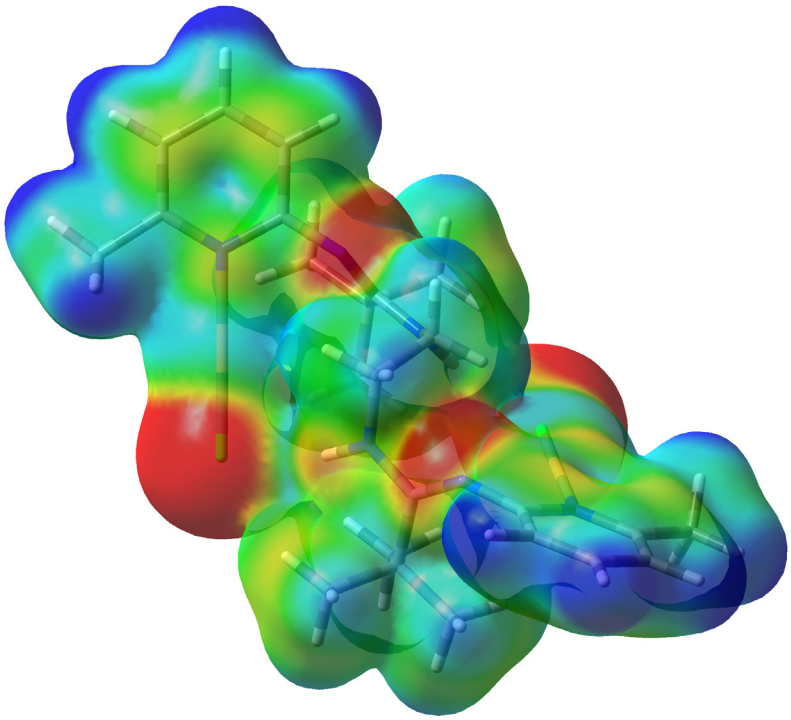

Figure S19: Electron density of **1a** mapped with electrostatic potential on the 0.006 au electron density isosurface. Color code (au): blue > 0.05706 > –0.02706 > red. Frontal view, transparent.

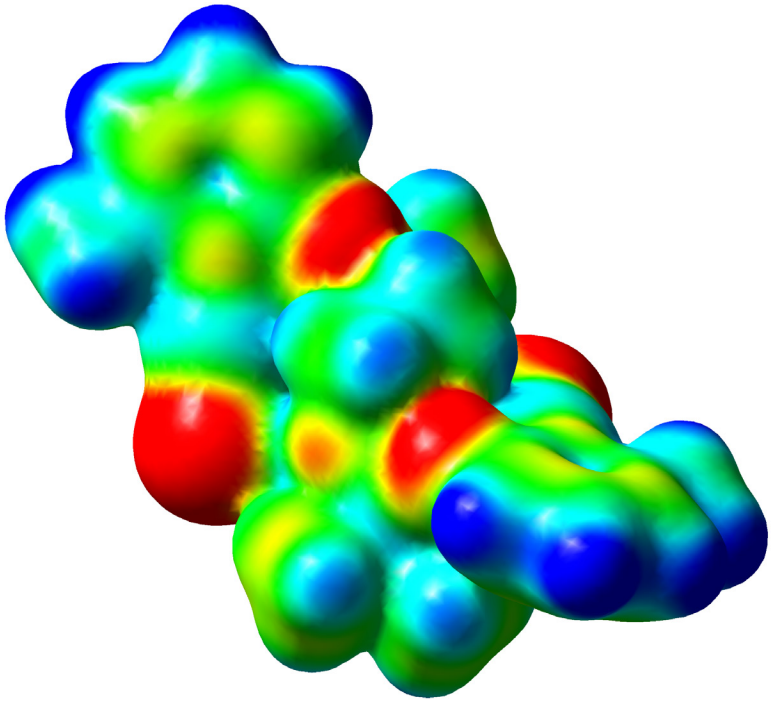

Figure S20: Electron density of **1a** mapped with electrostatic potential on the 0.006 au electron density isosurface. Color code (au): blue > 0.05706 > –0.02706 > red. Frontal view.

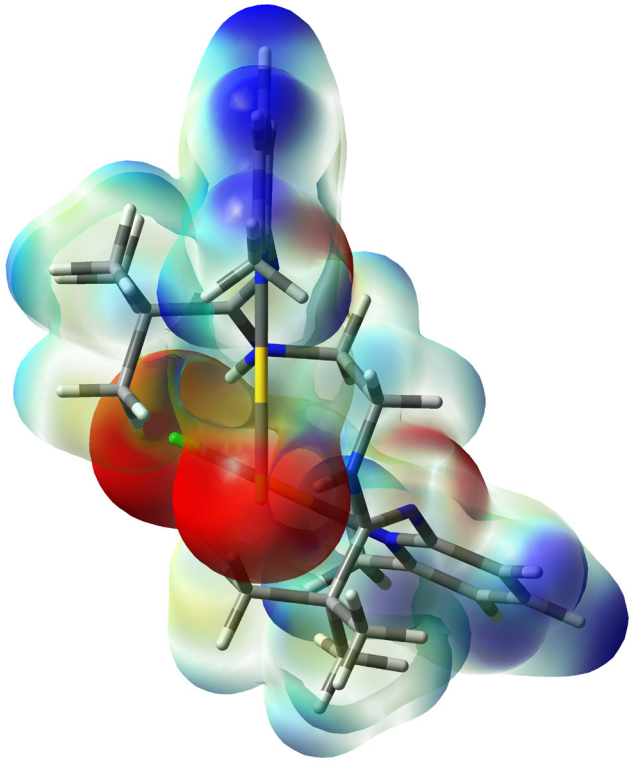

Figure S21: Electron density of **2a** mapped with electrostatic potential on the 0.007 au electron density isosurface. Color code (au): blue > 0.06348 > –0.02648 > red. Side view, transparent and fade.

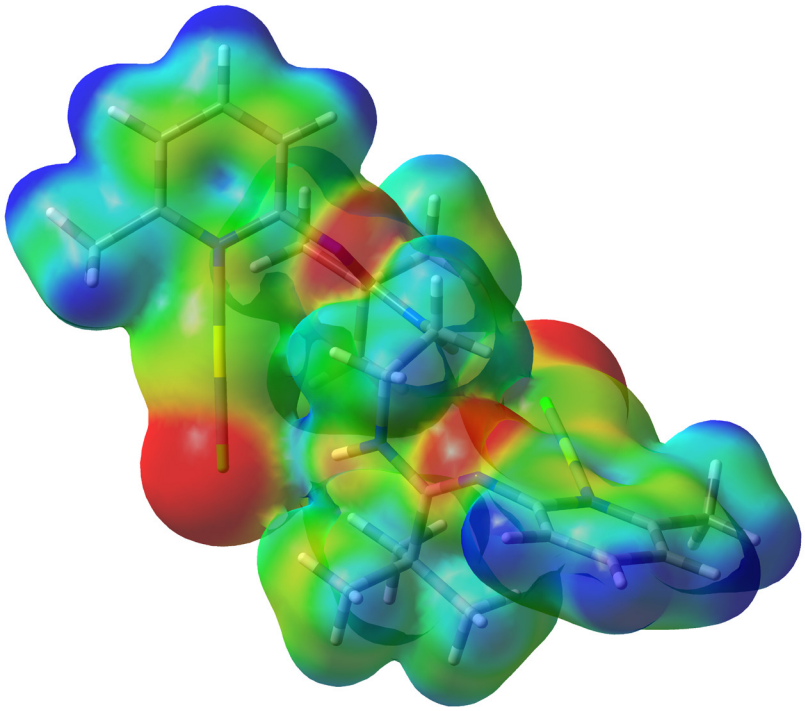

Figure S22: Electron density of **2a** mapped with electrostatic potential on the 0.007 au electron density isosurface. Color code (au): blue > 0.06348 > –0.02648 > red. Frontal view, transparent.

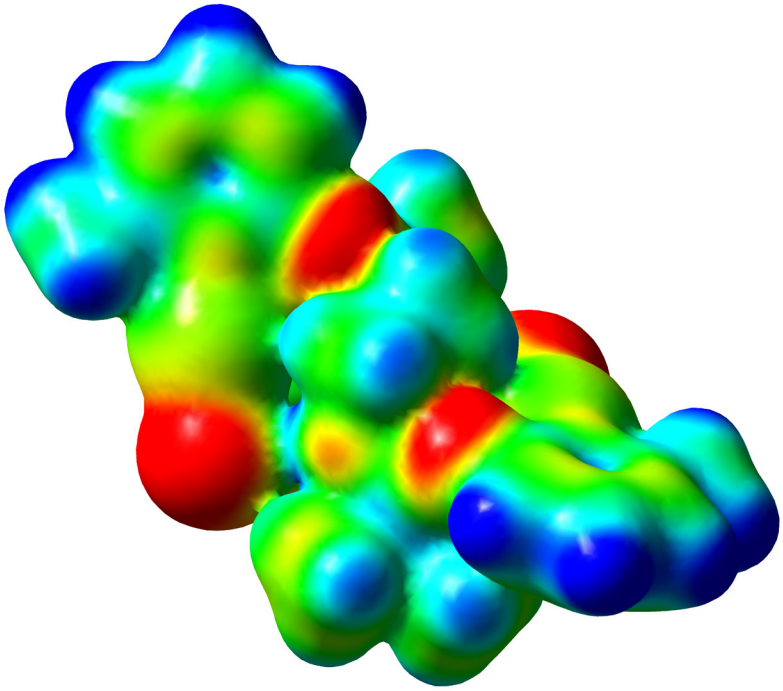

Figure S23: Electron density of **2a** mapped with electrostatic potential on the 0.007 au electron density isosurface. Color code (au): blue > 0.06348 > –0.02648 > red. Frontal view.

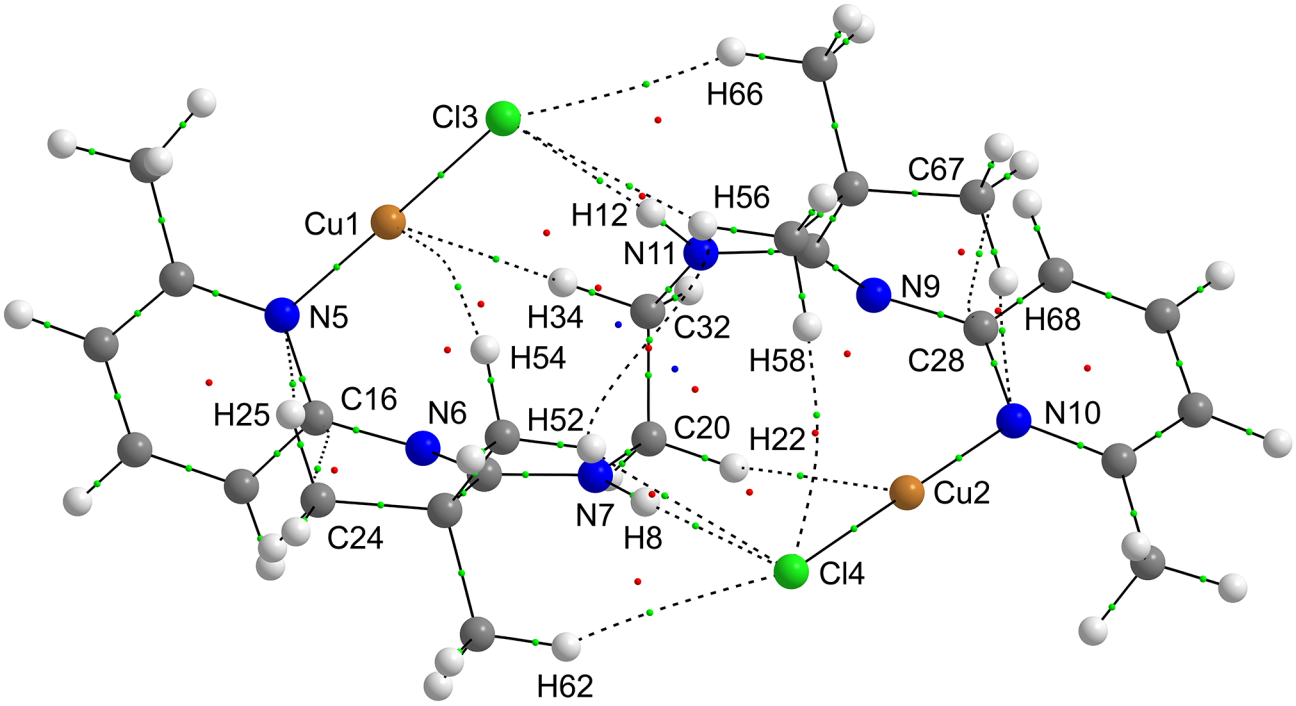

Figure S24: Atoms-in-molecules (AIM) molecular graph of **1a**. Bond critical points are denoted in green, ring critical points in red, and cage critical points in blue. See also Table S15.

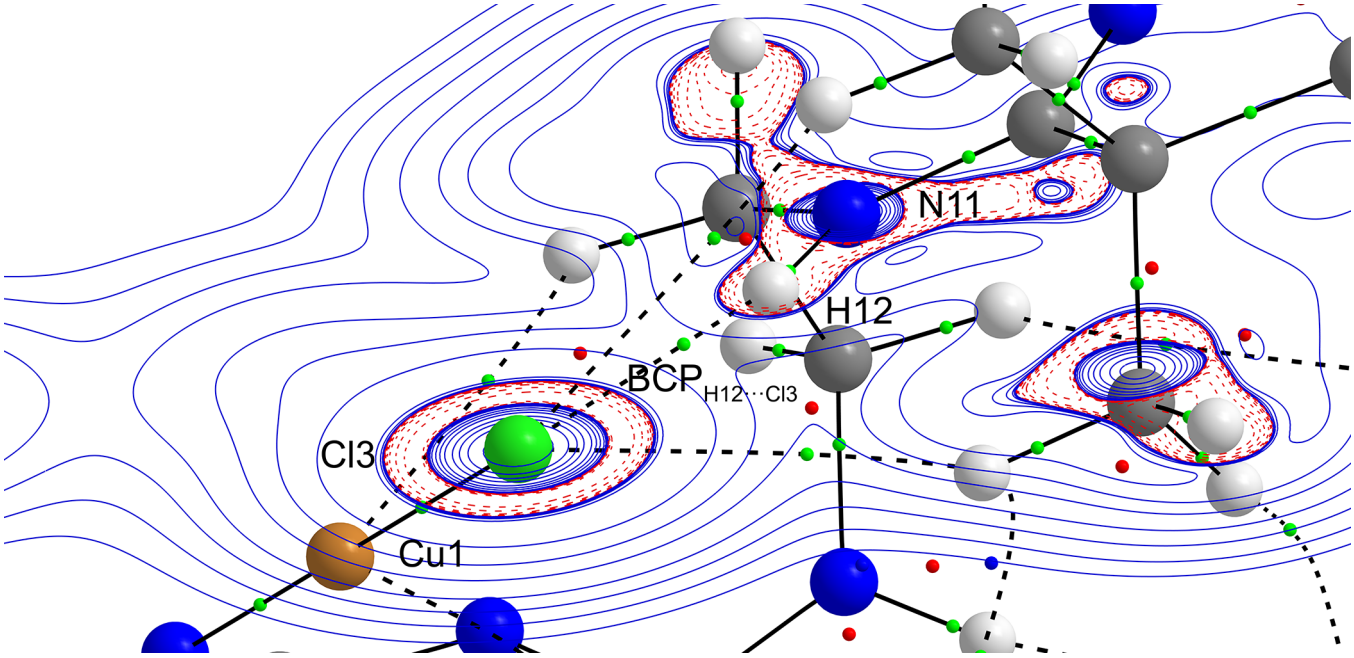

Figure S25: N–H···C*ipso* hydrogen bond region of the AIM molecular graph of **1a**. Contour map of the Laplacian of the electron density ($\nabla^2\rho(r)$) isosurfaces through the N(11)–H(12)–Cl(3) plane. Red contours show negative Laplacian ($\nabla^2\rho(r) < 0$) and blue contours show positive Laplacian ($\nabla^2\rho(r) > 0$) values. Bond critical points are denoted in green. See also Table S15.

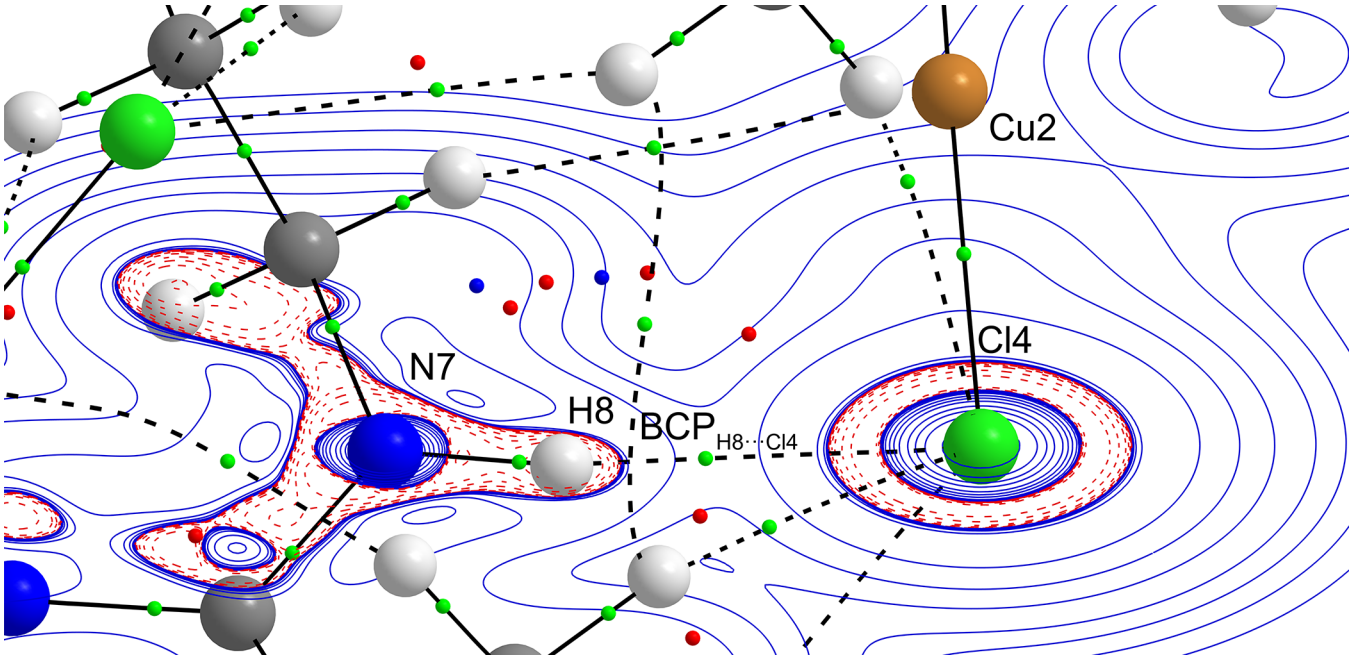

Figure S26: N–H···C*ipso* hydrogen bond region of the AIM molecular graph of **1a**. Contour map of the Laplacian of the electron density ($\nabla^2\rho(r)$) isosurfaces through the N(7)–H(8)–Cl(4) plane. Red contours show negative Laplacian ($\nabla^2\rho(r) < 0$) and blue contours show positive Laplacian ($\nabla^2\rho(r) > 0$) values. Bond critical points are denoted in green. See also Table S15.

Table S15: Topological parameters of selected intramolecular contacts in **1a** (see also Figs. S24–S26).

Bond Path A···B	Charge A	Charge B	d_{BP}(AB) [Å]	$\rho(r_{BCP})$ [eÅ^{-3}]	$\nabla^2\rho(r_{BCP})$ [eÅ^{-5}]	DI*	H	G	V
							[Hr Å^{-3}]		
N11···H12	–1.150399	0.422294	1.013427	0.332482	–1.671326	0.710957	–0.463304	0.045472	–0.508776
H12···Cl3	0.422294	–0.618215	2.333176	0.019163	0.061951	0.085090	0.001719	0.013768	–0.012049
Cu1···H34	0.495367	0.051972	2.838749	0.006649	0.016937	0.032115	0.000473	0.003762	–0.003289
Cu1···H54	0.495367	0.037766	2.864338	0.006963	0.017084	0.025440	0.000505	0.003767	–0.003262
H66···Cl3	0.041732	–0.618215	2.871786	0.007340	0.022687	0.040569	0.001104	0.004568	–0.003464
H56···Cl4	0.048147	–0.618215	2.874232	0.006974	0.022095	0.039771	0.001106	0.004418	–0.003312
H25···N5	0.026177	–1.159821	2.585245	0.010173	0.034630	0.031002	0.001392	0.007266	–0.005874
C16···C24	0.954468	–0.054525	2.941585	0.011559	0.045932	0.020536	0.001751	0.009732	–0.007981
H52···H56	0.042130	0.041732	2.987200	0.002203	0.007457	0.002731	0.000432	0.001432	–0.001000
N7···H8	–1.150361	0.422300	1.013513	0.332404	–1.670582	0.710406	–0.463159	0.045513	–0.508672
H8···Cl4	0.422300	–0.617604	2.327145	0.019414	0.062639	0.085867	0.001691	0.013969	–0.012278
Cu2···H22	0.495287	0.051638	2.838764	0.006653	0.016967	0.032180	0.000474	0.003768	–0.003294
H52···Cl4	0.042130	–0.617604	2.867750	0.007388	0.022890	0.040597	0.001113	0.004610	–0.003497
H62···Cl4	0.048555	–0.617604	2.849361	0.007301	0.023288	0.041417	0.001161	0.004661	–0.003500
H58···Cl4	0.038899	-0.617604	2.952993	0.006932	0.018716	0.041324	0.000814	0.003864	–0.003050
H68···Cl4	0.025995	–1.160111	2.593027	0.010082	0.034167	0.030459	0.001359	0.007183	–0.005824
C28···C67	0.954394	–0.054079	2.943400	0.011572	0.045728	0.020577	0.001744	0.009689	–0.007945

*) delocalization index

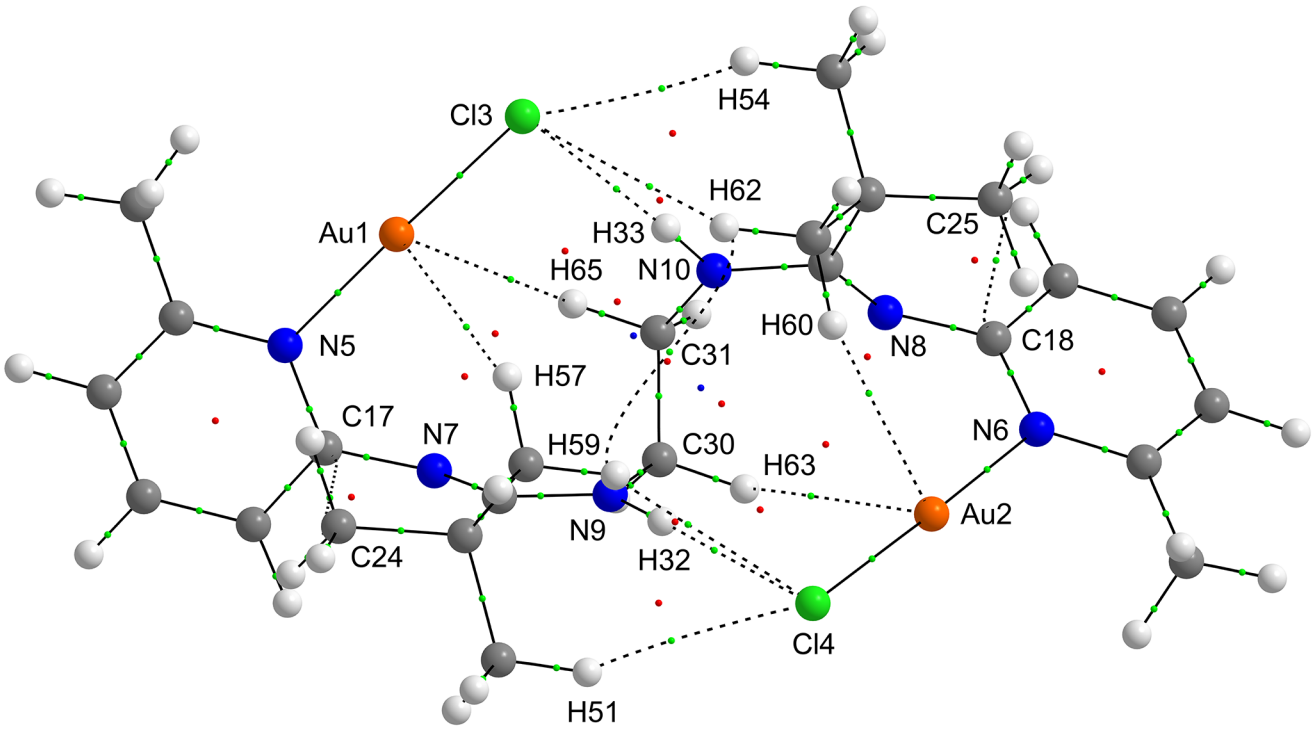

Figure S27: Atoms-in-molecules (AIM) molecular graph of **2a**. Bond critical points are denoted in green, ring critical points in red, and cage critical points in blue. See also Table S16.

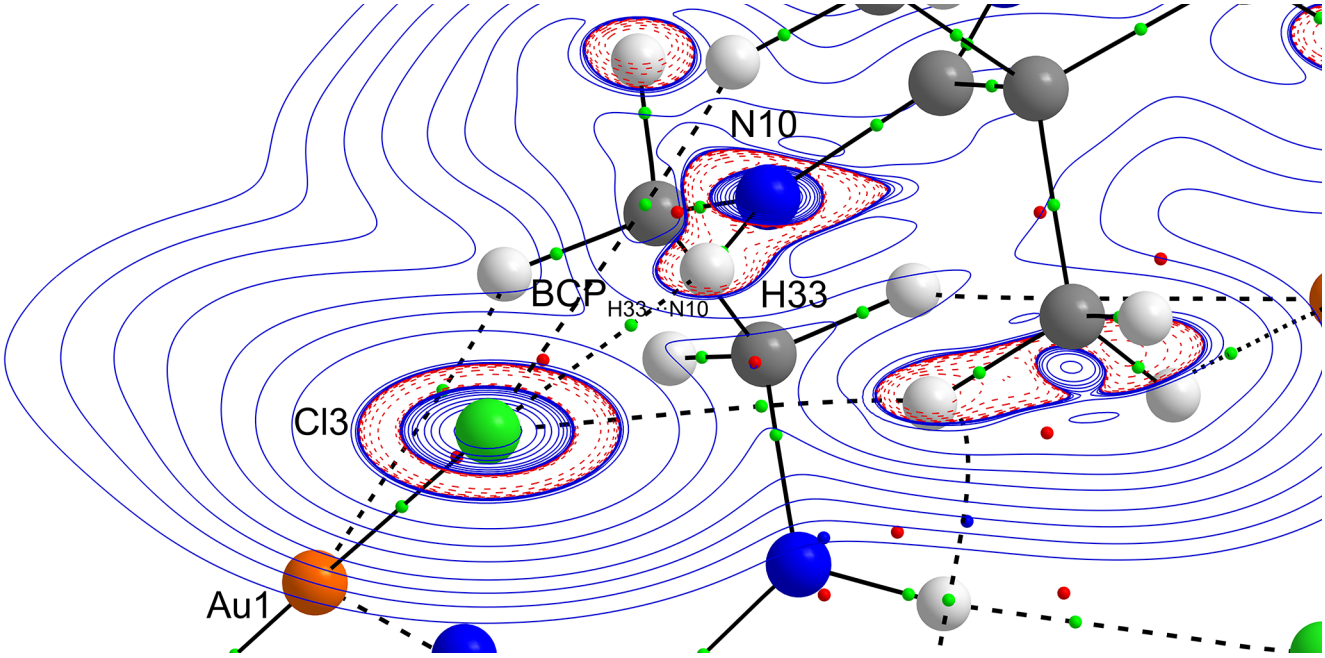

Figure S28: N–H···C*ipso* hydrogen bond region of the AIM molecular graph of **2a**. Contour map of the Laplacian of the electron density ($\nabla^2\rho(r)$) isosurfaces through the N(10)–H(33)–Cl(3) plane. Red contours show negative Laplacian ($\nabla^2\rho(r) < 0$) and blue contours show positive Laplacian ($\nabla^2\rho(r) > 0$) values. Bond critical points are denoted in green. See also Table S16.

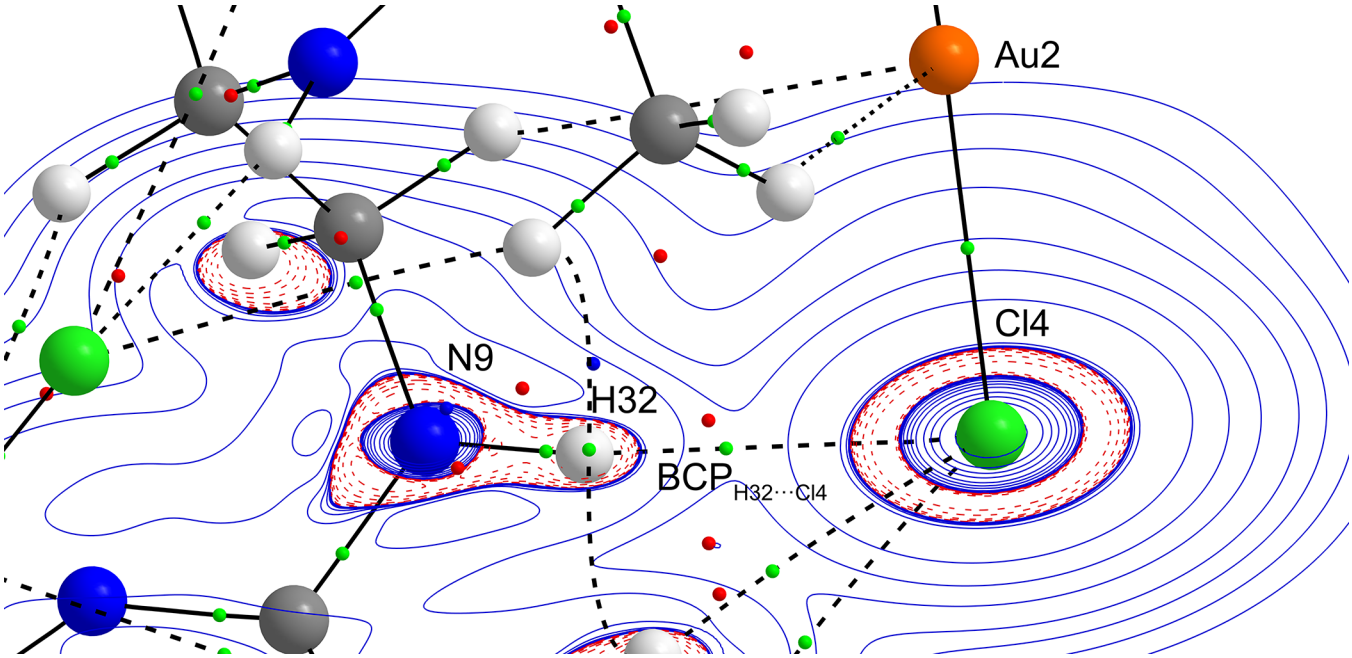

Figure S29: N–H···C*ipso* hydrogen bond region of the AIM molecular graph of **2a**. Contour map of the Laplacian of the electron density ($\nabla^2\rho(r)$) isosurfaces through the N(9)–H(32)–Cl(4) plane. Red contours show negative Laplacian ($\nabla^2\rho(r) < 0$) and blue contours show positive Laplacian ($\nabla^2\rho(r) > 0$) values. Bond critical points are denoted in green. See also Table S16.

Table S16: Topological parameters of selected intramolecular contacts in **2a** (see also Figs. S27–S29).

Bond Path A···B	Charge A	Charge B	d_{BP}(AB) [Å]	$\rho(r_{BCP})$ [eÅ^{-3}]	$\nabla^2\rho(r_{BCP})$ [eÅ^{-5}]	DI*	H	G	V
							[Hr Å^{-3}]		
N10···H33	–1.143940	0.416758	1.011016	0.334984	–1.680687	0.725528	–0.465674	0.045502	–0.511176
H33···Cl3	0.416758	–0.497839	2.445428	0.015012	0.049921	0.069023	0.001934	0.010546	–0.008612
Au1···H65	0.265976	0.062020	2.935329	0.008192	0.022524	0.042841	0.000708	0.004922	–0.004214
Au1···H57	0.265976	0.037892	3.072013	0.006516	0.017553	0.031886	0.000582	0.003806	–0.003224
H62···Cl3	0.040273	–0.497839	2.869551	0.007367	0.022650	0.041639	0.001102	0.004560	–0.003458
H54···Cl3	0.047693	–0.497839	2.835884	0.007459	0.023660	0.042365	0.001174	0.004742	–0.003568
C17···C24	0.953369	–0.055444	2.939975	0.011668	0.045503	0.020996	0.001715	0.009661	–0.007946
H59···H62	0.040270	0.040273	3.259865	0.001411	0.004915	0.001380	0.000318	0.000912	–0.000594
N9···H32	–1.144355	0.416747	1.011016	0.334985	–1.680698	0.725605	–0.465677	0.045502	–0.511179
H32···Cl4	0.416747	–0.497715	2.445433	0.015012	0.049921	0.069014	0.001934	0.010546	–0.008612
Au2···H63	0.265932	0.062033	2.935245	0.008193	0.022528	0.042841	0.000709	0.004923	–0.004214
Au2···H60	0.265932	0.037905	3.072029	0.006516	0.017552	0.031884	0.000583	0.003806	–0.003223
H59···Cl4	0.040270	–0.497715	2.869456	0.007368	0.022655	0.041647	0.001102	0.004561	–0.003459
H51···Cl4	0.047682	–0.497715	2.835839	0.007460	0.023663	0.042384	0.001173	0.004742	–0.003569
C18···C25	0.953390	–0.055443	2.939908	0.011669	0.045509	0.021034	0.001715	0.009663	–0.007948

*) delocalization index

Table S17: Cartesian coordinates for the geometry-optimized structure **1a** (RIDFT-D3/B3LYP/def2-TZVP).

Cu	–3.528013	–0.050483	–0.012364
Cu	3.464582	–0.241880	–0.580501
Cl	–2.906923	–2.045110	–0.408431
Cl	2.630133	0.698953	–2.294601
N	–4.118261	1.755599	0.339422
N	–1.880566	2.418983	0.289428
N	0.076987	1.488183	–0.320711
H	0.744783	1.231109	–1.038472
N	2.075996	–1.410537	1.784142
N	4.239563	–1.114323	0.959702
N	–0.014628	–1.170604	0.982301
H	–0.800544	–1.526503	0.450588
C	–1.116059	1.998550	–0.666153
C	–3.573909	4.065361	0.692505
H	–2.808595	4.825962	0.750650
C	–3.182671	2.743742	0.392196
C	–5.428277	2.041640	0.536842
C	–5.852798	3.327493	0.808740
H	–6.903472	3.526681	0.964251
C	0.482962	1.266863	1.052990
H	0.280766	2.159317	1.649196
H	1.558647	1.092437	1.046033
C	1.147974	–1.842326	0.992323
C	–2.787031	2.585342	–2.518352
H	–3.556048	1.892433	–2.180238
H	–2.877512	2.679007	–3.601761
H	–2.988000	3.565042	–2.083882
C	3.399601	–1.622179	1.903757
C	–4.902823	4.349922	0.890601
H	–5.214118	5.364321	1.108593
C	–1.377706	2.080419	–2.187872
C	–0.226192	0.069447	1.701895
H	0.127120	–0.032378	2.730339
H	–1.300593	0.250427	1.721581
C	5.582197	–1.226171	1.106027
C	–6.384295	0.889407	0.444580
H	–6.317383	0.416110	–0.538154
H	–7.411812	1.211016	0.608799
H	–6.132779	0.124779	1.183643
C	1.183470	–3.104347	0.098835
C	3.930315	–2.235641	3.058023
H	3.242027	–2.610824	3.801641
C	5.291733	–2.348473	3.200061
H	5.707911	–2.830328	4.076491
C	6.423230	–0.646888	0.007611
H	6.176727	–1.115137	–0.948685
H	7.485392	–0.787899	0.202627
H	6.224336	0.422082	–0.101289

C	6.138825	–1.841106	2.210370
H	7.213017	–1.915189	2.301886
C	–1.200017	0.681251	–2.813937
H	–0.178326	0.313623	–2.728265
H	–1.442186	0.732379	–3.877406
H	–1.866618	–0.045977	–2.345643
C	0.789839	–2.724773	–1.344210
H	–0.237154	–2.369100	–1.415660
H	0.876028	–3.607342	–1.981150
H	1.450296	–1.950760	–1.740340
C	–0.354908	3.068994	–2.790637
H	–0.465719	4.060710	–2.345722
H	–0.530787	3.157483	–3.864760
H	0.673304	2.739364	–2.650125
C	0.172309	–4.118701	0.677707
H	0.434015	–4.384510	1.704540
H	0.192389	–5.029460	0.075804
H	–0.847782	–3.737091	0.667843
C	2.566561	–3.765753	0.066708
H	3.313441	–3.121660	–0.395545
H	2.502032	–4.678570	–0.527750
H	2.916038	–4.042407	1.061412

Table S18: Cartesian coordinates for the geometry-optimized structure **1b** (RIDFT-D3/B3LYP/def2-TZVP).

Cu	–3.485716	–1.417268	0.267879
N	–4.638828	0.110860	–0.060239
N	–2.657965	1.231261	–0.081196
C	–1.762552	2.109439	0.265294
C	–3.979750	1.274030	–0.328132
C	–5.964468	–0.002210	–0.279770
N	–0.488168	1.792548	0.004717
H	0.266395	2.431196	0.228890
C	–1.959656	3.445662	1.024624
C	–4.674181	2.327663	–0.959192
C	–6.589424	–1.318944	0.075089
C	–6.694290	1.036470	–0.833605
C	–0.844607	3.615266	2.083133
C	–1.862431	4.611727	0.021057
C	–3.301606	3.480070	1.772358
C	–6.023398	2.203007	–1.201256
Cu	3.487724	1.418318	–0.241155
N	4.644364	–0.114402	0.050254
C	3.989624	–1.278801	0.323496
C	5.974806	–0.004906	0.240936
N	2.662854	–1.233425	0.103891
C	1.761749	–2.108438	–0.235921
N	0.491432	–1.792752	0.045394
H	–0.266438	–2.429111	–0.173942
C	1.946211	–3.439201	–1.008287

C	4.696033	–2.337651	0.931990
C	6.050592	–2.216938	1.144558
C	3.273057	–3.465413	–1.782794
C	0.811053	–3.603883	–2.046079
C	1.870869	–4.612639	–0.011611
C	6.715155	–1.048931	0.770220
C	6.593883	1.313542	–0.117898
C	0.077596	–0.518354	0.589563
C	–0.068112	0.518943	–0.536138
H	1.970687	–5.556927	–0.551412
H	2.666192	–4.569133	0.732727
H	0.914100	–4.621067	0.512116
H	3.297015	–4.354706	–2.414871
H	4.144643	–3.502383	–1.135924
H	3.368572	–2.590014	–2.427788
H	1.010511	–4.491517	–2.648613
H	0.762930	–2.743152	–2.715805
H	–0.170889	–3.740752	–1.592524
H	6.188278	2.106062	0.516503
H	6.349718	1.578120	–1.148559
H	7.676702	1.291546	–0.002338
H	7.779425	–0.936775	0.920317
H	6.598696	–3.030426	1.604565
H	4.160344	–3.224140	1.232788
H	–2.641826	4.562943	–0.739697
H	–0.894842	4.615934	–0.482399
H	–1.973217	5.560004	0.551689
H	0.146321	3.745443	1.647567
H	–1.052896	4.508295	2.674693
H	–0.812433	2.759713	2.760392
H	–4.159966	3.514842	1.107808
H	–3.336107	4.373601	2.397929
H	–3.412280	2.609219	2.421029
H	–6.370727	–1.573862	1.113898
H	–7.669007	–1.300644	–0.067885
H	–6.166070	–2.116017	–0.541771
H	–4.133227	3.212834	–1.254543
H	–6.562321	3.012089	–1.679545
H	0.894372	0.667258	–1.024649
H	–0.792468	0.165680	–1.268171
H	0.804892	–0.167776	1.320083
H	–0.884252	–0.664547	1.080149
H	–7.754653	0.921141	–1.007185
Cl	–2.364620	–3.239740	0.342974
Cl	2.366596	3.242120	–0.279680

Table S19: Cartesian coordinates for the geometry-optimized structure **1c** (RIDFT-D3/B3LYP/def2-TZVP).

C	2.315575	4.279884	1.166481
C	3.126049	5.248888	1.711320
C	2.794748	2.961324	1.058810
N	1.998435	1.962369	0.615044
C	2.117611	1.120613	–0.359088
N	1.440575	–0.037094	–0.261381
H	1.509765	–0.688514	–1.019976
C	0.760045	–0.482239	0.942892
N	–1.461356	0.076994	–0.026504
H	–1.629295	0.910041	–0.557962
C	–0.602001	0.189417	1.139909
C	–2.169654	–1.023311	–0.336213
N	–1.925228	–2.097143	0.341201
C	–2.668104	–3.195688	0.606547
C	–2.206279	–4.483078	0.276261
C	–2.948057	–5.580724	0.647276
C	4.403707	4.912659	2.163519
C	4.825465	3.599322	2.062860
N	4.032304	2.643017	1.527291
C	2.816917	1.350939	–1.721296
C	3.843036	2.490071	–1.679883
C	3.534487	0.072973	–2.198675
C	1.699313	1.734974	–2.717698
C	–3.067942	–0.885683	–1.589974
C	–3.822363	0.458496	–1.585806
C	–2.118709	–0.957088	–2.807871
C	–4.099485	–2.014156	–1.711587
N	–3.815906	–3.043519	1.321878
C	–4.137750	–5.407647	1.357625
C	–4.541616	–4.126028	1.685118
C	–5.794302	–3.854146	2.462832
Cu	–4.326465	–1.230476	1.778718
Cl	–4.753919	0.810728	2.125045
Cu	4.568410	0.785761	1.387254
Cl	5.002256	–1.262010	1.091479
C	6.173545	3.151090	2.542179
H	0.951489	0.945388	–2.808231
H	1.193840	2.650762	–2.404396
H	2.131308	1.905087	–3.705923
H	4.676919	2.252493	–1.020625
H	3.402941	3.431932	–1.354785
H	4.240310	2.639706	–2.685276
H	4.215125	–0.306321	–1.435142
H	2.840210	–0.728258	–2.463623
H	4.105382	0.298272	–3.101203
H	–1.106311	–0.260266	1.997350
H	–0.461620	1.249263	1.339883
H	0.628835	–1.559024	0.863547

H	1.394156	–0.274031	1.806770
H	–2.696070	–0.858614	–3.729342
H	–1.376781	–0.157022	–2.788024
H	–1.590882	–1.912548	–2.836752
H	–4.821359	–1.984786	–0.896418
H	–3.635268	–2.999413	–1.726779
H	–4.644484	–1.890307	–2.648949
H	–3.159012	1.316444	–1.720085
H	–4.374264	0.598639	–0.655246
H	–4.525384	0.477656	–2.420439
H	6.750495	3.981333	2.946935
H	6.735401	2.695578	1.723133
H	6.065113	2.385949	3.314771
H	5.055453	5.656188	2.599651
H	2.773143	6.269943	1.789440
H	1.319375	4.499595	0.810263
H	–4.733903	–6.255429	1.663715
H	–2.609277	–6.576571	0.388980
H	–1.278218	–4.576230	–0.269287
H	–6.323056	–4.775098	2.704187
H	–6.460795	–3.202169	1.892995
H	–5.556623	–3.329154	3.391272

Table S20: Cartesian coordinates for the geometry-optimized structure **1d** (RIDFT-D3/B3LYP/def2-TZVP).

C	0.414268	4.500240	2.029278
C	1.353130	3.581020	1.525130
C	0.715987	5.842448	2.022126
N	1.062360	2.264626	1.427028
C	1.608901	1.205121	1.925238
N	1.392392	0.040127	1.284633
C	2.373240	1.080478	3.264910
N	2.528644	4.022475	0.999837
C	1.937219	6.278335	1.503129
H	1.812793	–0.788462	1.661523
C	0.799786	–0.046109	–0.038239
C	1.372243	0.498584	4.287936
C	3.587658	0.141835	3.117385
C	2.874627	2.431859	3.789140
C	2.820337	5.343420	0.994181
C	–0.406699	–4.493468	–2.257801
C	–1.294217	–3.589841	–1.645489
C	–0.717438	–5.833848	–2.273944
N	–0.996208	–2.275610	–1.531085
N	–2.421592	–4.046385	–1.034575
C	–1.894518	–6.283364	–1.671298
C	–1.590587	–1.207959	–1.951380
N	–1.340114	–0.060320	–1.291403
C	–2.469367	–1.053113	–3.215820
H	–1.804282	0.769808	–1.609193

C	–0.729461	–0.015557	0.026306
C	–2.967340	–2.398316	–3.758607
C	–1.585478	–0.387084	–4.293579
C	–3.698755	–0.171613	–2.916537
C	–2.723266	–5.364490	–1.053347
Cu	3.715619	2.667726	0.285321
Cl	4.894253	1.046794	–0.388594
Cu	–3.497182	–2.712264	–0.132700
Cl	–4.518397	–1.099553	0.775840
C	–3.994660	–5.762269	–0.365537
C	4.143611	5.727931	0.403261
H	4.956391	5.228240	0.935917
H	4.302920	6.804418	0.445862
H	4.202076	5.402132	–0.638067
H	3.347884	2.276233	4.760169
H	2.065316	3.147672	3.928035
H	3.615055	2.870921	3.121295
H	4.230081	0.452179	2.291901
H	4.166442	0.158438	4.042430
H	3.300488	–0.899090	2.950111
H	0.513624	1.160224	4.415550
H	1.001691	–0.480416	3.981121
H	1.864347	0.385823	5.256140
H	2.193137	7.328157	1.484248
H	0.008091	6.559475	2.419653
H	–0.519857	4.123440	2.420501
H	1.130106	–0.975184	–0.499004
H	1.168716	0.785266	–0.641526
H	–1.053674	0.901728	0.514161
H	–1.100526	–0.859341	0.611307
H	–2.165545	–0.251304	–5.208703
H	–1.223304	0.591408	–3.975441
H	–0.718963	–1.008645	–4.527479
H	–4.362158	–0.174424	–3.783322
H	–4.248214	–0.539327	–2.048338
H	–3.436370	0.872117	–2.729018
H	–2.148875	–3.076292	–3.997055
H	–3.632482	–2.893314	–3.052033
H	–3.526707	–2.218749	–4.678355
H	0.493732	–4.106890	–2.713119
H	–0.051182	–6.538819	–2.755918
H	–2.156492	–7.331809	–1.670653
H	–4.171944	–6.834165	–0.440041
H	–3.957816	–5.481953	0.689955
H	–4.843500	–5.231350	–0.803357

Table S21: Cartesian coordinates for the geometry-optimized structure **2a** (RIDFT-D3/B3LYP/def2-TZVP).

Au	0.058704	–0.396406	3.611124
Au	–0.058835	–0.396204	–3.611139
Cl	1.840668	–1.621674	2.868603
Cl	–1.840938	–1.621223	–2.868555
N	–1.585032	0.732976	4.236003
N	1.585106	0.732869	–4.236025
N	–2.075632	1.107456	1.975941
N	2.075895	1.106936	–1.975963
N	–1.488360	0.325877	–0.053039
N	1.488691	0.325623	0.053138
C	–1.845709	0.955834	5.551132
C	–2.929448	1.716806	5.944774
C	–3.763703	2.274553	4.973478
C	3.764388	2.273609	–4.973434
C	–3.501250	2.052438	3.645259
C	3.501863	2.051523	–3.645223
C	–2.402464	1.250885	3.270641
C	2.402795	1.250344	–3.270649
C	–0.917282	0.349531	6.560445
C	–2.135004	0.148850	1.111630
C	2.135178	0.148393	–1.111595
C	–2.932270	–1.171221	1.224846
C	2.932099	–1.171876	–1.224857
C	–3.544878	–1.377635	2.615501
C	3.544600	–1.378376	–2.615546
C	–4.082615	–1.113227	0.194548
C	4.082479	–1.114280	–0.194583
C	–2.002494	–2.364839	0.919742
C	2.001967	–2.365239	–0.919816
C	–0.680595	1.492692	–0.353894
C	0.681095	1.492564	0.353977
H	–1.594011	–0.360641	–0.787674
H	1.594159	–0.360949	0.787748
C	1.845723	0.955886	–5.551139
C	2.929731	1.716495	–5.944746
C	0.916888	0.350231	–6.560464
H	–3.113118	1.878850	6.997088
H	–4.613818	2.878104	5.267064
H	4.615003	2.876462	–5.267007
H	–4.116719	2.466877	2.860100
H	4.117402	2.465822	–2.860045
H	0.102353	0.713381	6.416055
H	–1.235488	0.594758	7.572704
H	–0.887880	–0.737178	6.456403
H	–4.219910	–0.568698	2.894119
H	–4.125353	–2.301575	2.604290
H	–2.783058	–1.477398	3.387397
H	4.219857	–0.569617	–2.894133

H	4.124799	–2.302491	–2.604422
H	2.782722	–1.477863	–3.387425
H	–3.720023	–1.029187	–0.828823
H	–4.673251	–2.029000	0.262971
H	–4.742872	–0.267581	0.399460
H	3.719944	–1.030203	0.828805
H	4.672855	–2.030217	–0.263076
H	4.742975	–0.268809	–0.399455
H	–1.150714	–2.380414	1.601565
H	–2.561669	–3.293719	1.050111
H	–1.626995	–2.352381	–0.102082
H	1.150180	–2.380525	–1.601639
H	2.560863	–3.294279	–1.050242
H	1.626472	–2.352715	0.102008
H	–0.530573	1.512447	–1.431654
H	–1.220298	2.397024	–0.062644
H	0.531068	1.512337	1.431737
H	1.220954	2.396810	0.062745
H	3.113272	1.878791	–6.997045
H	–0.102575	0.714457	–6.415819
H	1.235038	0.595590	–7.572708
H	0.887060	–0.736492	–6.456698

Table S22: Cartesian coordinates for the geometry-optimized structure **2b** (RIDFT-D3/B3LYP/def2-TZVP).

Au	–3.491167	–1.606353	0.327189
N	–4.662636	0.085695	–0.082613
N	–2.674492	1.224842	–0.088912
C	–1.781285	2.103907	0.252932
C	–3.987552	1.249653	–0.342822
C	–5.995703	–0.005576	–0.299803
N	–0.506581	1.792715	–0.019206
H	0.237649	2.446057	0.191739
C	–1.980444	3.434439	1.021151
C	–4.672810	2.307037	–0.980723
C	–6.676826	–1.292646	0.059604
C	–6.703885	1.045326	–0.857124
C	–0.874005	3.590712	2.090595
C	–1.871273	4.608089	0.027159
C	–3.328983	3.465921	1.756662
C	–6.019332	2.201135	–1.230589
Au	3.507941	1.611972	–0.247343
N	4.682587	–0.097439	0.068778
C	4.010198	–1.263394	0.327740
C	6.023168	–0.017646	0.238935
N	2.689363	–1.226868	0.117380
C	1.781017	–2.095788	–0.210888
N	0.516271	–1.778139	0.097465
H	–0.236196	–2.427076	–0.095867
C	1.948302	–3.418786	–1.000172

C	4.711370	–2.336174	0.920855
C	6.066607	–2.242274	1.124688
C	3.268064	–3.443207	–1.786398
C	0.802413	–3.562069	–2.029361
C	1.873085	–4.603669	–0.016687
C	6.744663	–1.083465	0.748885
C	6.698512	1.272920	–0.119085
C	0.114025	–0.489499	0.619473
C	–0.086567	0.507603	–0.535251
H	1.960638	–5.541856	–0.569019
H	2.675731	–4.576010	0.720713
H	0.921304	–4.611910	0.516189
H	3.282122	–4.325614	–2.428269
H	4.145147	–3.491843	–1.147607
H	3.361975	–2.561095	–2.422361
H	0.990793	–4.442050	–2.646507
H	0.752620	–2.691448	–2.685959
H	–0.174975	–3.701363	–1.566807
H	6.373515	2.076076	0.546373
H	6.439365	1.574602	–1.135417
H	7.780882	1.176207	–0.043888
H	7.812826	–0.992289	0.882420
H	6.605212	–3.068622	1.572568
H	4.160420	–3.215641	1.214023
H	–2.644688	4.567787	–0.740495
H	–0.899716	4.614488	–0.468660
H	–1.984148	5.552280	0.564476
H	0.120225	3.722552	1.663534
H	–1.084326	4.478912	2.688667
H	–0.850465	2.728690	2.759883
H	–4.181114	3.509478	1.084412
H	–3.366821	4.353974	2.389670
H	–3.447609	2.589575	2.396374
H	–6.456033	–1.570715	1.091612
H	–7.755960	–1.204978	–0.060092
H	–6.320991	–2.107681	–0.574942
H	–4.116104	3.184011	–1.270939
H	–6.546250	3.015528	–1.712957
H	0.853798	0.645545	–1.067078
H	–0.835315	0.122836	–1.225210
H	0.871120	–0.111738	1.304325
H	–0.823807	–0.620068	1.157570
H	–7.765996	0.944863	–1.027402
Cl	–2.223250	–3.506281	0.579650
Cl	2.244363	3.525838	–0.387237

Table S23: Cartesian coordinates for the geometry-optimized structure **2c** (RIDFT-D3/B3LYP/def2-TZVP).

C	2.302417	4.261405	1.032732
C	3.083800	5.257323	1.566537
C	2.784996	2.939448	0.997884
N	1.997270	1.934535	0.565157
C	2.115844	1.063344	–0.381165
N	1.435172	–0.088573	–0.250223
H	1.478555	–0.751016	–1.001374
C	0.755688	–0.500482	0.966872
N	–1.457591	0.124284	0.003532
H	–1.600671	0.969133	–0.516968
C	–0.593526	0.196336	1.170072
C	–2.174285	–0.960698	–0.337620
N	–1.927754	–2.058690	0.297060
C	–2.658903	–3.161627	0.552996
C	–2.204046	–4.430259	0.146159
C	–2.912455	–5.552766	0.499628
C	4.341679	4.944485	2.082210
C	4.778104	3.632273	2.057877
N	4.008647	2.646140	1.530222
C	2.827721	1.249269	–1.742477
C	3.811570	2.425349	–1.740282
C	3.591293	–0.026850	–2.147617
C	1.716164	1.546772	–2.775557
C	–3.092176	–0.776202	–1.570059
C	–3.879734	0.546052	–1.482660
C	–2.161296	–0.751602	–2.804119
C	–4.090807	–1.927592	–1.740927
N	–3.778725	–3.055538	1.328778
C	–4.067853	–5.424165	1.270845
C	–4.476755	–4.166674	1.676425
C	–5.702489	–3.982870	2.519418
Au	–4.351360	–1.130149	1.940409
Cl	–4.897542	1.008050	2.491220
Au	4.621466	0.637786	1.501795
Cl	5.200662	–1.558517	1.381664
C	6.113541	3.248286	2.620308
H	0.999352	0.727079	–2.850277
H	1.169810	2.454463	–2.510449
H	2.161491	1.693045	–3.761489
H	4.639984	2.255431	–1.054951
H	3.328133	3.364964	–1.475491
H	4.224623	2.537848	–2.744189
H	4.289071	–0.337514	–1.369980
H	2.927556	–0.867859	–2.361069
H	4.152766	0.166631	–3.063538
H	–1.107100	–0.258186	2.019575
H	–0.431520	1.249642	1.387604
H	0.605871	–1.575857	0.905377

H	1.400908	–0.288218	1.821507
H	–2.757159	–0.627179	–3.710417
H	–1.446291	0.071624	–2.757210
H	–1.601589	–1.685216	–2.890182
H	–4.800578	–1.970418	–0.916443
H	–3.594417	–2.893806	–1.821526
H	–4.654887	–1.767365	–2.661317
H	–3.237504	1.426742	–1.555697
H	–4.441481	0.615697	–0.551008
H	–4.580705	0.602308	–2.317697
H	6.637948	4.122915	3.002952
H	6.732796	2.772764	1.856855
H	5.996237	2.526097	3.431049
H	4.973231	5.708113	2.512522
H	2.724559	6.278852	1.587223
H	1.320299	4.457930	0.627380
H	–4.639928	–6.291684	1.566592
H	–2.575559	–6.531578	0.181301
H	–1.302069	–4.483716	–0.446094
H	–6.175080	–4.941557	2.728823
H	–6.424883	–3.337417	2.015127
H	–5.450500	–3.500567	3.466394

Table S24: Cartesian coordinates for the geometry-optimized structure **2d** (RIDFT-D3/B3LYP/def2-TZVP).

C	0.470383	4.483596	2.115821
C	1.384768	3.571750	1.555122
C	0.758952	5.826709	2.108233
N	1.078081	2.262473	1.462712
C	1.597584	1.187675	1.951379
N	1.336890	0.031363	1.309643
C	2.389971	1.039859	3.271249
N	2.534100	4.027149	0.974493
C	1.948267	6.273087	1.531058
H	1.705297	–0.817430	1.696219
C	0.737206	–0.033627	–0.011524
C	1.420052	0.426497	4.306235
C	3.607402	0.113679	3.075764
C	2.888392	2.385148	3.813319
C	2.815984	5.355098	0.967373
C	–0.427950	–4.428168	–2.143297
C	–1.370129	–3.555306	–1.567130
C	–0.672733	–5.780018	–2.155107
N	–1.102633	–2.239191	–1.448806
N	–2.504371	–4.055878	–0.995122
C	–1.845715	–6.273338	–1.582823
C	–1.634679	–1.168267	–1.930269
N	–1.391782	–0.014190	–1.276344
C	–2.429468	–1.018294	–3.248097
H	–1.773693	0.832661	–1.653848

C	–0.791778	0.045773	0.044912
C	–2.894701	–2.366376	–3.811846
C	–1.476093	–0.364363	–4.273374
C	–3.669596	–0.126116	–3.036729
C	–2.742752	–5.392375	–1.006319
Au	3.816456	2.601578	0.117655
Cl	5.161029	0.979528	–0.740708
Au	–3.836205	–2.684965	–0.127044
Cl	–5.242082	–1.122844	0.741546
C	–4.008219	–5.879046	–0.366383
C	4.097013	5.791060	0.322107
H	4.954244	5.318941	0.806714
H	4.211666	6.872518	0.381884
H	4.120477	5.492033	–0.727940
H	3.387595	2.213464	4.768601
H	2.072702	3.085219	3.990239
H	3.606953	2.850072	3.140067
H	4.242071	0.456114	2.257665
H	4.198454	0.100875	3.993162
H	3.324239	–0.921188	2.871330
H	0.558918	1.077334	4.468108
H	1.049921	–0.550399	3.992130
H	1.936451	0.300087	5.259954
H	2.195534	7.324665	1.507351
H	0.067217	6.534379	2.548482
H	–0.438817	4.093288	2.549857
H	1.035509	–0.973539	–0.472539
H	1.133052	0.785700	–0.614187
H	–1.088828	0.984854	0.508759
H	–1.188221	–0.775291	0.645152
H	–1.996135	–0.236208	–5.224831
H	–1.130197	0.616552	–3.944645
H	–0.598847	–0.990625	–4.445710
H	–4.259402	–0.110313	–3.954846
H	–4.296938	–0.499942	–2.226588
H	–3.412481	0.911191	–2.811272
H	–2.061696	–3.042418	–4.001429
H	–3.600137	–2.860501	–3.145696
H	–3.399713	–2.191305	–4.763466
H	0.468276	–4.002428	–2.571012
H	0.041443	–6.458278	–2.605660
H	–2.057682	–7.332798	–1.572741
H	–4.085231	–6.963178	–0.437105
H	–4.042294	–5.591608	0.686651
H	–4.881351	–5.432165	–0.846514

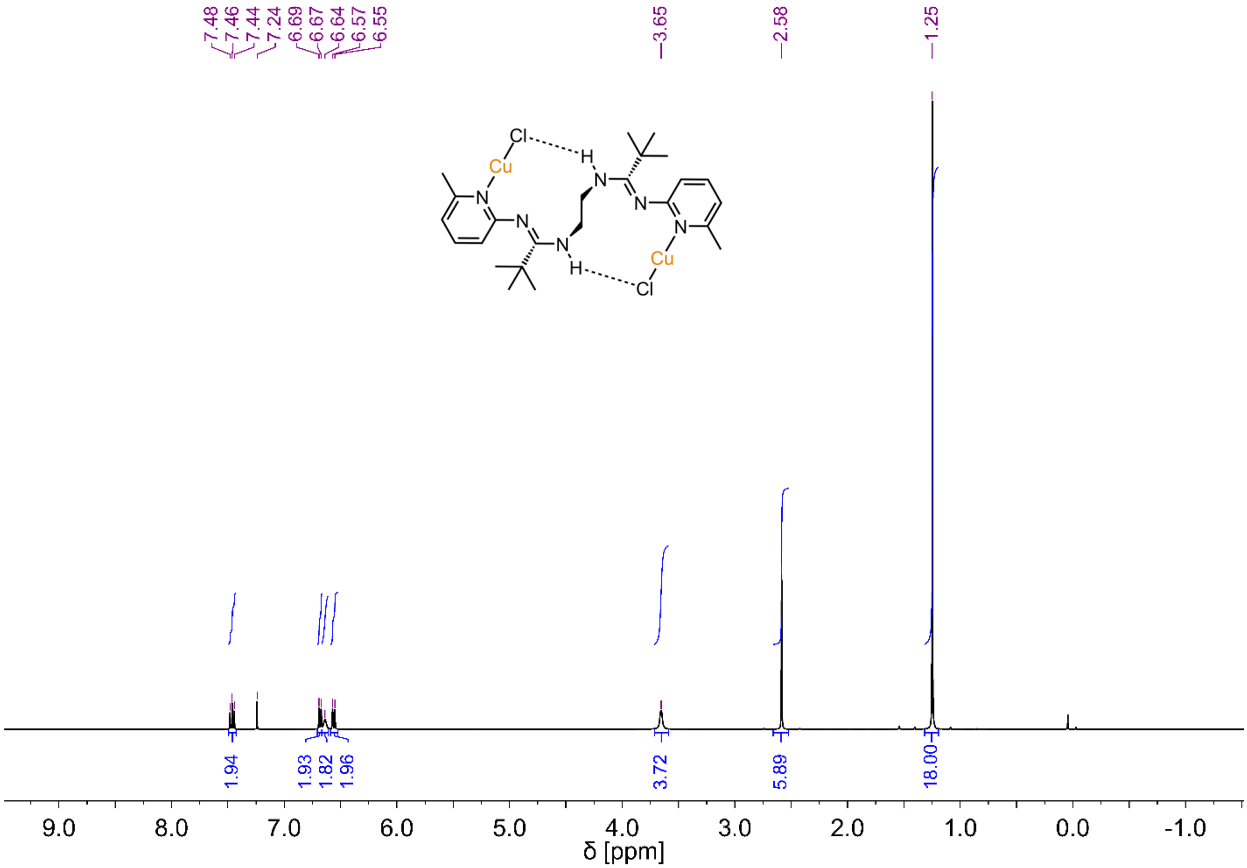

Figure S30: ^{1}H NMR spectrum of **1** ($CDCl_3$, 400.1 MHz).

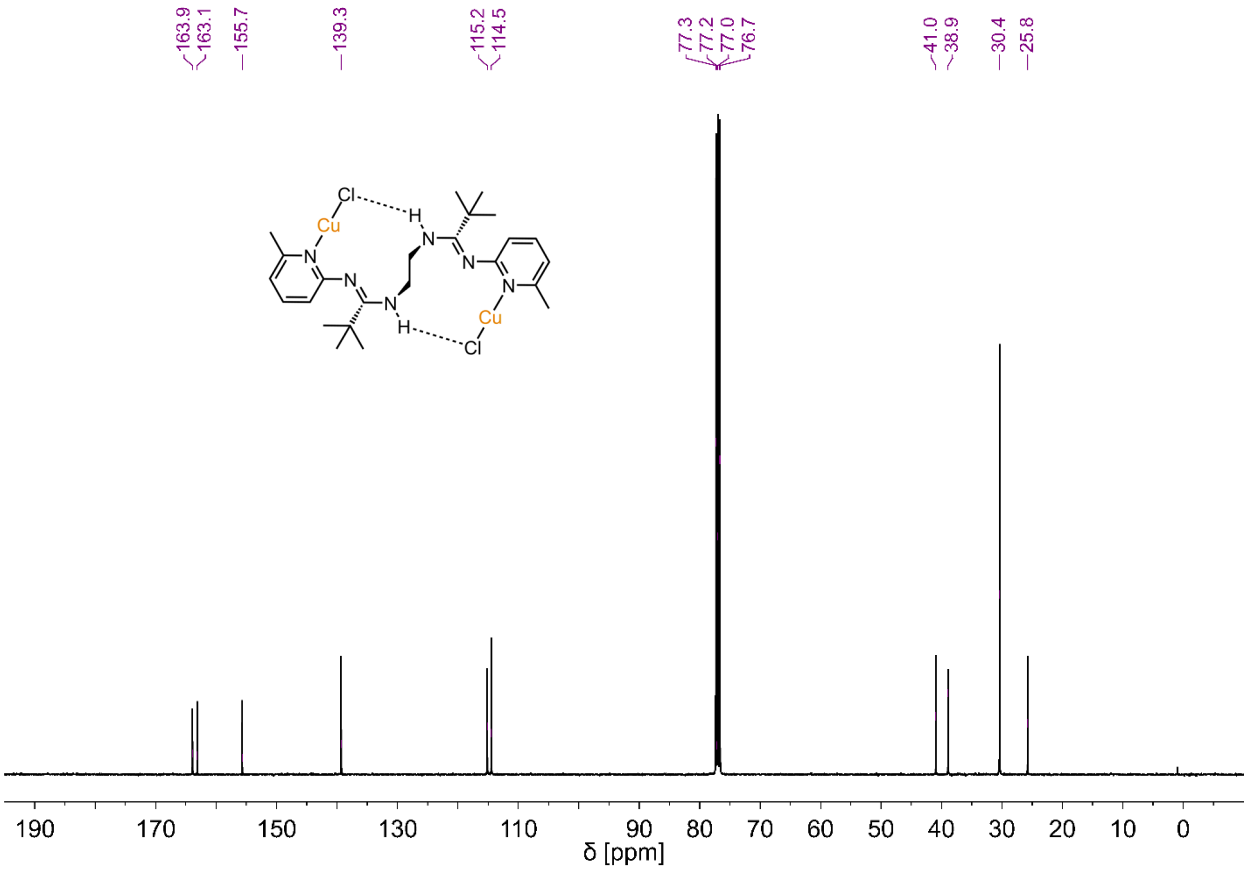

Figure S31: ^{13}C{^{1}H} NMR spectrum of **1** ($CDCl_3$, 100.6 MHz).

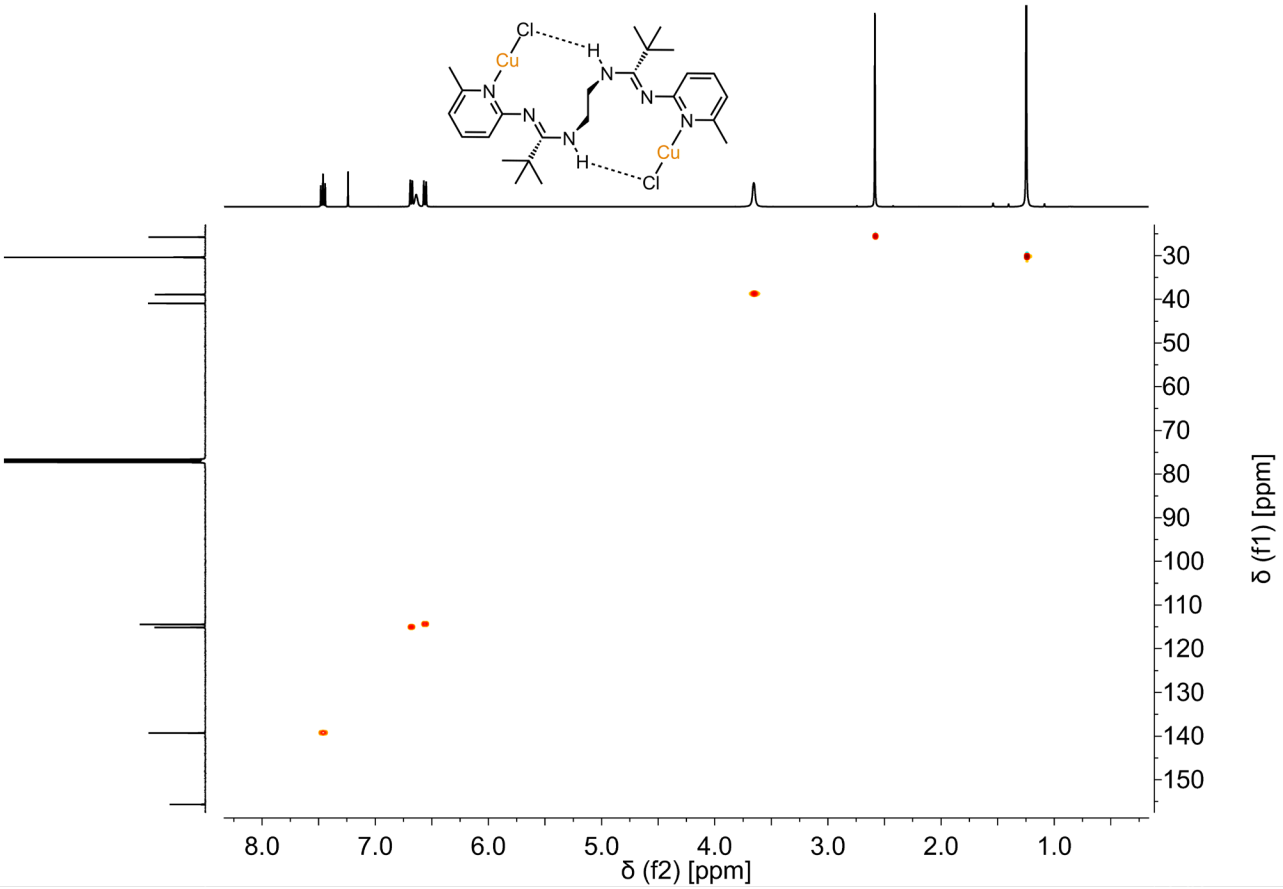

Figure S32: (^{1}H, ^{13}C)-HSQC NMR spectrum of **1** ($CDCl_3$, 100.6 MHz).

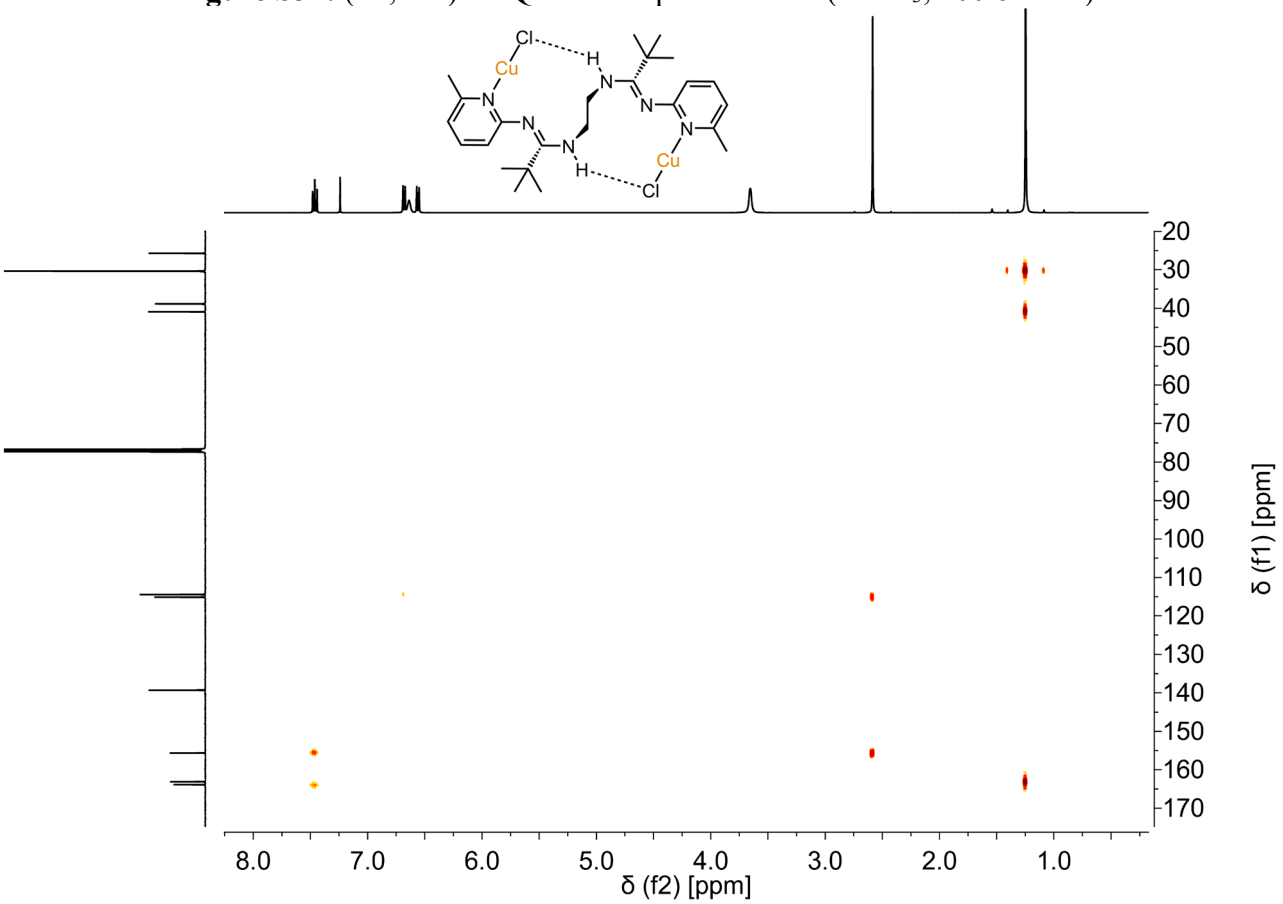

Figure S33: (^{1}H, ^{13}C)-HMBC NMR spectrum of **1** ($CDCl_3$, 100.6 MHz).

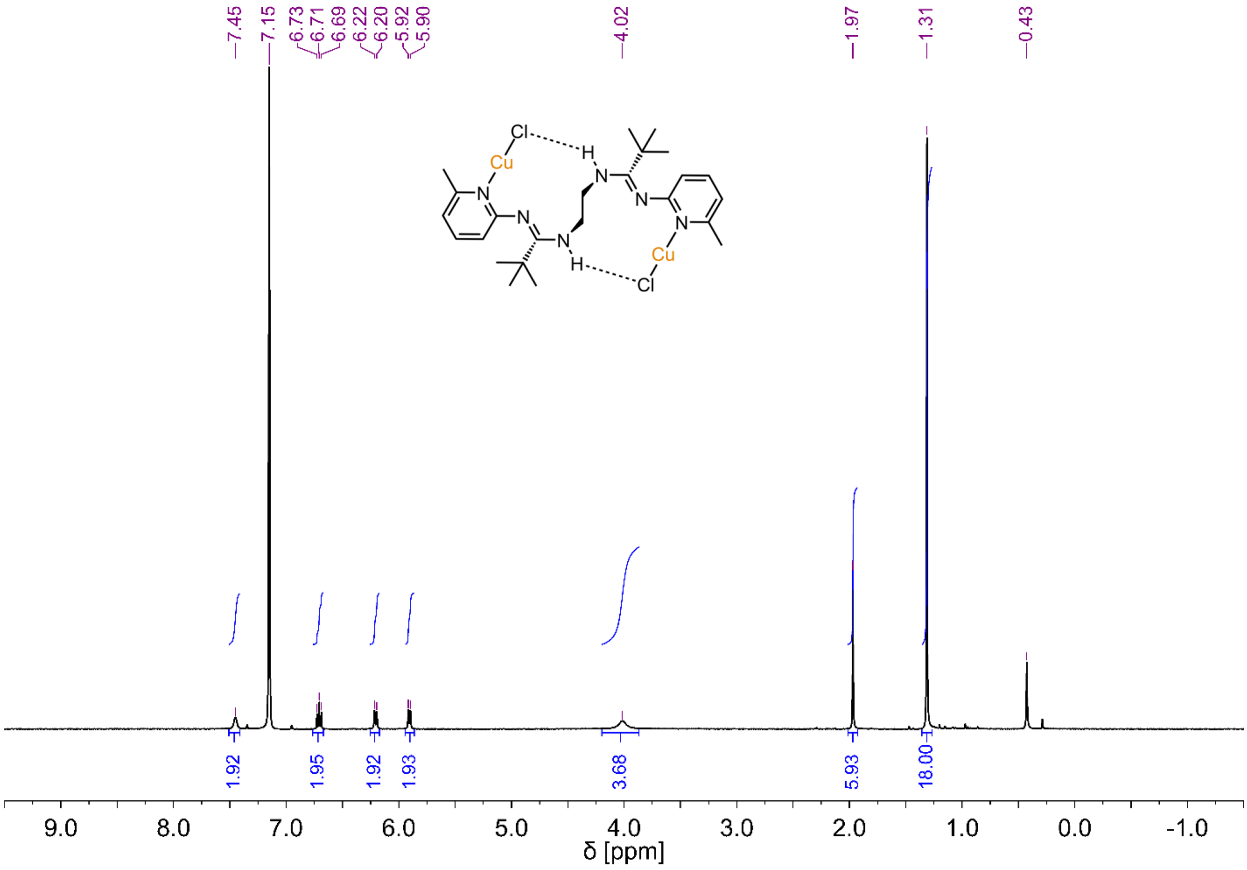

Figure S34: ^{1}H NMR spectrum of **1** (C_6D_6, 400.1 MHz).

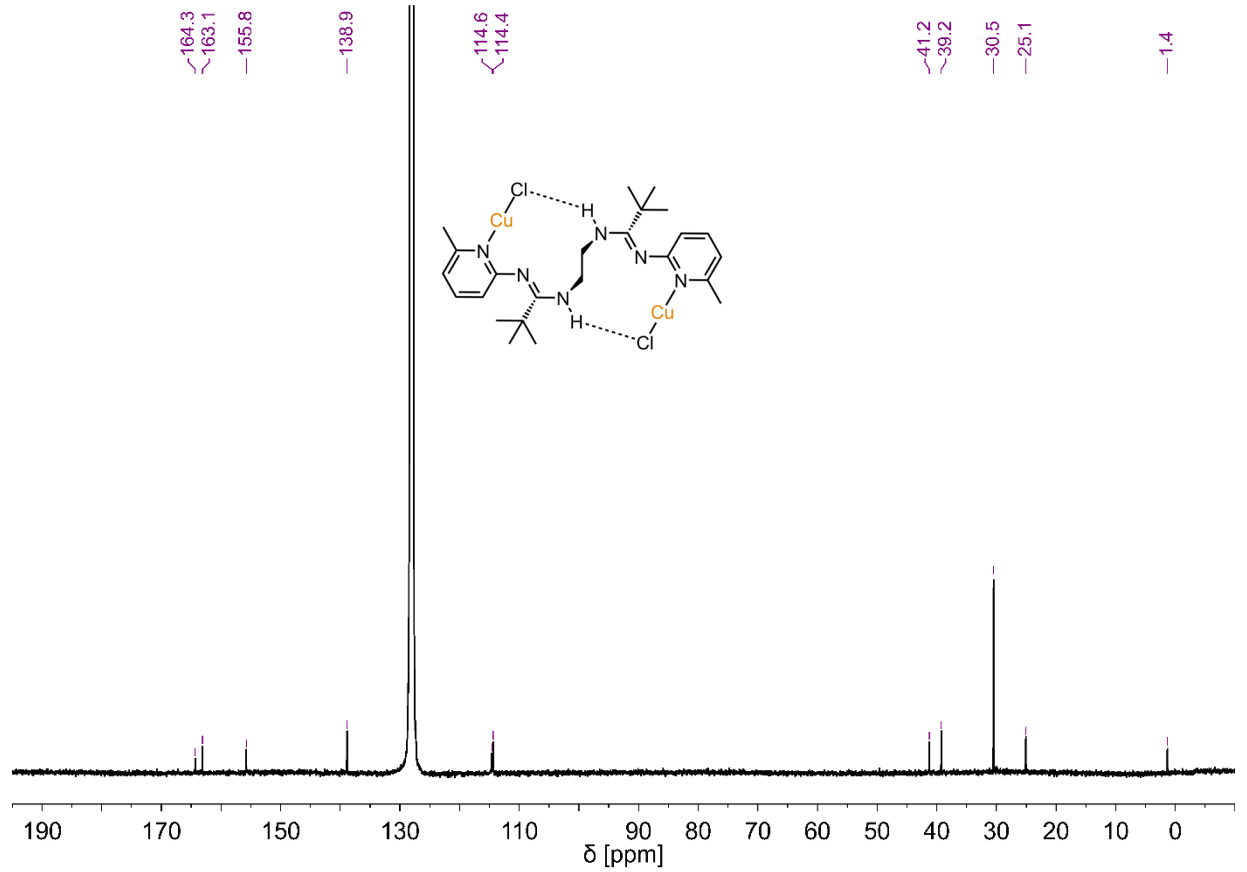

Figure S35: ^{13}C{^{1}H} NMR spectrum of **1** (C_6D_6, 100.6 MHz).

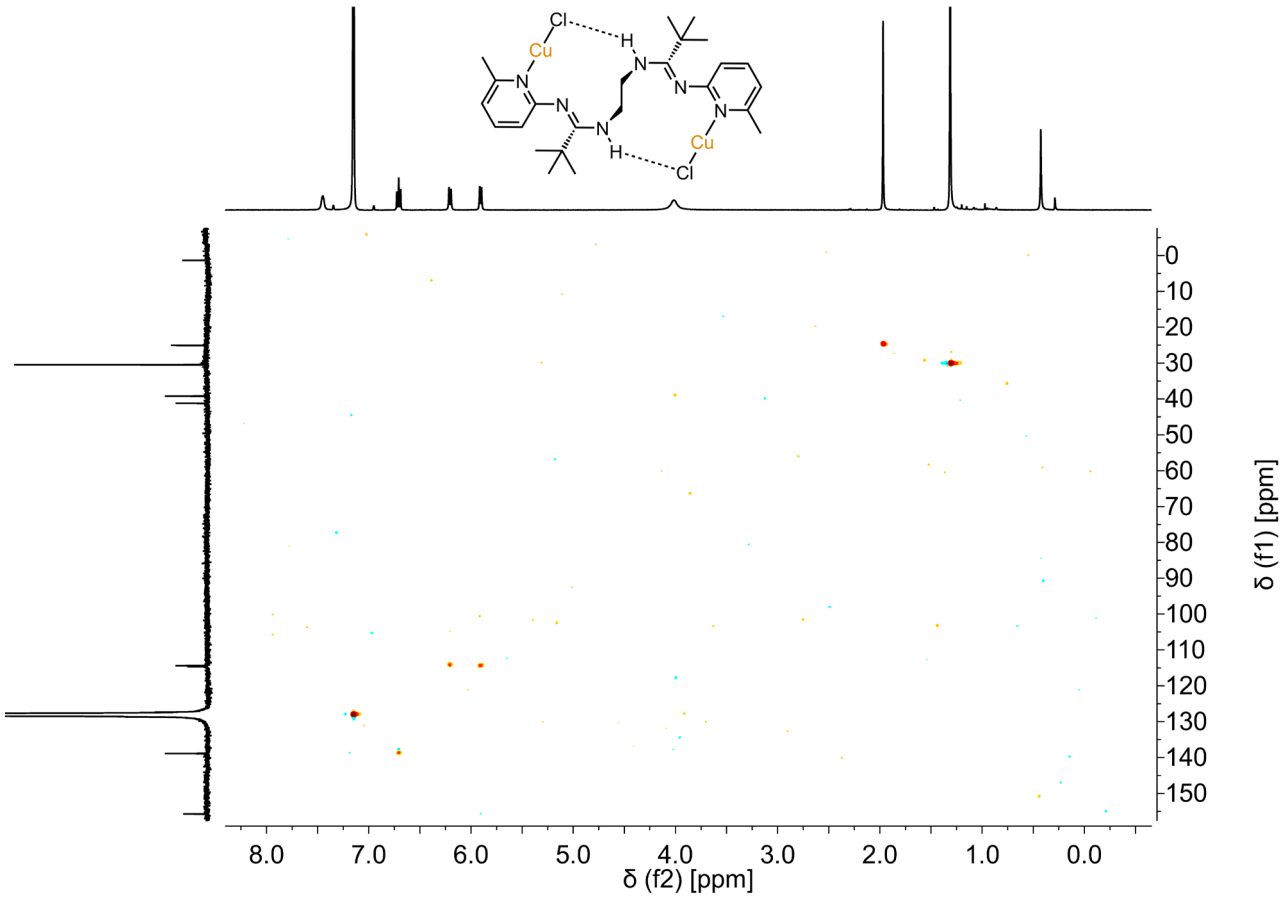

Figure S36: (^{1}H, ^{13}C)-HSQC NMR spectrum of **1** (C_6D_6, 100.6 MHz).

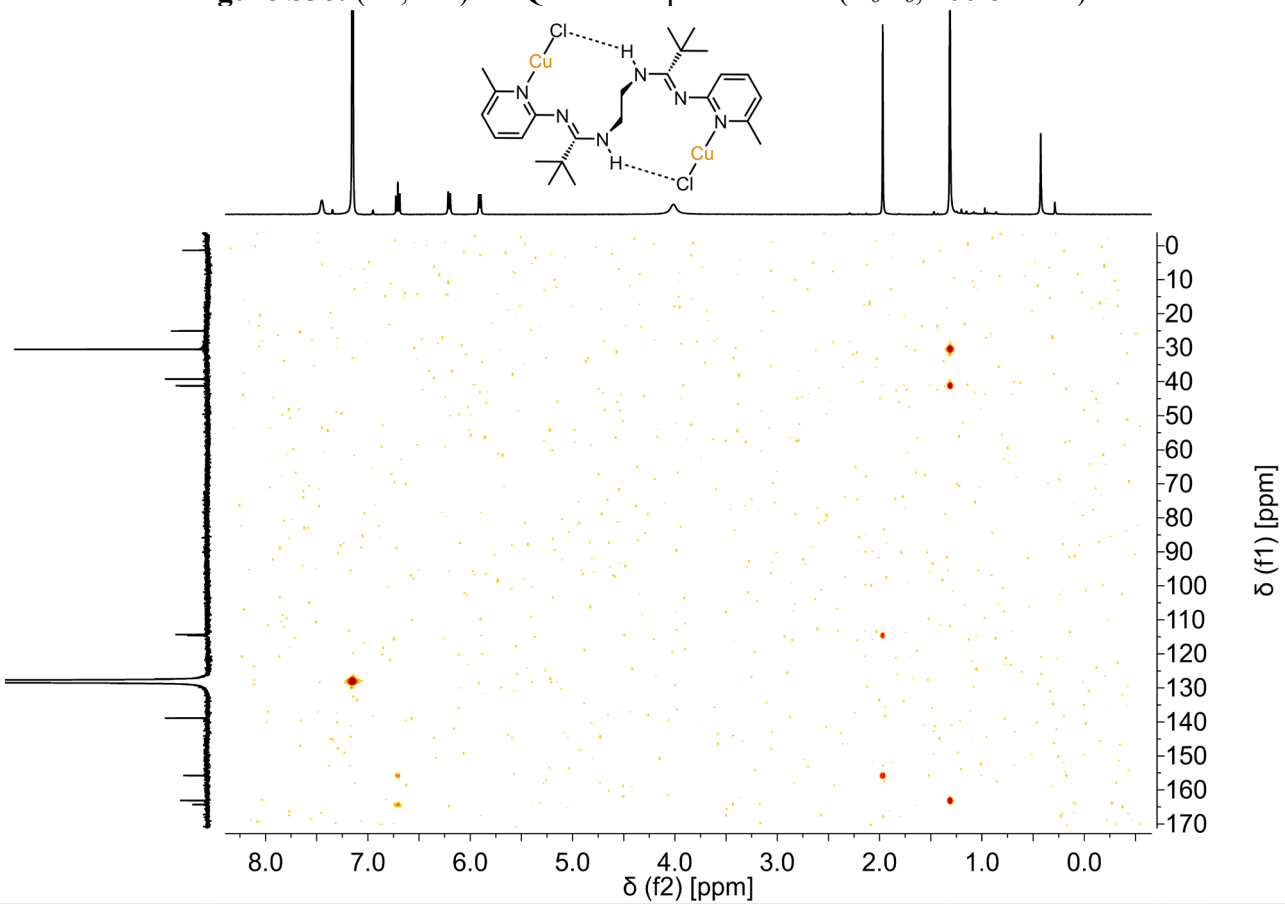

Figure S37: (^{1}H, ^{13}C)-HMBC NMR spectrum of **1** (C_6D_6, 100.6 MHz).

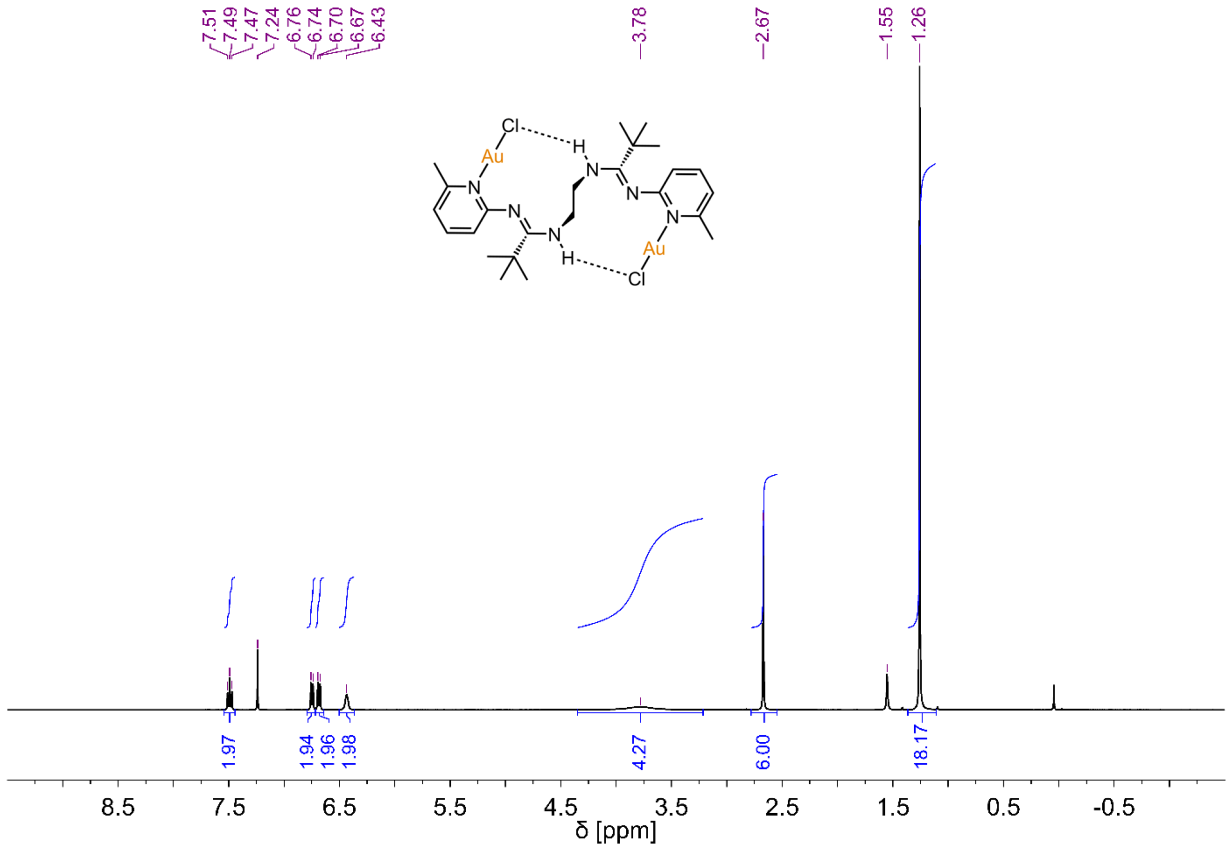

Figure S38: ^{1}H NMR spectrum of **2** ($CDCl_3$, 400.1 MHz).

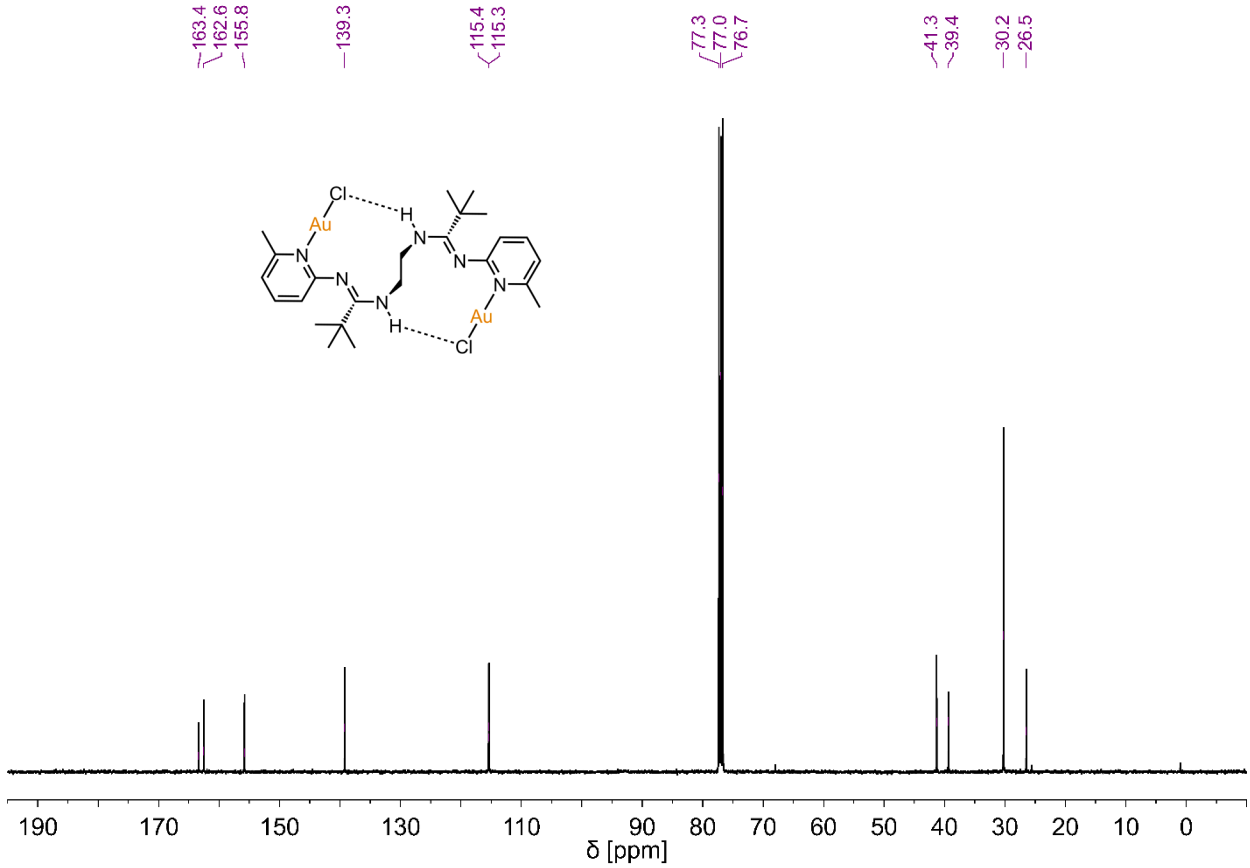

Figure S39: $^{13}C\{^{1}H\}$ NMR spectrum of **2** ($CDCl_3$, 100.6 MHz).

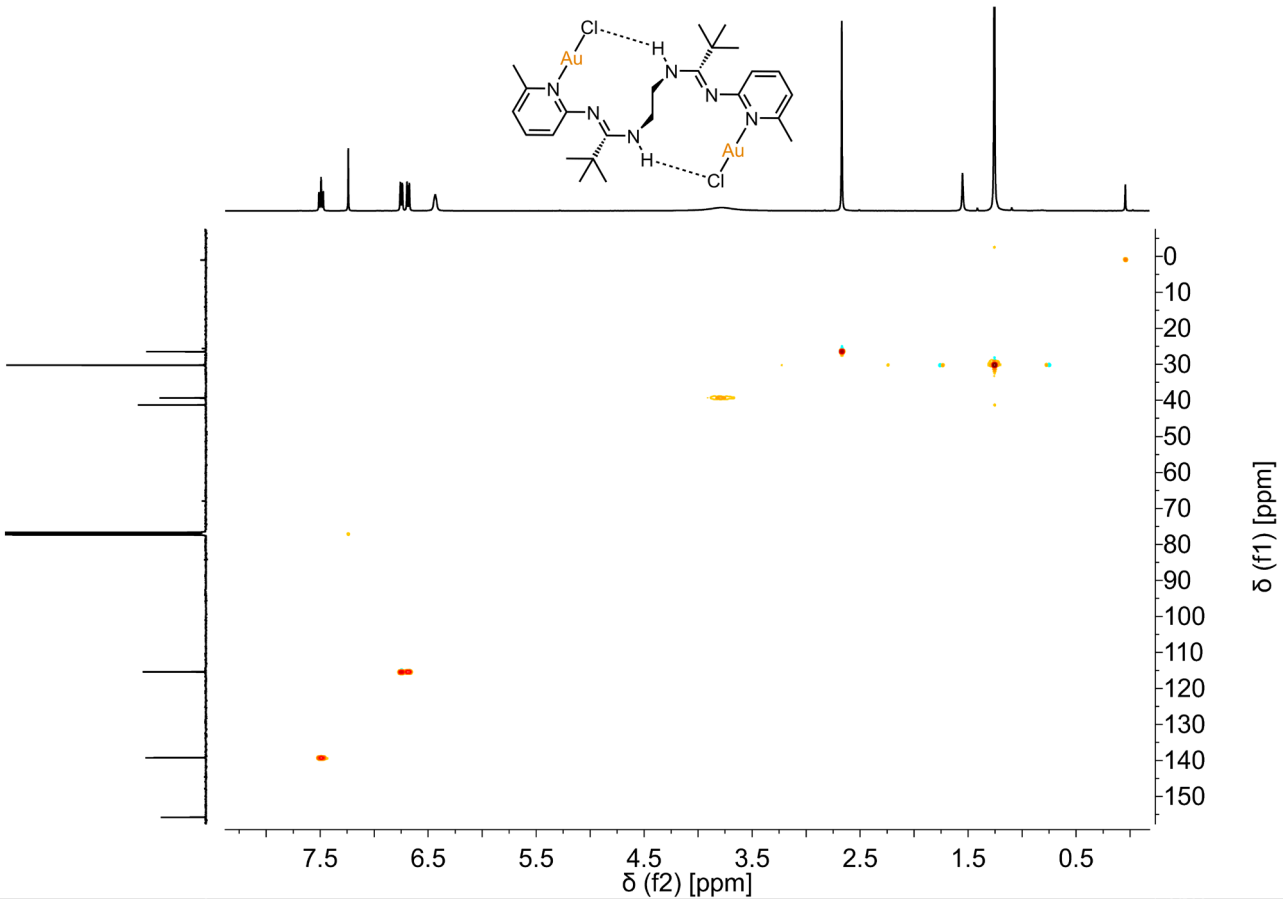

Figure S40: (^{1}H, ^{13}C)-HSQC NMR spectrum of **2** ($CDCl_3$, 100.6 MHz).

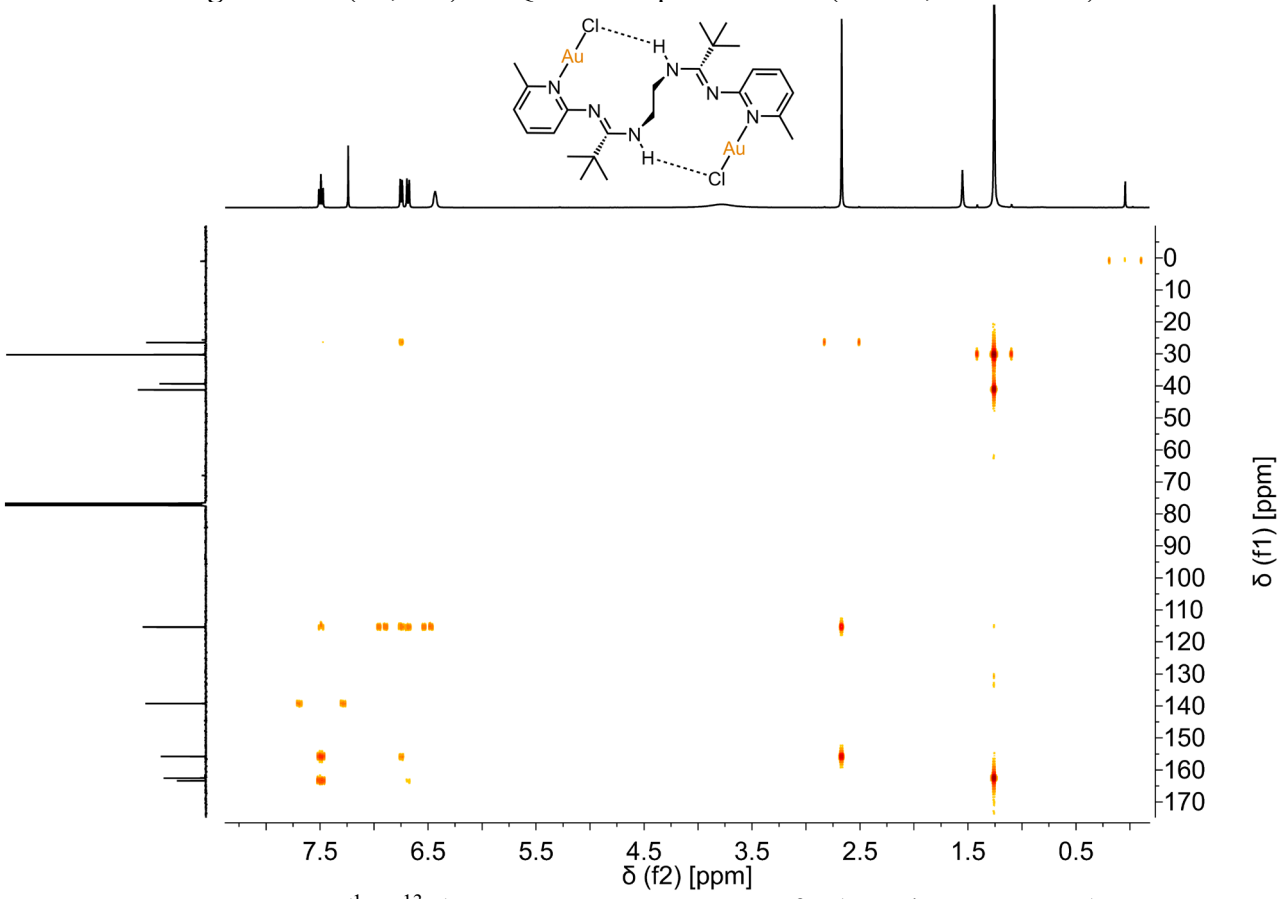

Figure S41: (^{1}H, ^{13}C)-HMBC NMR spectrum of **2** ($CDCl_3$, 100.6 MHz).

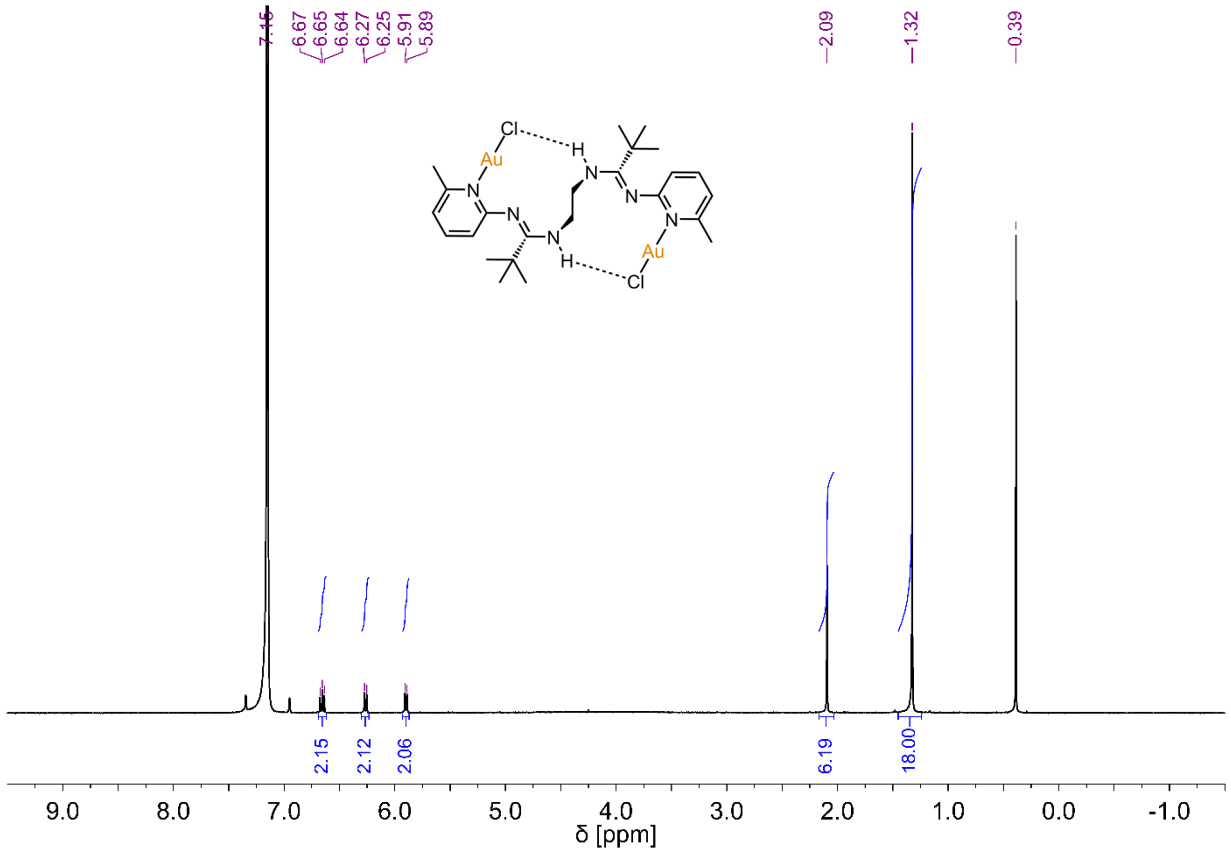

Figure S42: ^{1}H NMR spectrum of **2** (C_6D_6, 400.1 MHz).

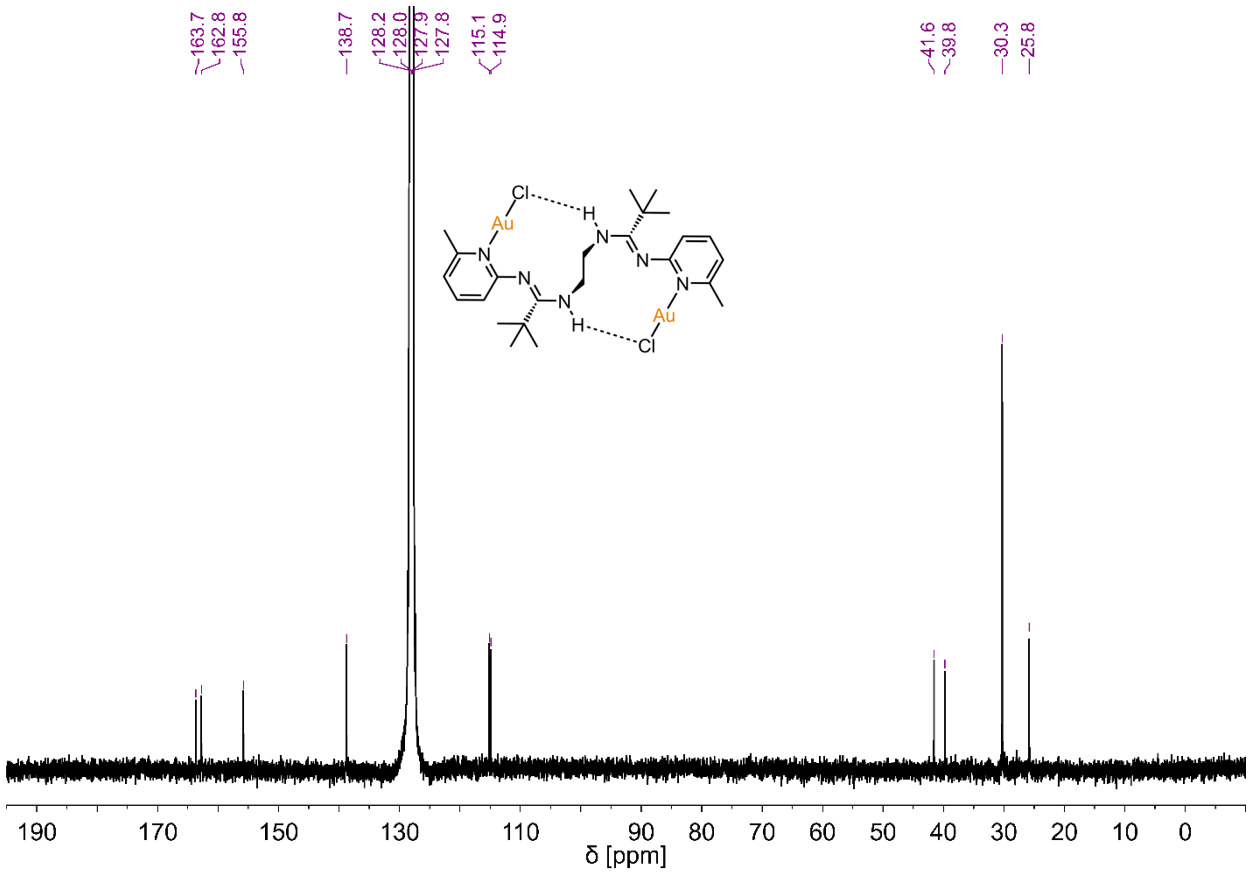

Figure S43: ^{13}C{^{1}H} NMR spectrum of **2** (C_6D_6, 100.6 MHz).

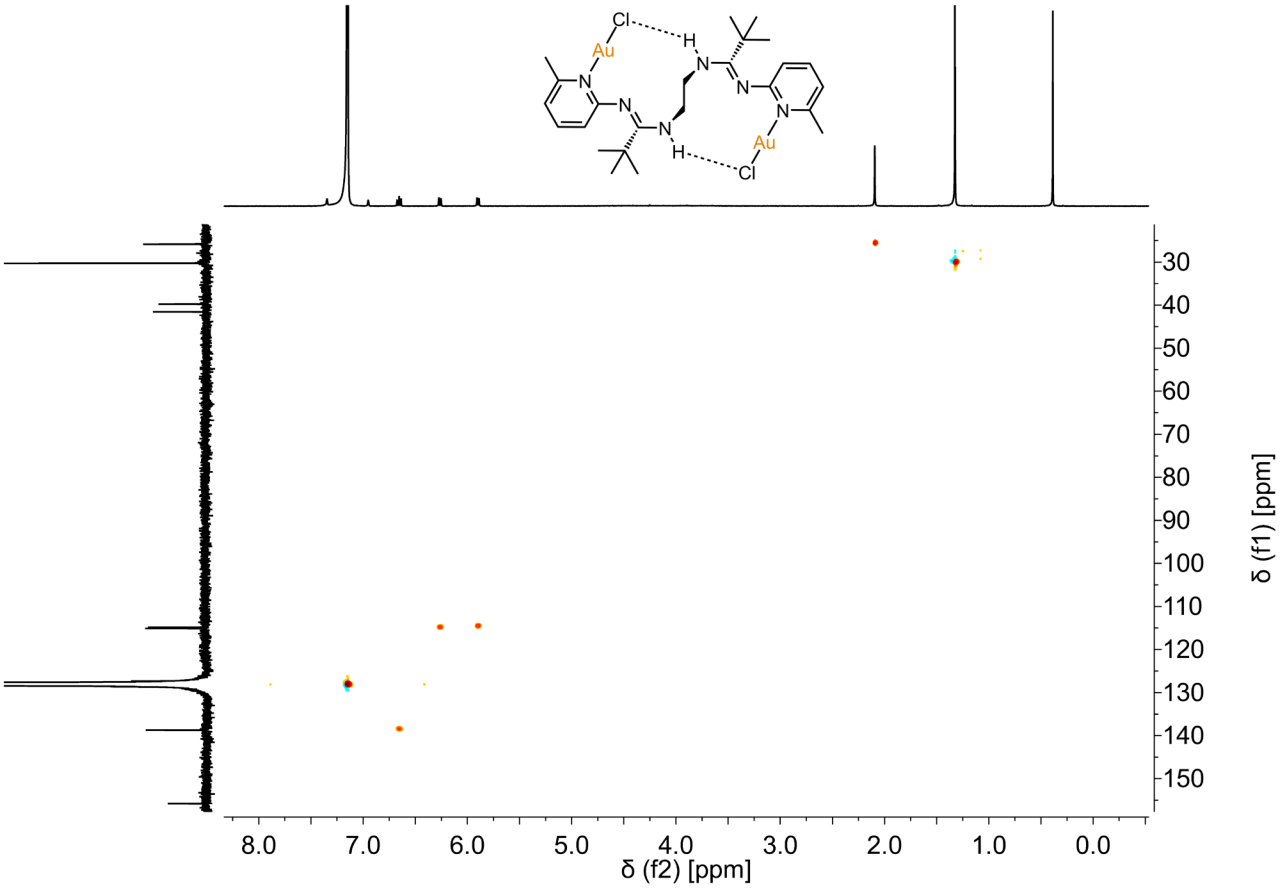

Figure S44: (^{1}H, ^{13}C)-HSQC NMR spectrum of **2** (C_6D_6, 100.6 MHz).

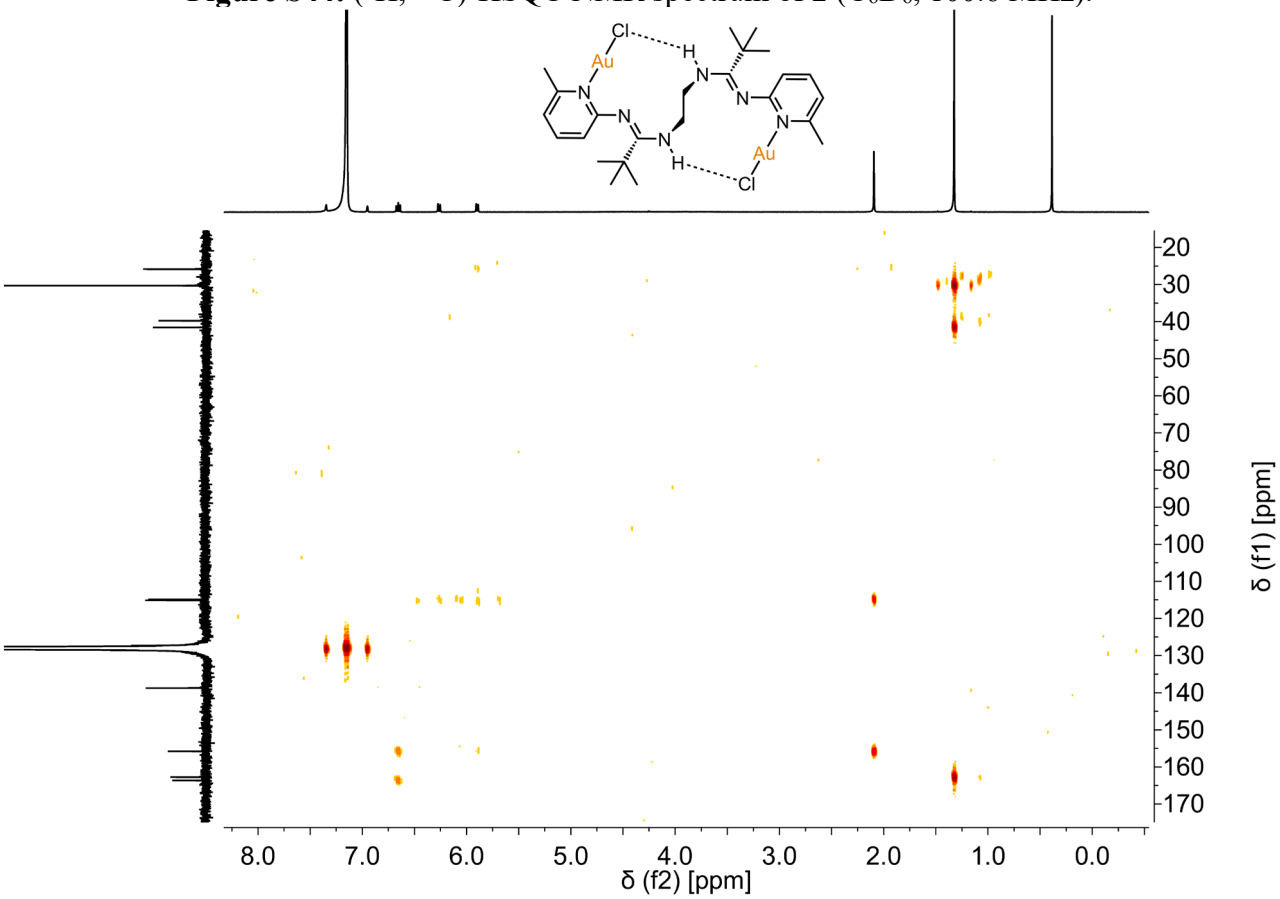

Figure S45: (^{1}H, ^{13}C)-HMBC NMR spectrum of **2** (C_6D_6, 100.6 MHz).

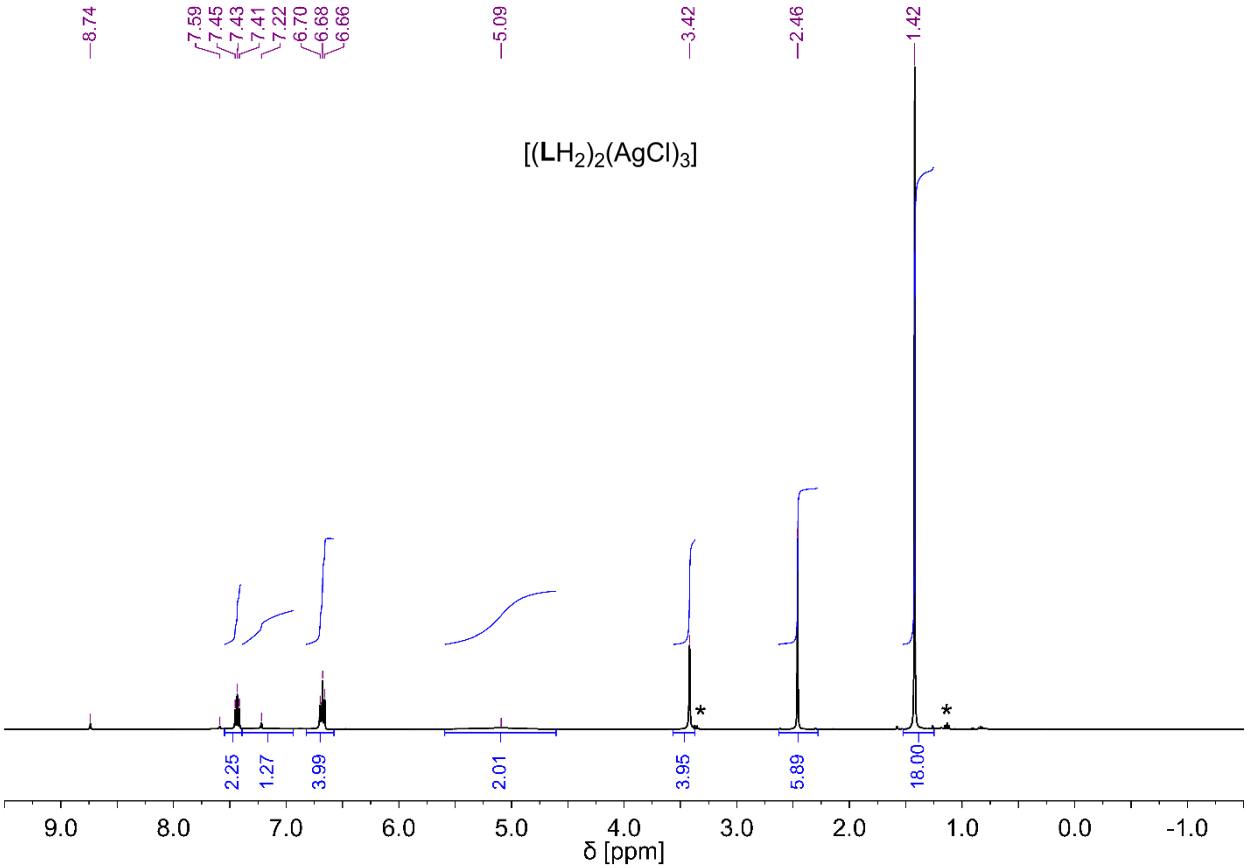

Figure S46: ^{1}H NMR spectrum of **3'** (C_5D_5N, 400.1 MHz, *) residual diethyl ether).

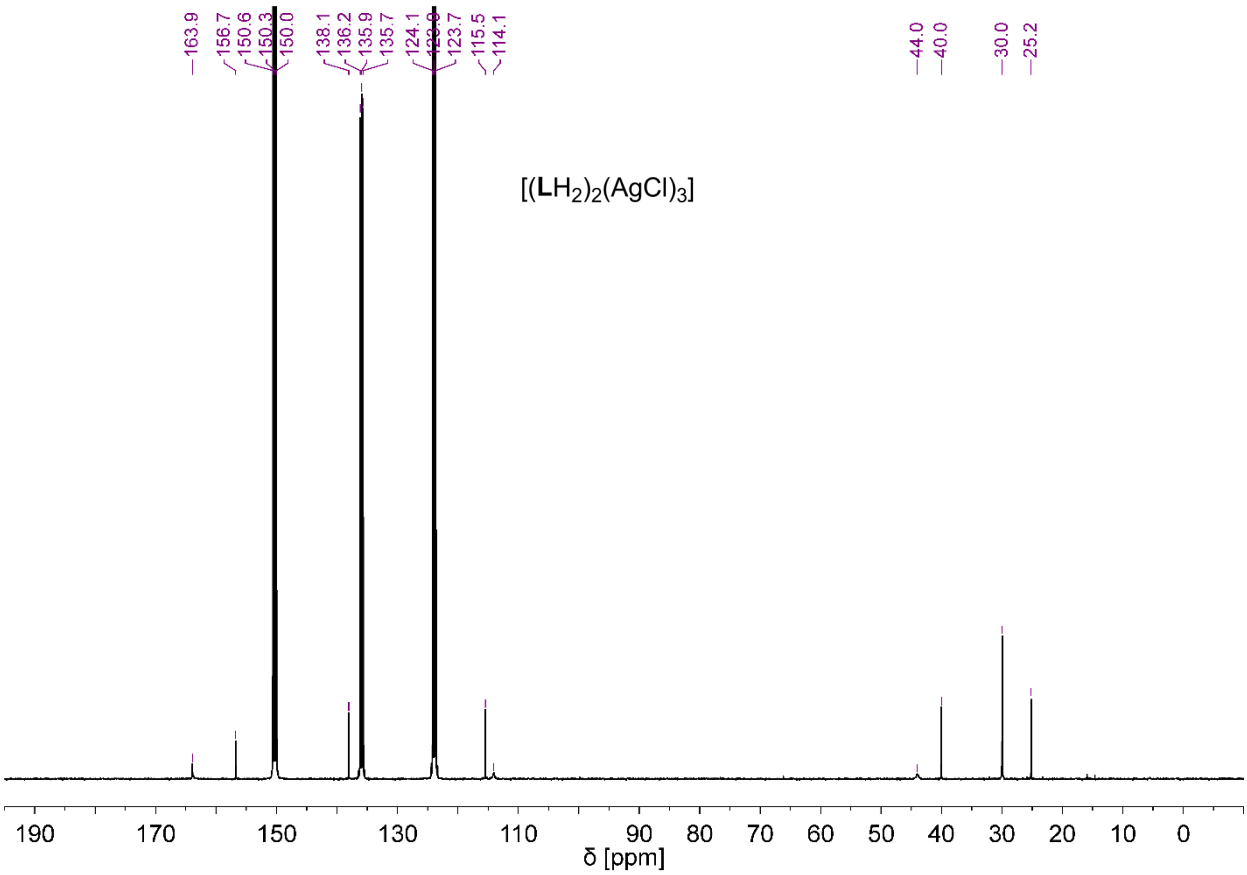

Figure S47: ^{13}C{^{1}H} NMR spectrum of **3'** (C_5D_5N, 100.6 MHz).

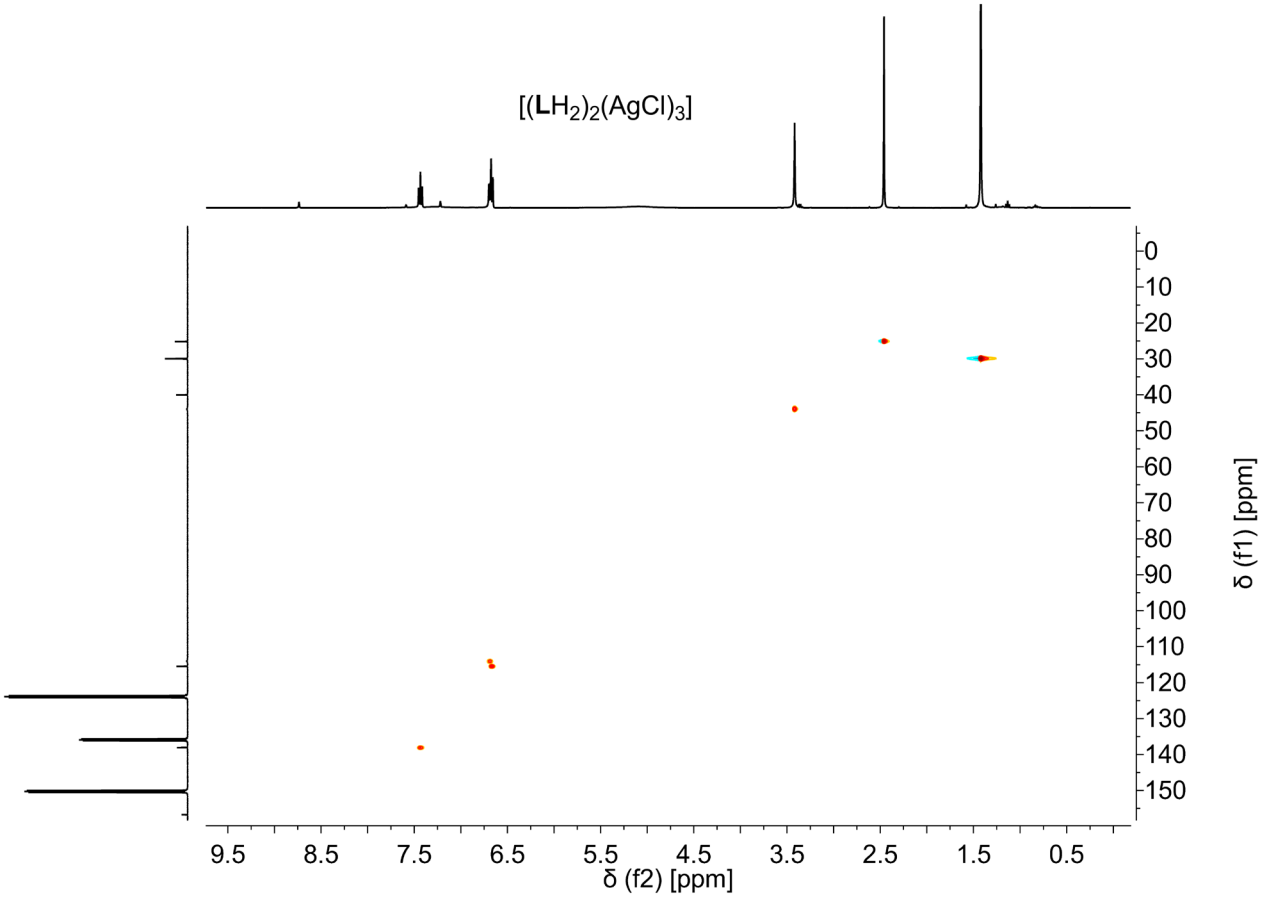

Figure S48: (^{1}H, ^{13}C)-HSQC NMR spectrum of **3'** (C_5D_5N, 100.6 MHz).

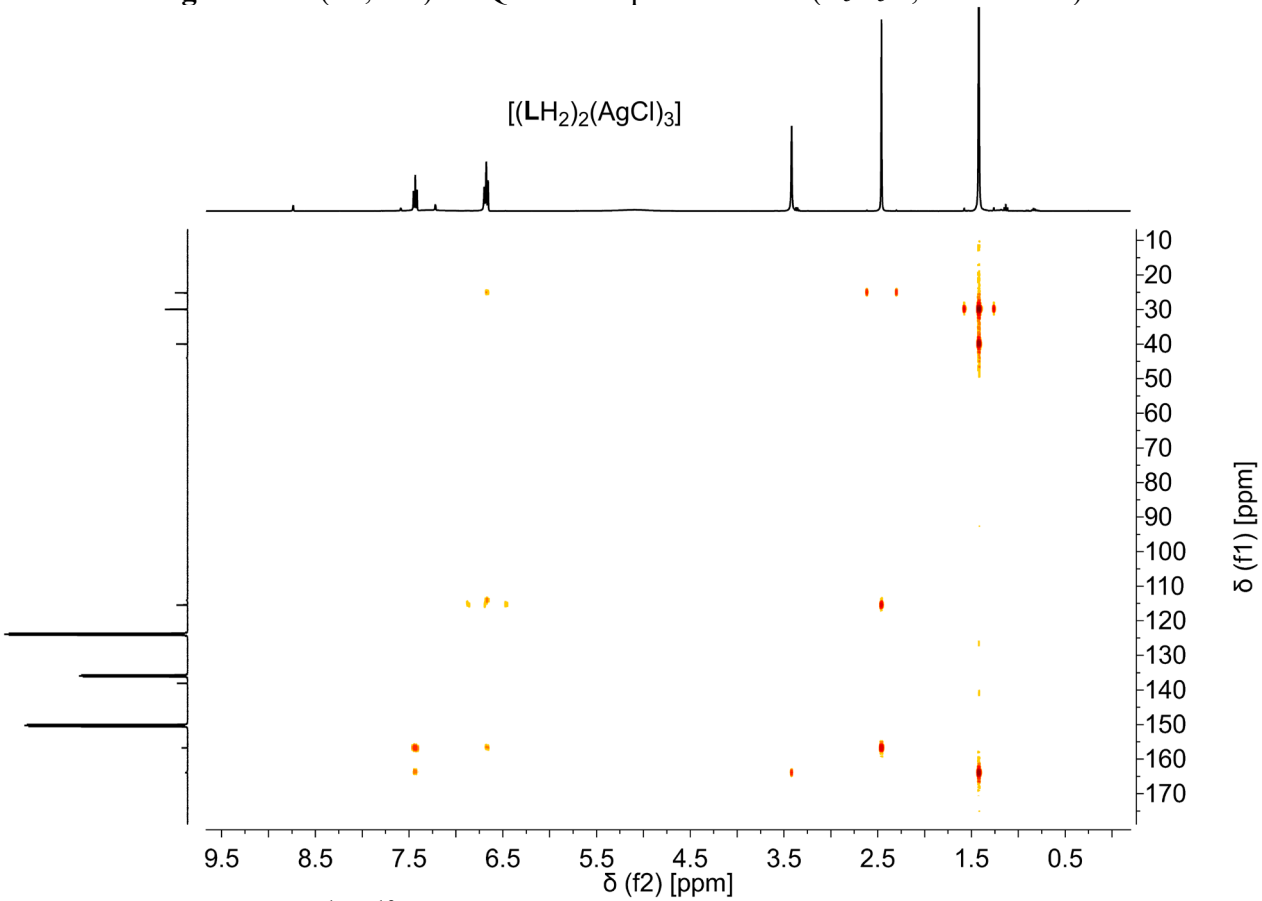

Figure S49: (^{1}H, ^{13}C)-HMBC NMR spectrum of **3'** (C_5D_5N, 100.6 MHz).

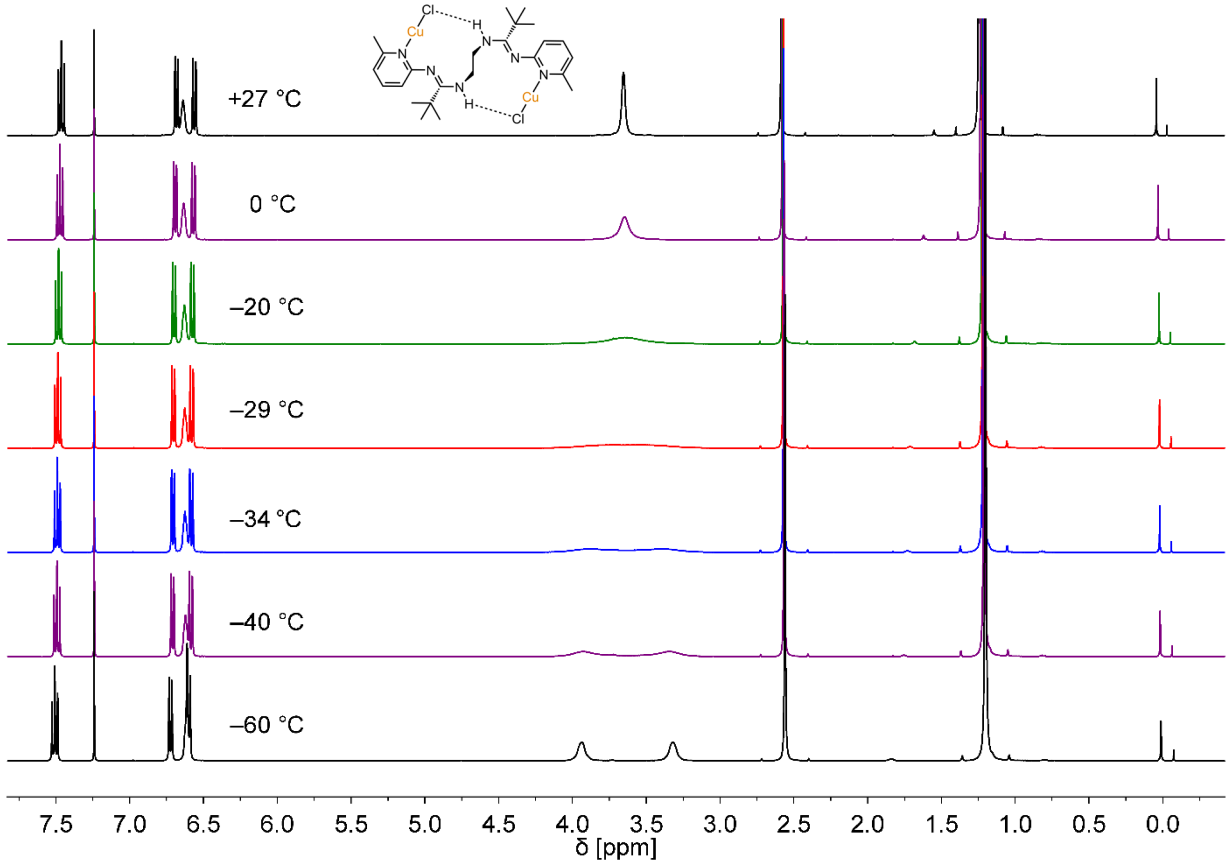

Figure S50: Variable-temperature ^{1}H NMR spectra of **1** ($CDCl_3$, 400.1 MHz).

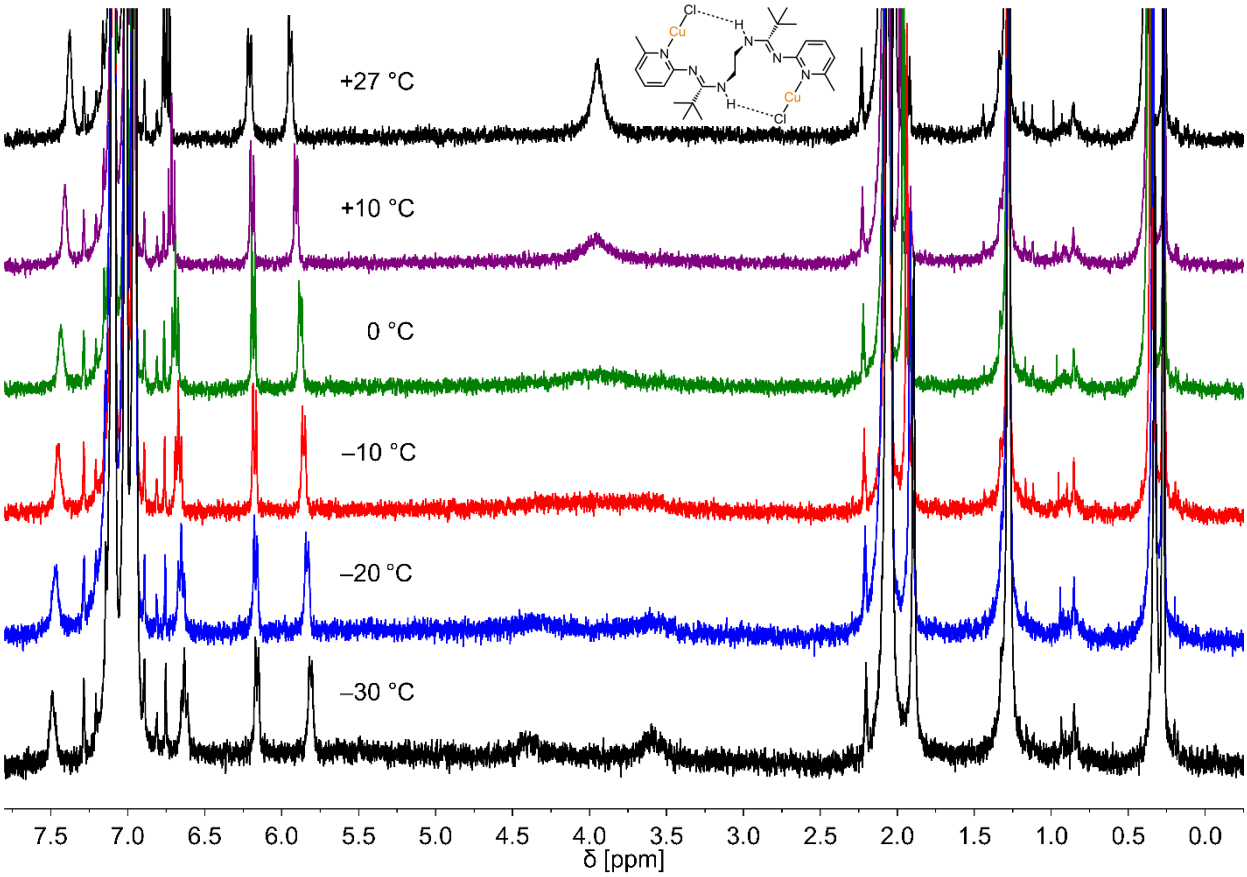

Figure S51: Variable-temperature ^{1}H NMR spectra of **1** (C_7D_8, 400.1 MHz).

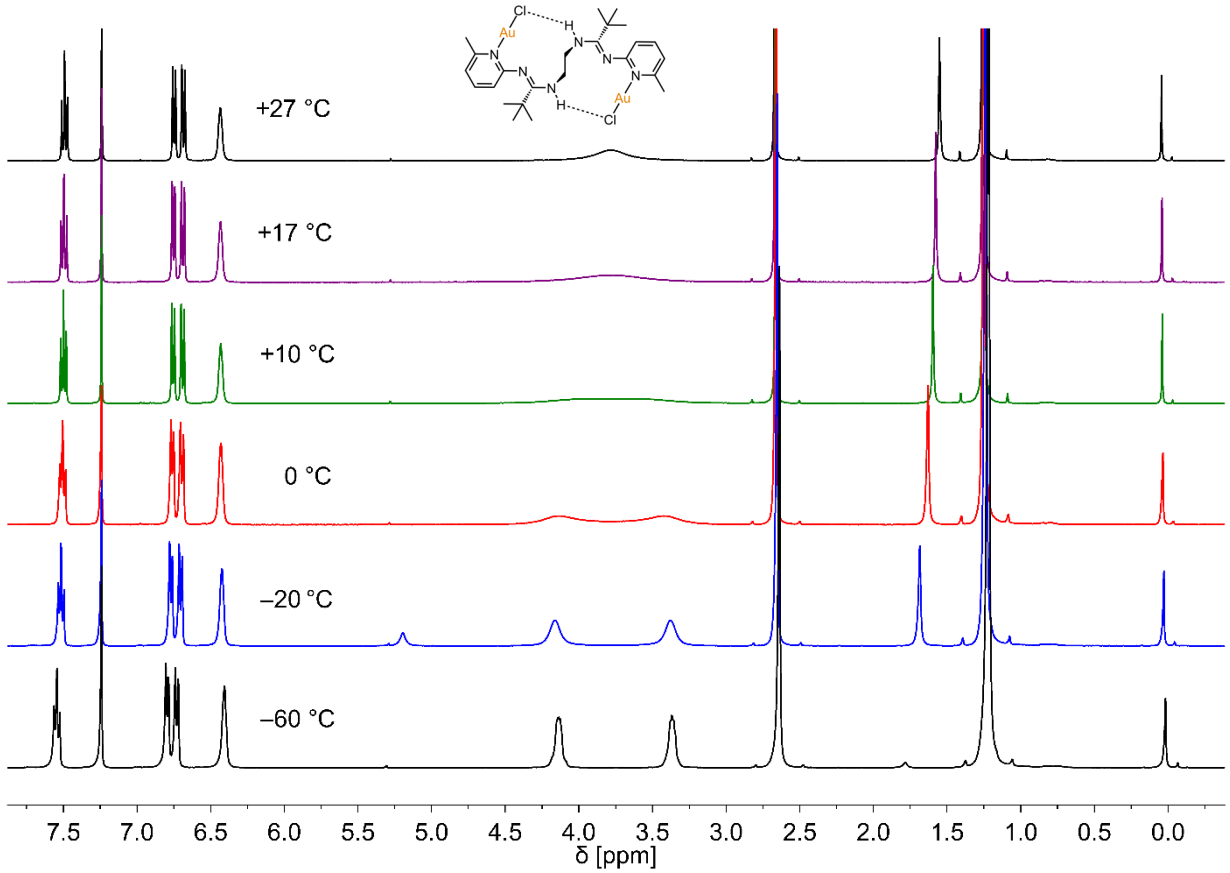

Figure S52: Variable-temperature ^{1}H NMR spectra of **2** ($CDCl_3$, 400.1 MHz).

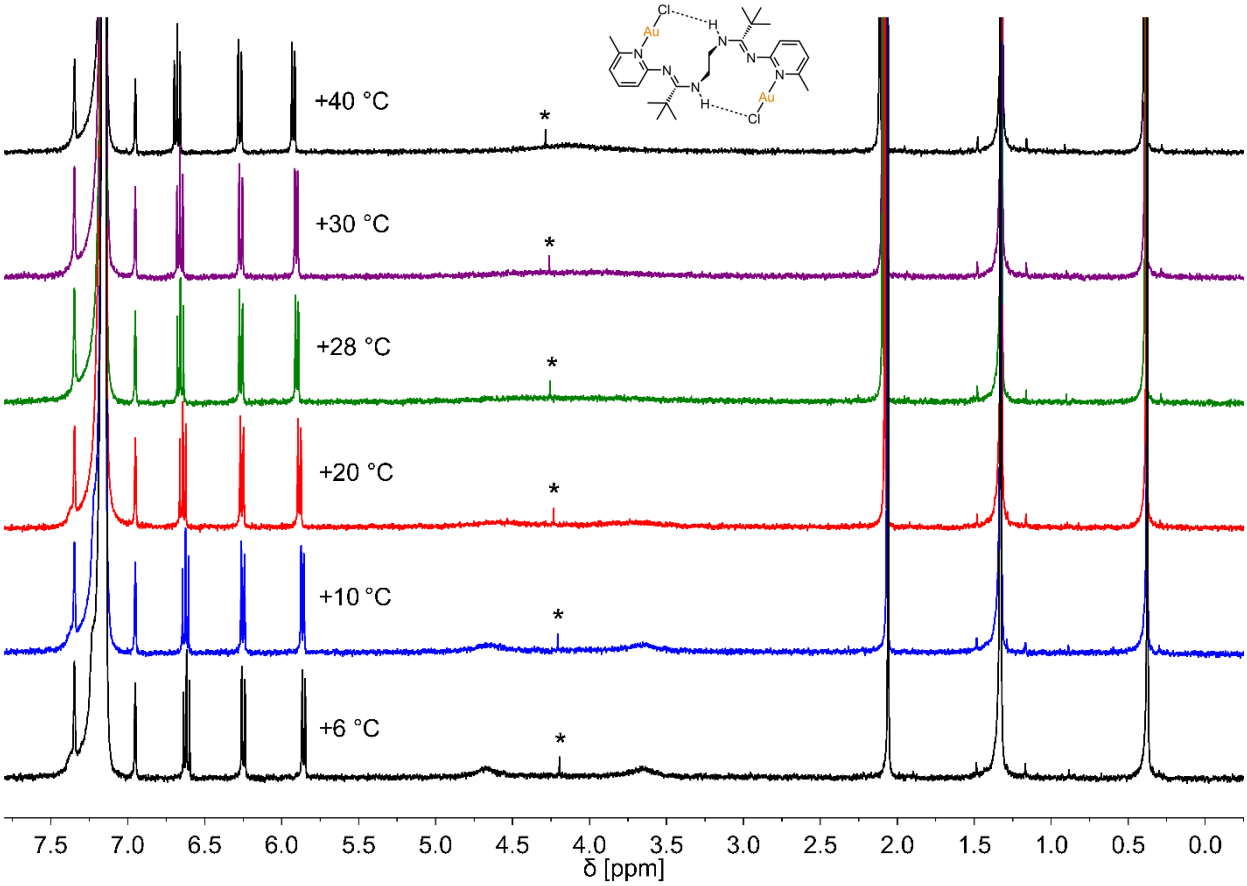

Figure S53: Variable-temperature ^{1}H NMR spectra of **2** (C_6D_6, 400.1 MHz, *) residual CH_2Cl_2).

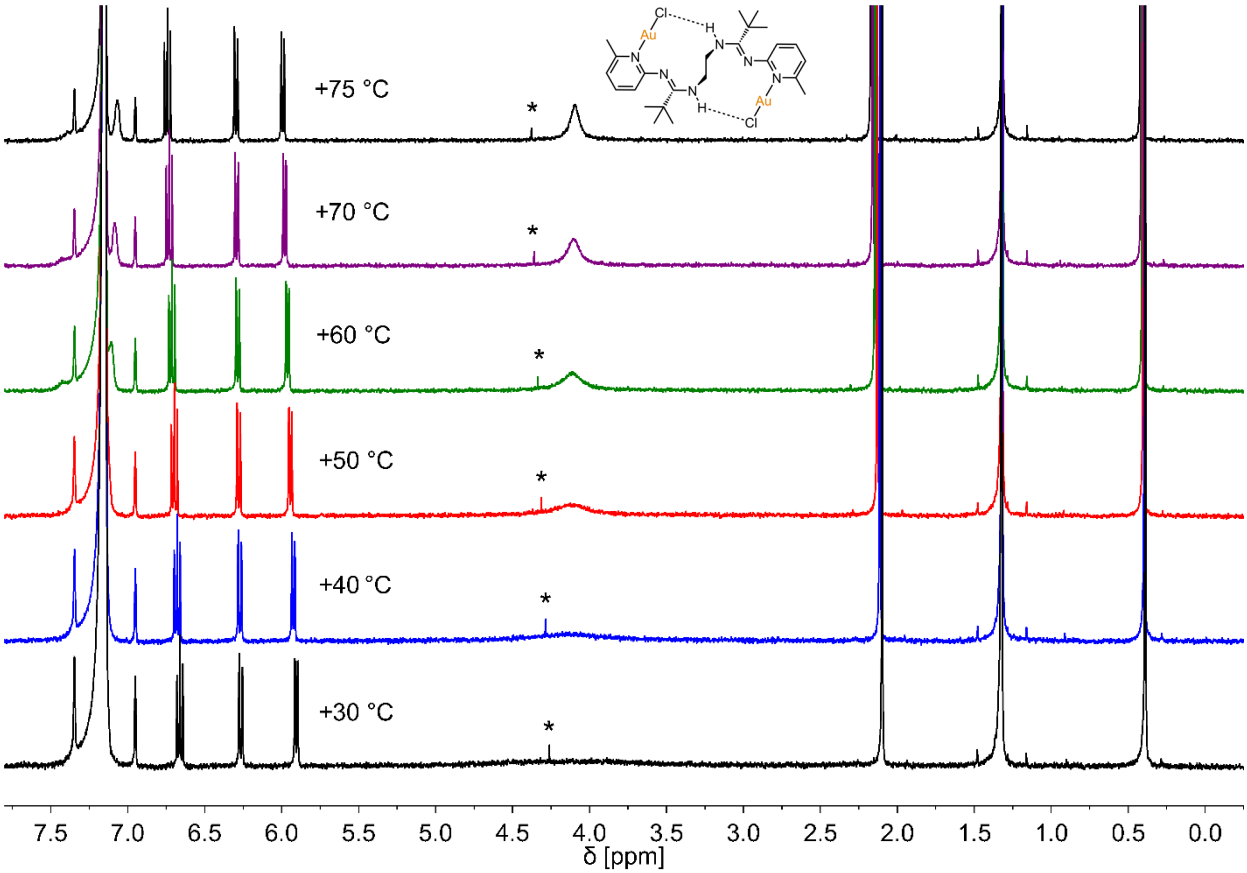

Figure S54: Variable-temperature ^{1}H NMR spectra of **2** (C_6D_6, 400.1 MHz, *) residual CH_2Cl_2).

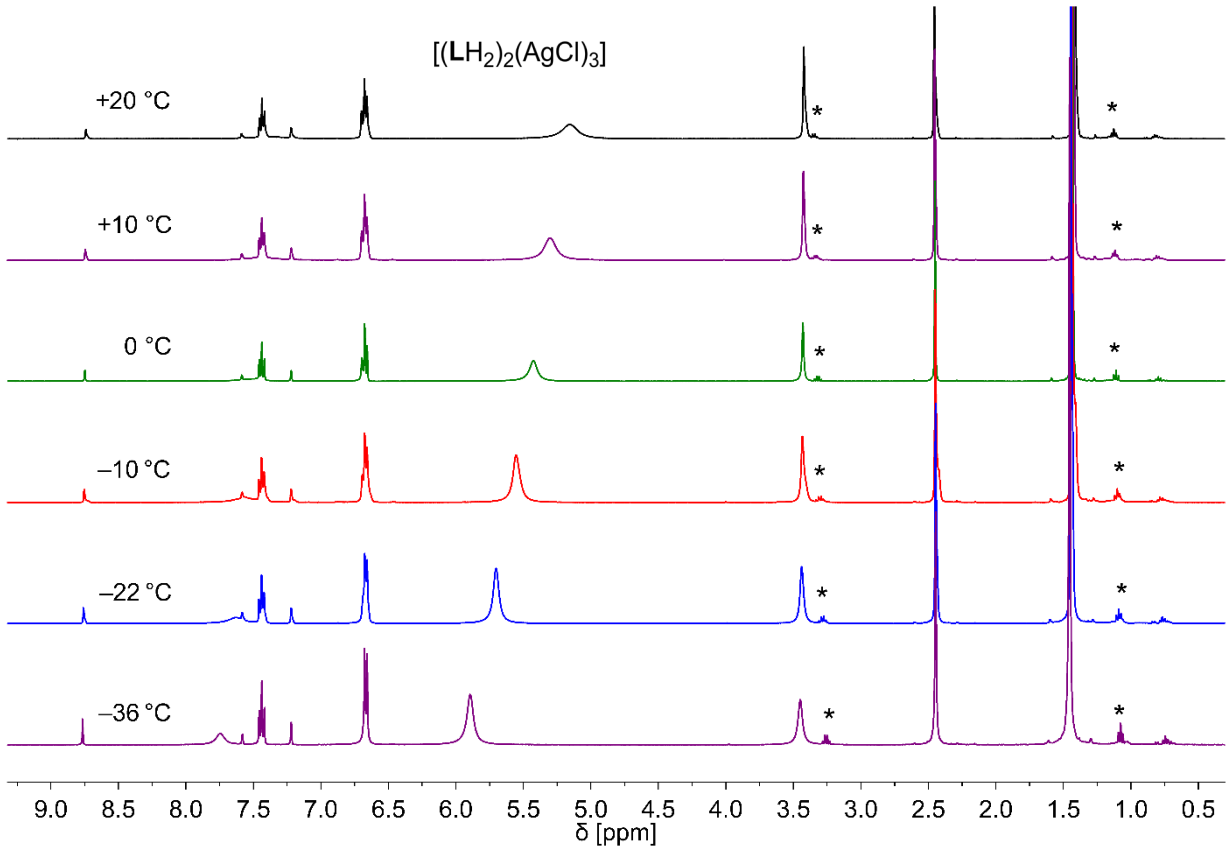

Figure S55: Variable-temperature ^{1}H NMR spectra of **3'** (C_5D_5N, 400.1 MHz, *) residual diethyl ether).

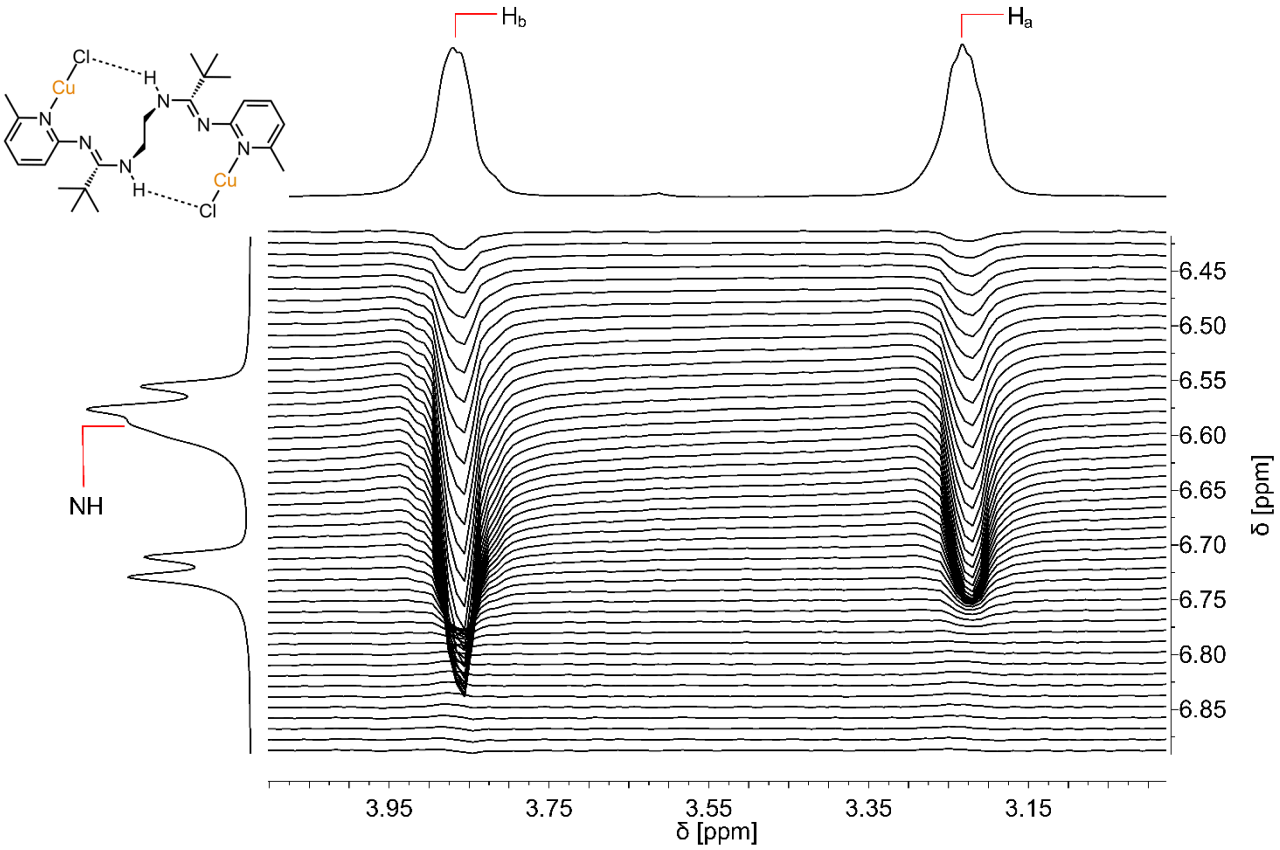

Figure S56: CH_2/NH cross peaks of the NOESY NMR spectrum of **1** (CD_2Cl_2, 400.1 MHz, –90 °C).

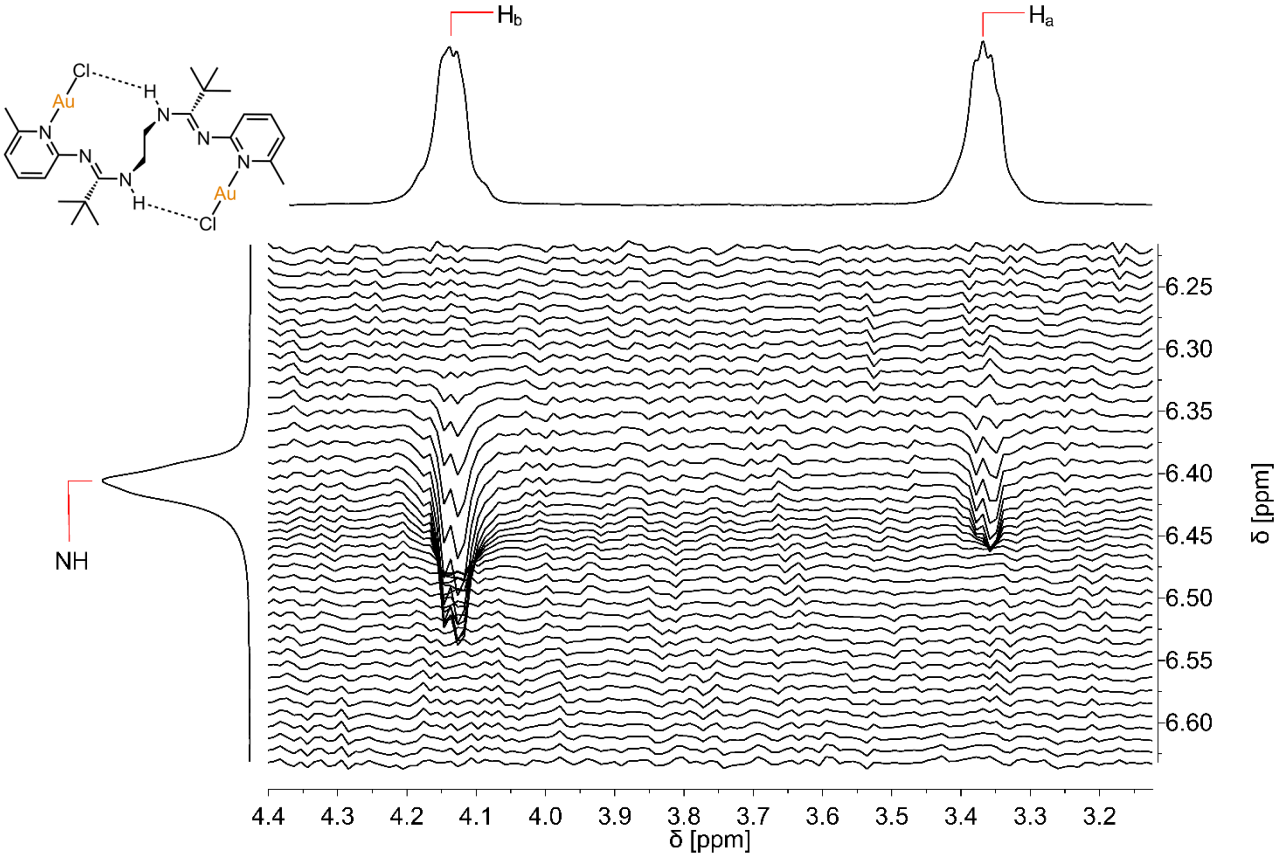

Figure S57: CH_2/NH cross peaks of the NOESY NMR spectrum of **2** ($CDCl_3$, 400.1 MHz, –60 °C).

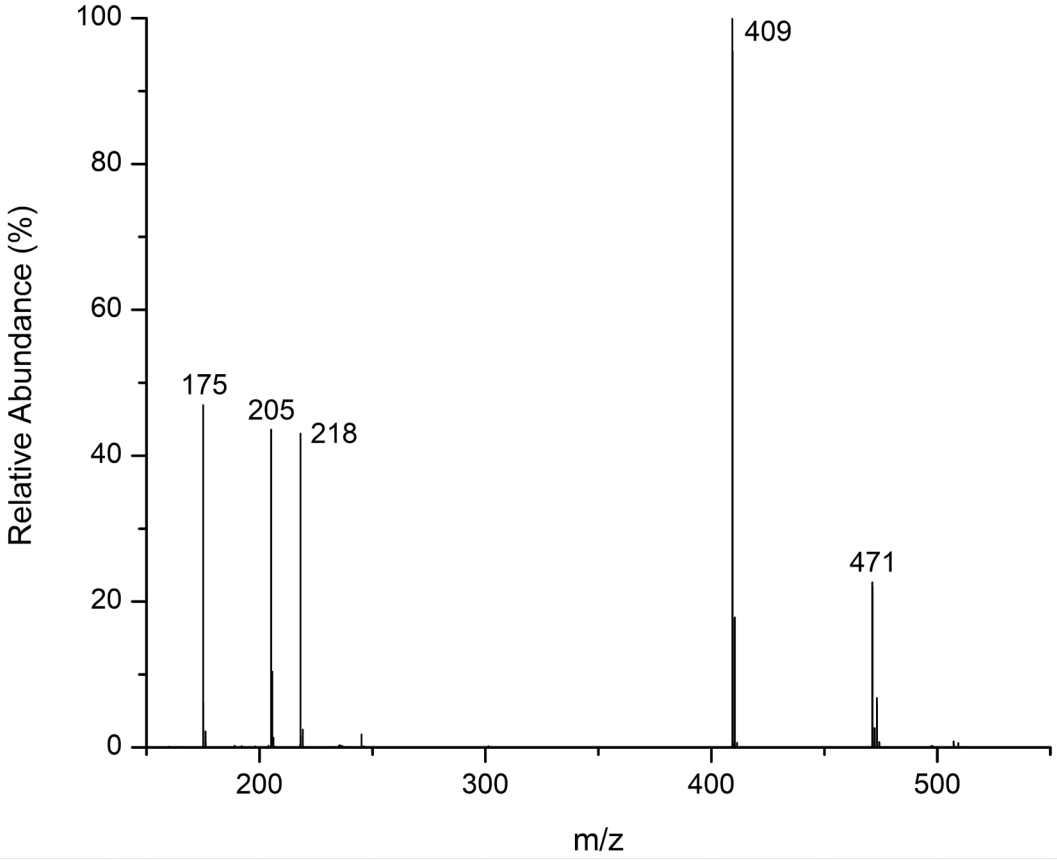

Figure S58: ESI(+)-MS spectrum of **1**.

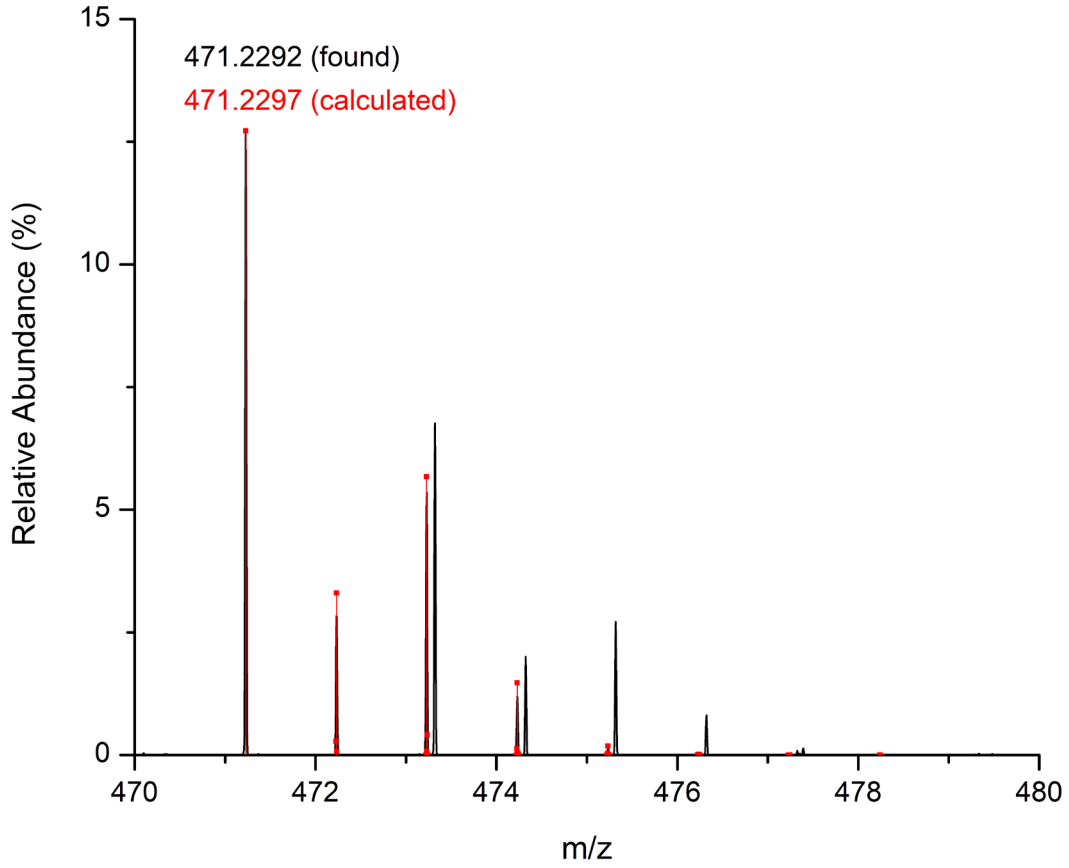

Figure S59: High-resultion ESI(+)-MS peak region of $[\mathbf{L}H_2Cu]^+$ (black) and calculated isotopic pattern (red).

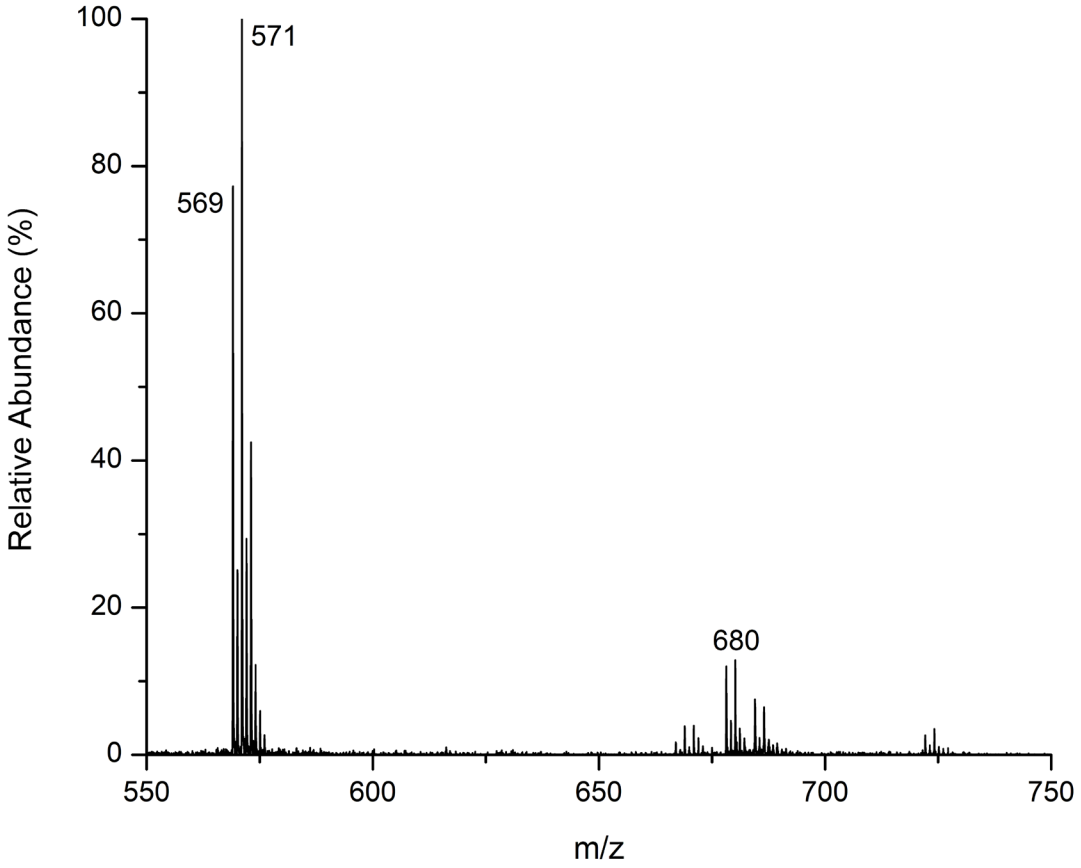

Figure S60: MALDI(+)-MS spectrum of **1**.

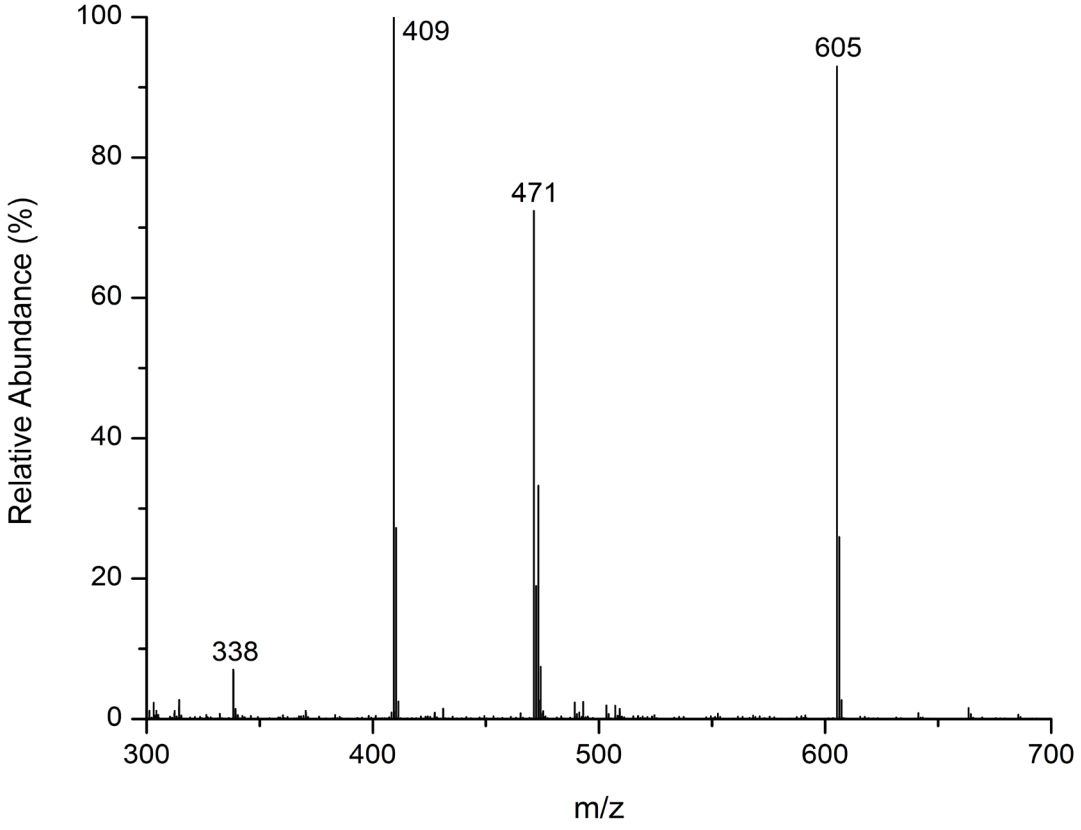

Figure S61: ESI(+)-MS spectrum of **2**.

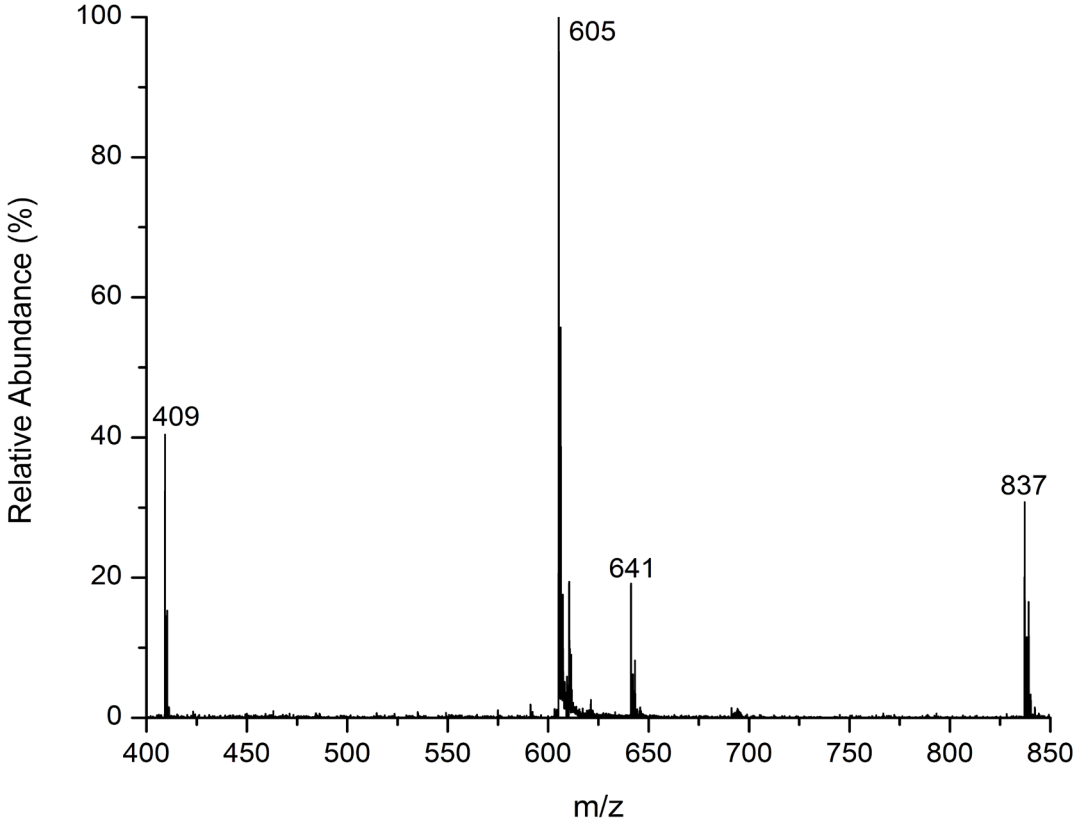

Figure S62: MALDI(+)-MS spectrum of **2**.

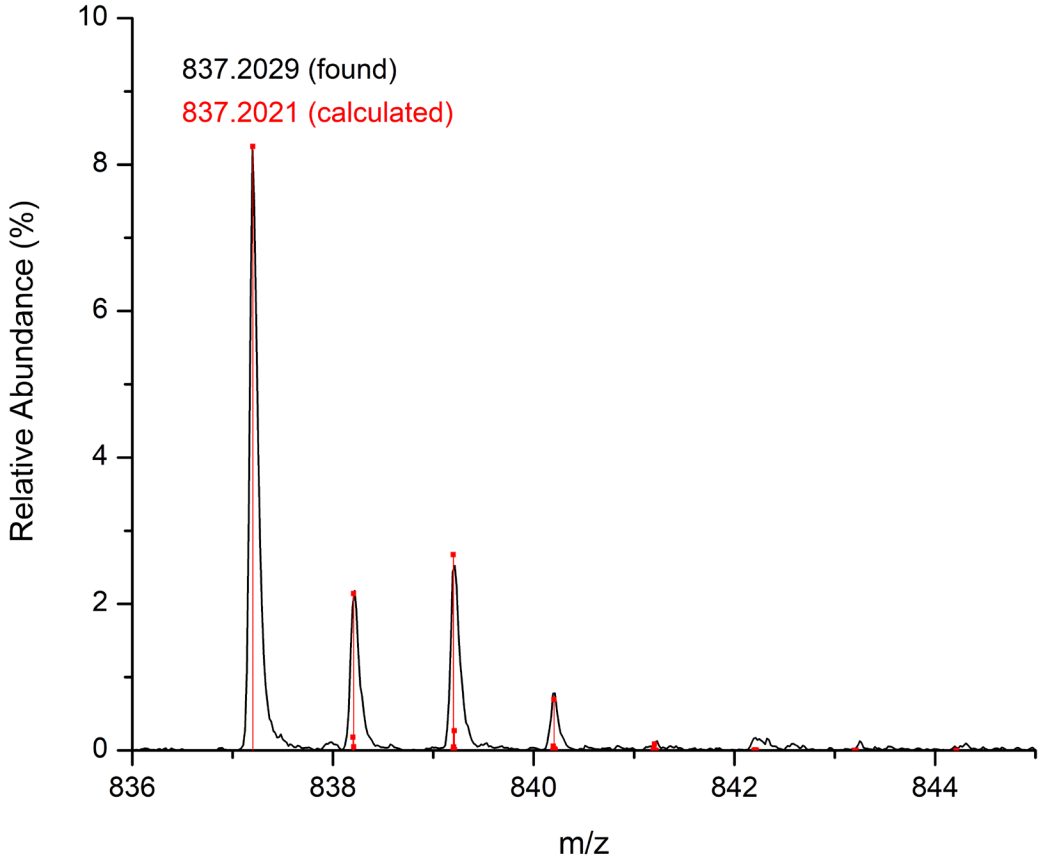

Figure S63: High-resultion MALDI(+)-MS peak region of $[M - Cl]^+$ (**2**, black) and calculated isotopic pattern (red).

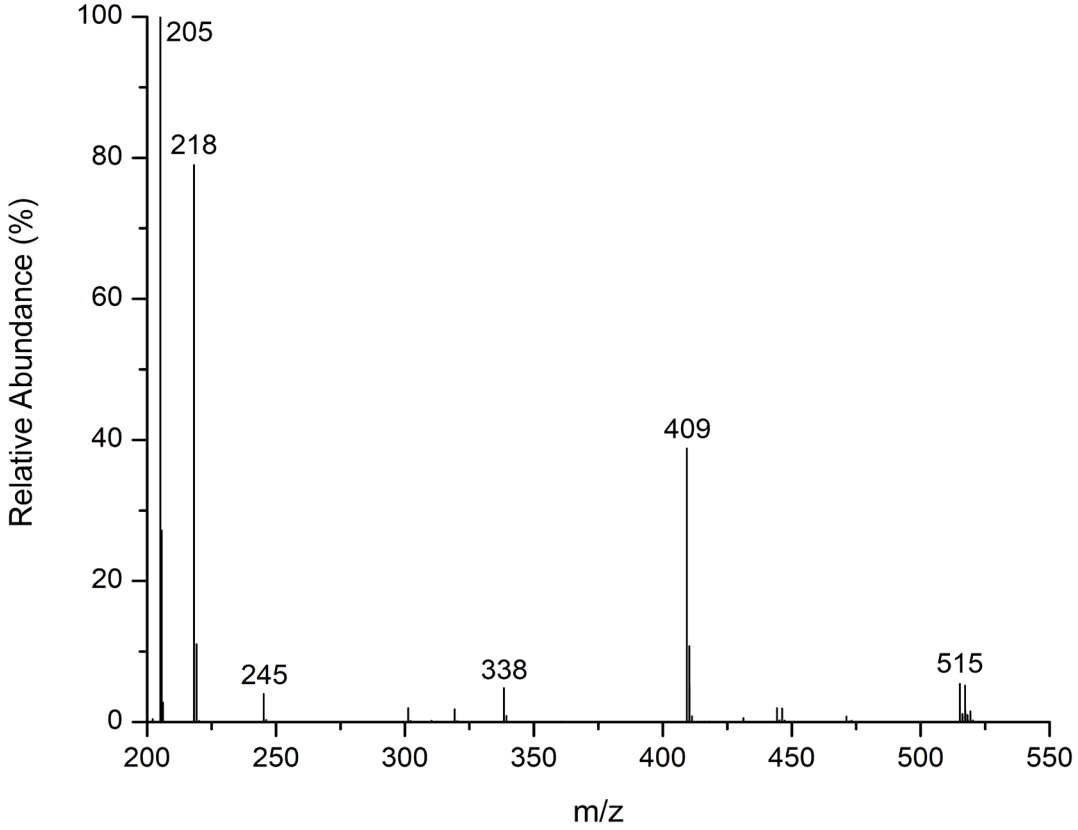

Figure S64: ESI(+)-MS spectrum of **3'**.

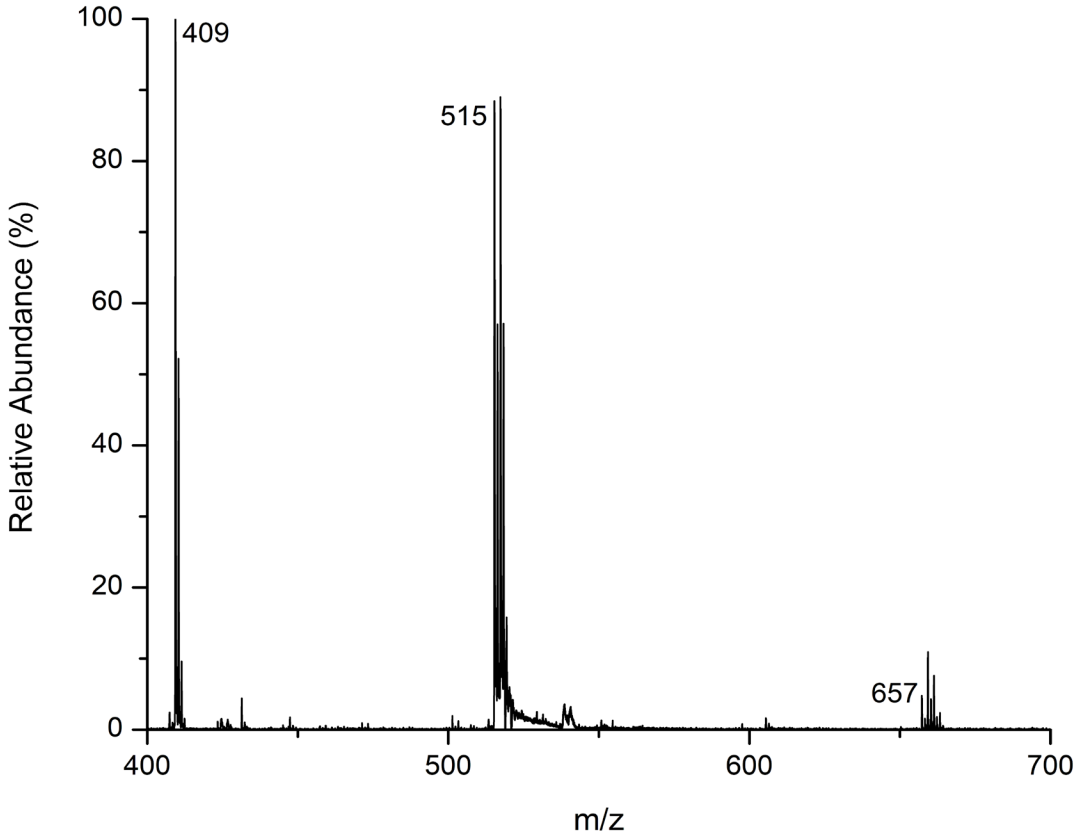

Figure S65: MALDI(+)-MS spectrum of **3'**.

Footnotes

[S1] For all representations of XRD molecular structures, both in the manuscript and the SI, the following program was used: *DIAMOND: Crystal and Molecular Structure Visualization* (version 3.2k); CRYSTAL IMPACT, Dr. H. Putz and Dr. K. Brandenburg GbR, Kreuzherrenstr. 102, 53227 Bonn (Germany).

[S2] O'Dea, C.; Ugarte Trejo, O.; Arras, J.; Ehnbom, A.; Bhuvanesh, N.; Stollenz, M. *J. Org. Chem.* **2019**, *84*, 14217–14226.

[S3] Arras, J.; Ugarte Trejo, O.; Bhuvanesh, N.; Stollenz, M. *Chem. Commun.* **2022**, *58*, 1418–1421.

[S4] Gutowsky, H. S.; Holm, C. H. *J. Chem. Phys.* **1956**, *25*, 1228–1234.

[S5] Günther, H. In *NMR-Spektroskopie*; Georg Thieme Verlag; Stuttgart, New York, *1992*, pp. 310–312.

[S6] Elemental analysis indicates co-precipitation of 0.7 equivalents of AgCl per monomeric unit of the dried solvent-free complex [(**L**H_2)$_2$(AgCl)$_3$] (**3'**). Despite the excess of **L**H_2 in the reaction solution, attempts to crystallize pure complex **3** resulted in co-crystallization of AgCl in varying amounts. The reported elemental analysis of **3'** represents the best available result.

[S7] (a) *APEX2: Program for Data Collection on Area Detectors*; BRUKER AXS Inc., 5465 East Cheryl Parkway, Madison, WI 53711–5373 USA. (b) *APEX3: Program for Data Collection on Area Detectors*; BRUKER AXS Inc., 5465 East Cheryl Parkway, Madison, WI 53711–5373 USA.

[S8] Sheldrick, G.M. *SADABS: Program for Absorption Correction of Area Detector Frames*; University of Göttingen, Göttingen, Germany, 2008.

[S9] (a) Sheldrick, G.M. *Acta Crystallogr.* **2008**, *A64*, 112–122. (b) Sheldrick, G. M. *Acta Crystallogr.* **2015**, *C71*, 3–8.

[S10] (a) Spek, A. L. *PLATON: A Multipurpose Crystallographic Tool*, Utrecht University, Utrecht, The Netherlands 2008. (b) Spek, A. L. *J. Appl. Cryst.* **2003**, *36*, 7–13.

[S11] (a) Ahlrichs, R.; Bär, M.; Häser, M.; Horn, H.; Kölmel, C. *Chem. Phys. Lett.* **1989**, *162*, 165−169. (b) Furche, F.; Ahlrichs, R.; Hättig, C.; Klopper, W.; Sierka, M.; Weigend, F.*Wiley Interdiscip. Rev.: Comput. Mol. Sci.* **2014**, *4*, 91−100. (c) TURBOMOLE V7.4.1 2019, A development of University of Karlsruhe and Forschungszentrum Karlsruhe GmbH, 1989−2007; TURBOMOLE GmbH, 2007. http://www.turbomole. com.

[S12] (a) Lee, C.; Yang, W.; Parr, R. G. *Phys. Rev. B: Condens. Matter Mater. Phys.* **1988**, *37*, 785−789. (b) Becke, A. D. *Phys. Rev. A: At., Mol., Opt. Phys.* **1988**, *38*, 3098−3100. (c) Becke, A. D. *J. Chem. Phys.* **1993**, *98*, 5648−5652.

[S13] (a) Eichkorn, K.; Treutler, O.; Öhm, H.; Häser, M.; Ahlrichs, R. *Chem. Phys. Lett.* **1995**, *242*, 652−660. (b) Eichkorn, K.; Weigend, F.; Treutler, O.; Ahlrichs, R. *Theor. Chem. Acc.* **1997**, *97*, 119−124; (c) Sierka, M.; Hogekamp, A.; Ahlrichs, R. *J. Chem. Phys.* **2003**, *118*, 9136−9148.

[S14] (a) Grimme, S. *J. Comput. Chem.* **2004**, *25*, 1463–1473. (b) Grimme, S. *J. Comput. Chem.* **2006**, *27*, 1787–1799. (c) Grimme, S.; Antony, J.; Ehrlich, S.; Krieg, H. *J. Chem. Phys.* **2010**, *132*, 154104.

[S15] Weigend, F.; Ahlrichs, R. *Phys. Chem. Chem. Phys.* **2005**, *7*, 3297−3305.

[S16] Deglmann, P.; Furche, F.; Ahlrichs, R. *Chem. Phys. Lett.* **2002**, *362*, 511−518.

[S17] Frisch, M. J.; Trucks, G. W.; Schlegel, H. B.; Scuseria, G. E.; Robb, M. A.; Cheeseman, J. R.; Scalmani, G.; Barone, V.; Petersson, G. A.; Nakatsuji, H.; Li, X.; Caricato, M.; Marenich, A. V.; Bloino, J.; Janesko, B. G.; Gomperts, R.; Mennucci, B.; Hratchian, H. P.; Ortiz, J. V.; Izmaylov, A. F.; Sonnenberg, J. L.; Williams-Young, D.; Ding, F.; Lipparini, F.; Egidi, F.; Goings, J.; Peng, B.; Petrone, A.; Henderson, T.; Ranasinghe, D.; Zakrzewski, V. G.; Gao, J.; Rega, N.; Zheng, G.; Liang, W.; Hada, M.; Ehara, M.; Toyota, K.; Fukuda, R.; Hasegawa, J.; Ishida, M.; Nakajima, T.; Honda, Y.; Kitao, O.; Nakai, H.; Vreven, T.; Throssell, K.; Montgomery, J. A., Jr.; Peralta, J. E.; Ogliaro, F.; Bearpark, M. J.; Heyd, J. J.; Brothers, E. N.; Kudin, K. N.; Staroverov, V. N.; Keith, T. A.; Kobayashi, R.; Normand, J.; Raghavachari, K.; Rendell, A. P.; Burant, J. C.; Iyengar, S. S.; Tomasi, J.; Cossi, M.; Millam, J. M.; Klene, M.; Adamo, C.; Cammi, R.; Ochterski, J. W.; Martin, R. L.; Morokuma, K.; Farkas, O.; Foresman, J. B.; Fox, D. J. *Gaussian 16*, Revision A.03; Gaussian, Inc.: Wallingford CT, USA, 2016.

[S18] (a) Perdew, J. P.; Yue, W. *Phys. Rev. B* **1986**, *33*, 8800−8802. (b) Becke, A. D. *Phys. Rev. A* **1988**, *38*, 3098−3100.

[S19] (a) Schäfer, A.; Huber, C.; Ahlrichs, R. *J. Chem. Phys.* **1994**, *100*, 5829−5835.(b) Weigend, F.; Ahlrichs, R. *Phys. Chem. Chem. Phys*. **2005**, *7*, 3297−3305.

[S20] (a) Bader, R. F. W. *Atoms in Molecules: A Quantum Theory*, Oxford University Press, Oxford, UK, 1990. (b) Bader, R. F. W. *Chem. Rev.* **1991**, *91*, 893−928.

[S21] Keith, T. A. *AIMAll*, Version 19.10.12; TK Gristmill Software: Overland Park KS, USA, 2019.

[S22] Grimme, S.; Ehrlich, S.; Goerigk, L. *J. Comput. Chem*. **2011**, *32*, 1456–1465.

[S23] Hariharan, P. C.; Pople, J. A. *Theor. Chim. Acta*, **1973**, *28*, 213–222.

[S24] (a) Figgen, D.; Rauhut, G.; Dolg, M.; Stoll, H. *Chem. Phys*. **2005**, *311*, 227–224. (b) Peterson, K. A.; Puzzarini, C. *Theor. Chem. Acc*. **2005**, *114*, 283–296.

[S25] Dennington, R.; Keith, T. A.; Millam, J. M. *GaussView*, Version 6.0.16; Semichem Inc.: Shawnee Mission, KS, USA, 2016.

[S26] These interatomic distances and torsion angles were calculated with the program DIAMOND 3.2k; the standard deviations are therefore not identical to those reported in the CIF.

[S27] Häfelinger, G.; Kuske, F. K. H. In The Chemistry of Amidines and Imidates; Patai, S., Rappoport, Z., Eds.; John Wiley & Sons, Ltd.: Chichester, UK, 1991; pp 1−100.

[S28] The ESDs of the corresponding bond distances in **3** are too large to be discussed.

[S29] Calderón-Díaz, A.; Arras, J.; Miller, E. T.; Bhuvanesh, N.; McMillen, C. D.; Stollenz, M. *Eur. J. Org. Chem.* **2020**, *22*, 3243–3250.